CONFIDENTIAL- VERTROUWELIJK

DEVELOPMENT OF THE THESSA ELECTRODE: A THERMO-ELECTRICAL STIMULATION ELECTRODE FOR NOCICEPTIVE CUTANEOUS FIBERS

EXPLORATION OF THE FUNCTIONALITY OF A HEAT CONDUCTING INTRA-EPIDERMAL ELECTRICAL STIMULATION ELECTRODE

UNIVERSITY OF TWENTE.

M.J. MAAN

MASTER THESIS

JUNE 2022

Supervisors
Dr. ir. J.R. Buitenweg
N. Jansen MSc
Committee
Dr. ir. J.R. Buitenweg
N. Jansen MSc
Dr. H.G.E. Meijer

Biomedical Signals and Systems Group

Faculty of Electrical Engineering, Mathematics and Computer Science

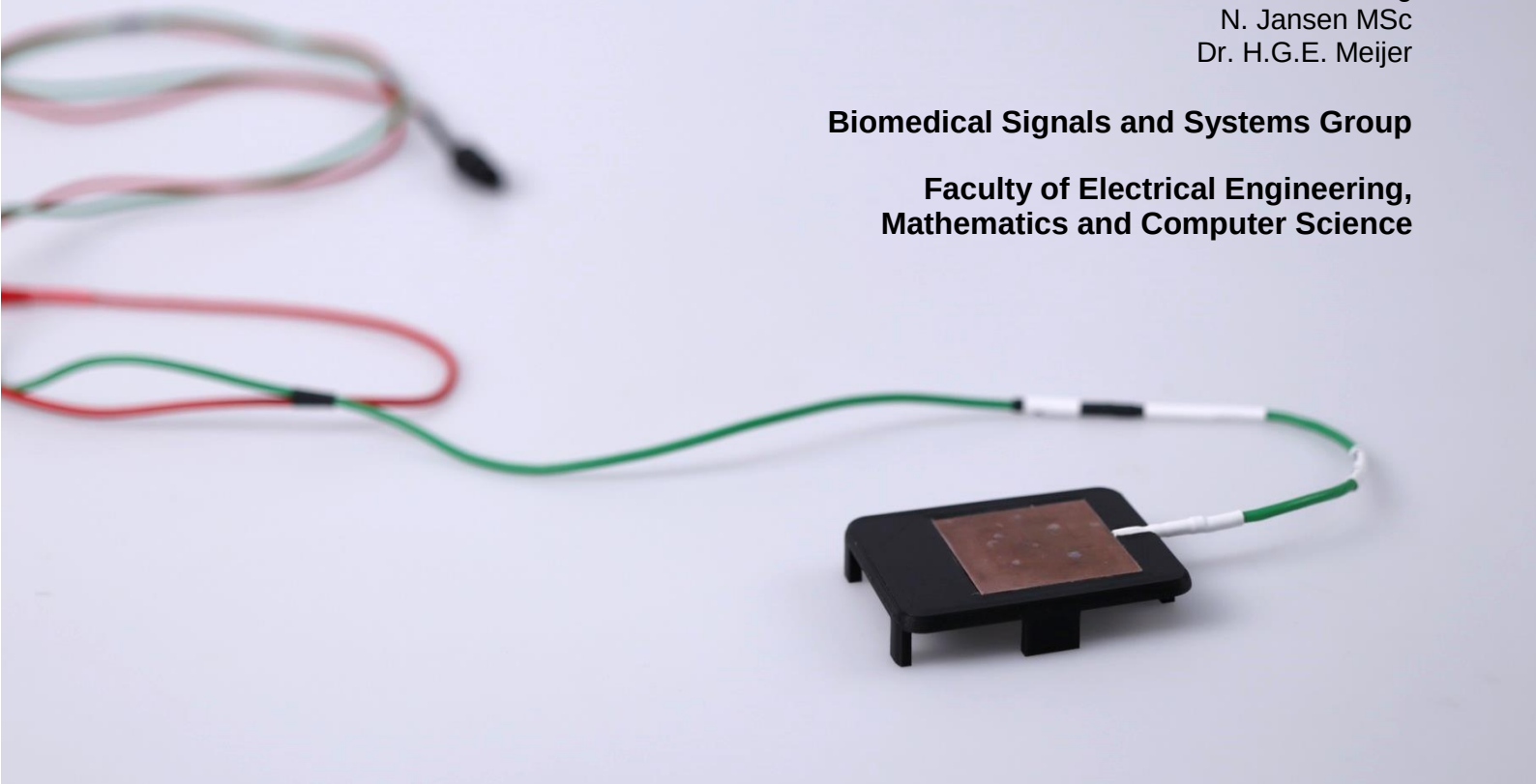

PREFACE

'Onderzoek alles, behoud het goede' – 1 Tessalonicenzen 5:21

In this report I present my master thesis: *Development of the ThESSA electrode: a thermo-electrical stimulation electrode for nociceptive cutaneous fibers*. I did this assignment for my master Biomedical Engineering at the research group Biomedical Signals and Systems at the University of Twente. I really enjoyed the variety of activities during my assignment, such as the practical activities at the workshop, discussing ideas for the design, cooperation in the development of the electrode, discussing the outcomes of measurements, the clinical experience, helping others with their problems, finding solutions for failures in the equipment, being frustrated about the "user-friendly" software and I even enjoyed the literature study

During my assignment I learned to cope with the everlasting struggles of science: there is always an extra measurement that can be performed; one answer found will lead to several new questions; writing is deleting (although there is still some progress possible for me); there is always progress possible, and so on. At the end, I was able to apply the things learned during study Biomedical Engineering, and I have even learned some things more: the existence of the Γ-function (quite complex).

When I first started on the topic pain during my Bachelor assignment, I was reserved about the topic. What would possibly be nice about research on pain?! It was Jan who convinced me that it was a really interesting topic, with a very enthusiastic theory about combined thermo-electrical stimulation. Now, a few years later, I completed several assignments related to this topic, which I really enjoyed.

I would like to use this opportunity to thank Jan, for guiding me through the project and keeping me focused on the important parts. Thank you for helping me with outlining the difficult structure of this thesis. I appreciated all the critical questions and feedback when I was over enthusiastic about certain explanations or potential solutions, although I didn't always show it at these moments. I now know that these questions improved my final work. Thank you for taking the time to supervise me during my assignment!

Niels, you turned out to be a nice example of a *day-to-day* supervisor. Thank you for your time to answer my endless questions and for the collaboration we had within this project. I appreciated your enthusiasm and our discussions about the challenges that occur during my assignment, although it often ended in 'That is science…'. I want to thank you also for the helpful feedback on my report. Bottom line: thank you for all the effort!

Hil, although you were not very present during my master assignment, you were present during large amount of math courses that I followed starting from the first quartile of my bachelor. Thank you for that and for the question you asked to help me focusing on my message. It was the simple question 'which story do you have to tell?'. I hope it has its effect, although my chaotic nature sometimes takes over.

I also want to thank Boudewijn, Frodo and Marcel for their help during the time that I was working on my research, and the possibility to discuss any topic related to this. In addition, I would like to thank the students from BSS, whom I could bother with the rest of my questions. Thank you for the interest in my project and the struggles related to this, and of course for the nice coffee breaks!

Furthermore, I would like to thank the subjects that participated in my experiments, without you I couldn't complete my research. And last but not least, I want to thank my family for their patience when I tried to explain the complicated topics were I was working on, I hope you will understand something of it on the end!

This all together really made my assignment more pleasant, thank you all!

Hanneke Maan

June 3th, 2022

ABSTRACT

Chronic pain is considered to have a major impact in the quality of life and daily activities. Due to lack of a sufficiently sophisticated device, the knowledge of assessing pain is currently limited. Therefore, the need for new and improved treatments is desired. Recently, we developed a thermo-electrical stimulation electrode that was designed to selectively stimulate the nociceptive system. An explorative study is presented in this research to the functionality of this thermal electrical stimulation electrode for the selective activation of nociceptors. The functionality of the electrode was tested with several thermal and impedance measurements, which showed high dependence on the skin's thermoregulatory system in the temperature measurements and increased electrical conduction of the skin when heat was applied in the impedance measurements. Subsequently, psychophysical exploration was performed on a group of six subjects, who completed normal and heated nociceptive detection threshold tasks (NDT task and H-NDT task, respectively). The research parameters within this exploration were the detection rate, stimulation amplitude and perception of the stimuli. The strength of the thermal stimulus was obtained by completing a subjective heat pain detection threshold (HPDT) task. Application of this temperature during the H-NDT task showed presumed affection of the detection rate. Analysis of the stimulation amplitude was subdivided into initial NDT (NDT_0) and slope of the NDT. This explorative study provides the indication of a potential increase of NDT_0 during the H-NDT task, although statistical evidence is needed to support these findings. This study had its limitations in the unexpected role of the thermoregulation system of the skin in applying thermo-electrical stimulaton, and the functionality of the software protocol.

SAMENVATTING

Chronische pijn wordt geacht van grote invloed te zijn op de kwaliteit van leven en dagelijkse activiteiten. De kennis om pijn te meten is ontoereikend, doordat er geen voldoende geavanceerd meetinstrument beschikbaar is. Daarom is er grote behoefte aan nieuwe en verbeterde behandelmethodes. Recent is een thermo-electrische stimulatie electrode ontworpen voor het selectief stimuleren van het nociceptive systeem. In dit onderzoek wordt een explorative studie gepresenteerd over de functionaliteit van deze thermisch-electrictrische stimulatie electrode voor de selectieve activatie van nociceptors. De functionaliteit van de electrode is getest met verschillende thermische en impedantie metingen. Deze metingen tonen respectievelijk de sterke afhankelijkheid van het thermoregulatief systeem, en de verhoogde electrische conductie van de huid wanneer deze wordt bloodgesteld aan warmte. Daaropvolgend is een psychofysische exploratie gedaan op een groep van zes proefpersonen die een normale en een verwarmde nociceptive detectiedrempel test uitvoerden (respectievelijk een NDT taak en een H-NDT taak). De onderzoeksparameters binnen deze exploratie waren de mate van detectie, de stimulatie amplitude en de waarneming van de stimuli door de proefpersoon. De sterkte van de thermische puls wordt bepaald door de proefpersoon een subjectieve hitte pijn detectie drempel (HPDT) taak te voltooien. Bij het toepassen van deze temperatuur tijdens de H-NDT taak werd een vermoedelijke invloed van de temperatuur op de detectiegraad te zien. De analyse van de stimulatie amplitude was onderverdeeld in een initiële NDT (NDT_0) en de helling van de NDT. Bevindingen uit dit onderzoek laten zien dat de NDT_0 vermoedelijk verhoogt tijdens de H-NDT taak, hoewel er nog statistisch bewijs nodig is om dit te kunnen onderbouwen. Dit onderzoek had zijn beperkingen in te onverwachte rol van het thermoregulatiesysteem van de huid in het toedienen van de thermisch-electische stimulatie en in de werking van het software protocol.

TABLE OF CONTENTS

Preface iii
Abstract v
Samenvatting v
Acronyms xi
1. Introduction 1
2. Background 3
2.1 Physiology of the skin 3
2.1.1 Nociceptors 3
2.1.2 Heat regulation 5
2.2 Dysfunction of the nociceptive pathways 5
2.2.1 Current assessment 5
2.2.2 Characterization 6
2.3 Current Methods 6
2.3.1 Laser stimulation 6
2.3.2 Contact heat stimulation 6
2.3.3 Intra-Epidermal Electrical Stimulation 7
2.4 Research implications 8
3. Design 9
3.1 Analysis of the problem 9
3.1.1 Problem definition 9
3.1.2 List of requirements 9
3.2 Synthesis I 10
3.2.1 Morphological map 10
3.2.2 Concept Design 1: The simple etched microneedle electrode 11
3.2.3 Concept Design 2: The etched hollow microneedle electrode 11
3.2.4 Concept Design 3: Redesign of microneedles array patches 11
3.2.5 Concept Design 4: Electrode with embedded needles 12
3.2.6 Design selection 12
3.3 Synthesis II: Development of the prototype 13
3.3.1 First prototype 13
3.3.2 Second prototype 14
3.3.3 Tape selection 14
3.3.4 Holder 15
4. Functionality of the Electrode 16
4.1 Thermal conduction 16
4.1.1 Method 16
4.1.2 Functional optimization 17

4.1.3 Overall Discussion 23
4.2 Electrical impedance 26
4.2.1 Method 26
4.2.2 Evaluation 27
4.2.3 Concluding Summary 31
5. Psychophysical exploration 32
5.1 Method 32
5.1.1 Subjects 32
5.1.2 Study design 32
5.1.3 Materials 33
5.1.4 Stimuli 34
5.1.5 Procedure 34
5.1.6 Analysis plan 35
5.2 Results 37
5.2.1 Study design 37
5.2.2 Group-level results 37
5.2.3 Individual subject analysis 39
5.3 Discussion 45
5.3.1 Technical feasibility of the study protocol 45
5.3.2 Group-level results 46
5.3.3 Individual subject analysis 47
6 General Discussion 50
6.1 Design 50
6.2 Functionality of the Electrode 50
6.3 Temperature measurements 50
6.4 Psychophysical exploration 51
6.5 Future prospective 51
References 52
Appendices 55
Appendix A 56
A.1 Detailed description of the production process of the prototypes 56
Application of the template 56
Length of the needles 56
Finishing the back of the electrode 56
A.2 Additional pictures measurements 57
Imprint electrode thermal conduction measurement 4 (with the concept electrode) 57
Oxidation of the electrode 57
A.3 Calculation of the temperature via calibration curve 58

A.4 Additional figures impedance measurements 60
A.5 Study design elaborated recommendations 63
A.6 Temperature comparison of the skin 63
A.7 Temperature comparison of the first measurements 64
A.8 Estimated NDTs 64
A.9 Individual values for comparing the subjects 65
A.10 Additional pictures of the psychophysical exploration 66

ACRONYMS

ADL – activities of daily living

ATP – adenosine triphosphate

CGRP – calcitonin gene-related peptide

CH-fiber – heat sensitive C-fiber

ChR2 – channelrhodopsin

CI – confidence interval

CNS – central nervous system

CPE – constant phase element

CRPS – complex regional pain syndrome

DP – double pulse

ET-1 – endothelin-1

H-NDT – heated NDT (nociceptive detection threshold)

HPDT – heat pain detection threshold

IES – Intra-epidermal electrical stimulation

IL-1β – interleukin 1β

IL-6 – interleukin 6

IPI – interpulse interval

MMS – medoc main station

NDT – nociceptive detection threshold

NGF – nerve growth factor

NoP – number of pulses

P2 – purinergic receptors

PNI – peripheral nerve injury

PGE_2 – prostaglandin E_2

QST – quantitative sensory testing

SC – stratum corneum

SP – substance P

SP – single pulse

TES – Thermal electrical stimulation

ThESSA electrode – thermo-electrical stimulation for specific activation electrode

TT – target temperature

1. INTRODUCTION

In the Netherlands, one in five adults suffers of chronic pain, which is two million people. Causes of chronic pain can be osteoarthritis and rheumatoid arthritis (42%), herniated/deteriorating discs of fracture of the spine (21%), surgery or traumatic injury (15%), migraine headache (7%), nerve damage or whiplash (both 4%) [1]. Chronic pain is considered to have a major impact in the quality of life and daily activities, such as work and social life. Therefore, the need for new and improved treatments of chronic pain is demanded [1]. However, to develop those treatments, the physiological and the psychological aspects to pain should be investigated more extensively, as thorough knowledge of these aspects to chronic pain is still insufficient.

Evaluating processing of pain via nociceptive pathways (pain sensitive neurons) is an important tool to understand the onset and progression of chronic pain. Nociceptive pathways can be evaluated via selective stimulation of nociceptors (Aδ- and C-fibers). Selective stimulation requires care, as tactile fibers (Aβ-fibers) can also be easily activated due to their lower threshold.

For selectivity, several methods have been proposed, for instance: thermal (laser) stimulation [2], contact heat stimulation with thermodes [3], and intra-epidermal electrical stimulation (IES) [4, 5]. The first two methods are based on the thermal sensitivity of nociceptors, as tactile fibers are thermally insensitive. These methods are based on the research on temperature and touch receptors, which was in 2021 rewarded with the Nobel Prize in Medicine. David Julius and Ardem Patapoutian got this prize for their discoveries of temperature and touch receptors (TRPV1 and Piezo1 respectively) [6]. IES on the other hand, is based on the difference in the depth of the nerve endings in the skin. As all methods have their own advantages as disadvantages, they will be explained as following.

Laser stimulation has a high energy density per unit area, which makes it possible to create a temperature increase proportional to 1000 °C/s [2]. This results in the activation of nociceptors in milliseconds. Although this characteristic is useful for reaction time measurements, it is also a limitation. The high energies transmitted by laser stimulation damage the skin when it is not applied briefly and with care [2]. Skin burns or eye damage can be the result when laser stimuli are not applied with caution [3].

An alternative for laser stimulation is contact heat stimulation applied with a thermode [7]. This is for instance used within quantitative sensory testing (QST), an assessment method for e.g. peripheral neuropathy. QST can be used for examination of certain physiological sensations, such as touch, vibration, pinprick/sharp pain, warmth, cold, painful warmth and painful cold [8].

In comparison with laser stimulation, thermodes are safer to use for longer time. This is due to a safety mechanism that switches the thermode off before the skin is exposed to noxious heat for too long [9]. However, this technique is limited for use in a clinical setting, presumably due to lack of standardized methods and robust reference values [3]. Nevertheless, selective activation of the nociceptors is often performed with thermal stimulation. It can even selectively activate C-fibers which have a lower thermal threshold (~40 °C) than Aδ-fibers (~46 °C) [2]. However, thermal activation of nociceptors via contact heat stimulation requires some time [2]. Therefore, a more controlled stimulation would be desired to get more qualitative stimuli, for instance with a method that stimulates the nociceptor directly with an electrical stimulus, such as IES.

Electrical stimulation is another method to assess the sensory system, as QST does in a broader way. IES applies a high current density to the epidermis, while the current density is limited in the deeper located dermis. This results in stimulation of the superficial layers of the skin, where the nociceptive Aδ- and C-fibers are located. IES can therefore selectively stimulate the nociceptors, which is perceived as a pin-prick sensation at the detection level (perceptual threshold). However, when the skin is stimulated at an intensity equal or below twice the perceptual (nociceptive) threshold, deeper located neurons might be stimulated as well [4]. Electrical stimulation of the superficial layers can be achieved by one (or several) needle(s) penetrating the stratum corneum, where the needles act as a cathode and are surrounded by a concentric anode [5].

A challenging difficulty in using the IES electrode is its high sensitivity, since selective activation of nociceptors only remains within a small range of stimulus intensities. Considering this, the sensitivity might be reduced by combining IES with thermal stimulation. Application of combined thermo-electrical stimulation has been previously explored in computational models in MATLAB and COMSOL, showing the possible potential for this technique [10, 11].

Combination of thermal and electrical stimulation might give more controlled stimulation compared to thermal stimulation only [12]. During the combined stimulation, it is desired to have a constant temperature, such that it is well controlled, accurate, and reproducible. To prevent for excessive activation of the thermosensitive nociceptors by a too high temperature pulse, it is necessary to heat the skin just below the nociceptive threshold. In this case the activation via the electrical stimulus will not disappear in a spike train of action potentials. With this approach, it is attempted to get the thermosensitive nociceptor in a slightly lowered activation threshold, since it is already partly activated. Hypothetically, this makes it possible to activate C-fibers with a lower electrical stimulus than is needed to activate Aδ-fibers.

The aim of this research is to design an intra-epidermal electrode which is compatible with the application of heat via a thermode (TSA2, Medoc, Israel). In particular, we want to explore the functionality of this thermal electrical stimulation electrode for the activation of nociceptors and gain more insight in the stimulus response relation. Accordingly, the research question is defined as follows: How can we test the functionality of a thermal electrical stimulation electrode in terms of detection rate, stimulation amplitude and perception of the stimuli?

In line with this, the following sub questions will be addressed:

1. How can we simultaneously stimulate the skin thermally and electrically?
2. How can we verify that the temperature of the skin reaches the desired temperature?
3. What is the nociceptive detection threshold with the new electrode?
4. How is the nociceptive detection threshold affected by an increase of skin temperature of the stimulated skin area?

As mentioned, a thermal electrical stimulation electrode will be designed whereof a prototype will be made and tested for its functionality. Additionally, a set-up will be realized such that it can verify the temperature of the skin. Furthermore, a protocol is developed for testing subjects with this electrode. The obtained electrical and thermal-electrical stimulation results will be analyzed and compared in the context of exploration of the quality and content of the nociceptive detection thresholds.

2. BACKGROUND

2.1 PHYSIOLOGY OF THE SKIN

The skin is essential in regulating the body temperature and sensation of pressure, temperature, and touch. Therefore, understanding the physiology of the skin is fundamental, before stimulation of the skin with thermal and electrical stimuli will be valuable. The layers of the skin include the epidermis, dermis and the hypodermis.

The epidermis is the outermost layer and can be classified as thick or thin depending on the width of the epidermis [13]. Thick (glabrous) skin can be found at the palms of the hands and the soles of the feet. Of this, the epidermis has a width of 0.8-1.5mm [13]. Additionally, thin skin can be found on the rest of the body and has an epidermis thickness of 0.07-0.15mm [13]. It consists of four layers: outermost the stratum corneum, followed by the stratum granulosum, stratum spinosum and stratum basalis. The free nerve endings of Aδ- and C-fibers are located in the epidermis, specifically in the stratum granulosum till the stratum basalis. This means that the dead stratum corneum has to be penetrated for good intra-epidermal electrical stimulation. For an overview of the skin layers and their sensory receptors, see Figure 2.1.

Underneath the epidermis is the dermis. It has a thickness of 0.3mm to 3.0 mm, which is much thicker than the epidermis [13]. The dermis is responsible for nutrition and temperature regulation, which is regulated by their blood vessels. Furthermore, the (larger) nerves are also located here, which are responsible for sensation of touch and pressure. The receptors of these nerves (Aβ-fibers) are Merkel, Meissner, Pacinian (also found in the hypodermis) and Ruffini cells [14].

The third layer is the hypodermis, or subcutaneous tissue, which is located above the muscles. It consists mostly of fat cells, and serves as insulation to cold. The hypodermis contains larger blood vessels and nerves (also Aβ-fibers) compared to the dermis. Although the Aβ-fibers are not the main focus of this research, it is important to know their location in the skin, as it is possible that these will be activated unintentionally as well.

2.1.1 NOCICEPTORS

The axons are named in the 1920s and 1930s, and are categorized according to the conduction velocity. The main categories are A (the fastest), B and C (the slowest), where A- and B-fibers are myelinated and C-fibers not. A- and C-fibers are motor and sensory neurons, whereas B-fibers are related to the autonomic nervous system. A-fibers are divided in three subcategories based on their conduction velocity as well. Aα-fibers are the fastest, followed by Aβ-fibers and as slowest Aδ-fibers [14].

Aδ- and C-fibers can be labelled as nociceptors, as they can detect noxious (painful) stimuli (i.e. heat). The heat detection threshold for C-fibers is approximately 40°C, whereas for Aδ-fibers it is 46°C [2]. Basbaum et al. addressed that the Aδ-fibers can be further subdivided in two main classes. Type I Aδ-fibers have relatively high heat thresholds, (>50°C), whereas type II have a much lower heat threshold (always > 42 °C) [15, 16]. This last type is almost certainly responsible for ‘first’ pain caused by noxious heat [16].

The heat threshold of nociceptors is most likely originating from a combination of TRPV receptors (pronounced as ‘Trip V’). Basbaum et al. mentioned that the TRPV1 receptor has a threshold of 43°C, which is present in both Aδ- (type II) and C-fibers. The TRPV2 threshold is 52°C and this receptor is only present in type I Aδ-fibers. [16] Remarkable is that the thresholds of these receptors are higher than the thresholds of the Aδ- and C-fibers indicated before. It is presumed that two other types of TRPV channels are responsible for this: TRPV3 and TRPV4. TRPV3 is activated at temperatures between 34 and 39°C, whereas TRPV4 is activated between 25°C and 35°C [17]. Those channels are highly expressed in keratinocytes and epithelial cells, both present in the epidermis. According to Chung et al. [18] and Peier et al. [19], a functional interplay is involved in detecting heat between the keratinocytes and the nociceptors.

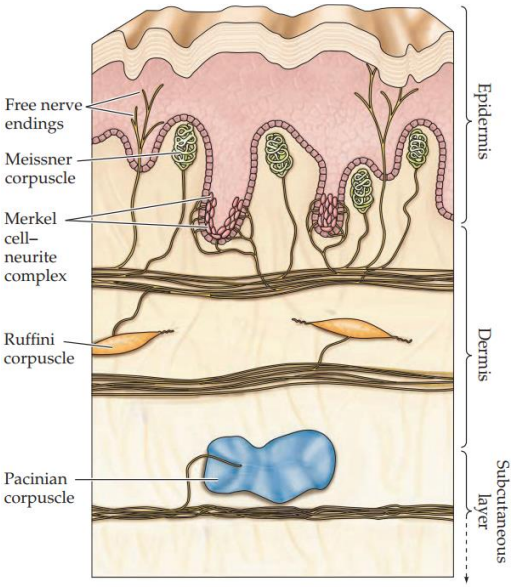

Figure 2.1 Schematic representation of the sensory receptors in the glabrous skin. Reprinted from Purves et. al [20].

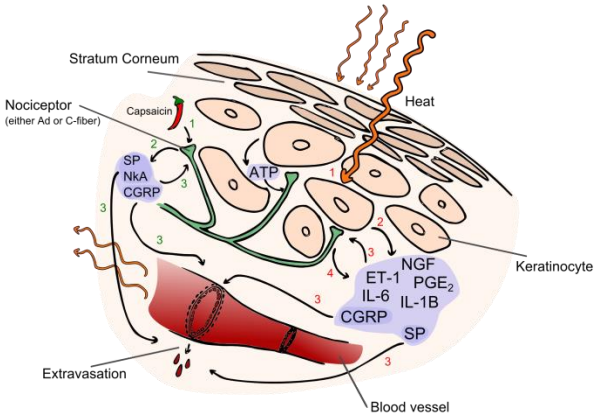

Figure 2.2 Different processes in the skin, when regulating the heat. The 'red' path contains the process when heat is applied externally, with temperatures in the range of 25-42°C. At 42 °C the blood vessels are diluted maximally. The 'green' path consists of the process when capsaicin is used to activate the TRPV1 receptors.

Keratinocytes can be stimulated with thermal, mechanical or chemical stimuli, and can lead to the release of several neuroactive molecules which will act on the peripheral neurons. Baumbauer et al. [21] did research on this phenomena by using mice expressing channelrhodopsin (ChR2) in keratinocytes. These channels are sensitive to (blue) light and can be used to determine the contribution of keratinocytes in the signaling pathway of sensory stimulation. Regularly, ChR2 is used in optogenetics to control biochemical pathways, as the natural light-sensitive channel can be found only in green algae. Therefore, the synthetic ChR2 is very powerful for the use of specifically stimulation of certain cells, in this case the keratinocytes, as the sensory neurons will not be activated by light.

Light activation of ChR2-keratinocytes could evoke nocifensive behaviors, such as paw lifting, biting and licking. This was found by Baumbauer et al. [21], suggesting that there is communication between keratinocytes and sensory fibers. Stimulation with blue light was sufficient to induce action potentials in several types of sensory neurons and potentiated a response to natural stimulation in other afferents. For instance, the heat sensitive C (CH) fibers responded to keratinocyte activation by light, which normally react only to noxious heat due to expression of TRPV1. This indicates that keratinocytes are able to communicate with CH-fibers.

The neuroactive molecules mentioned before, include nerve growth factor (NGF), prostaglandin E_2 (PGE_2), the neuropeptides substance P (SP) and calcitonin gene-related peptide (CGRP), adenosine triphosphate (ATP), protons, β-endorphins, endothelin-1 (ET-1), interleukin 1β (IL-1β) and interleukin 6 (IL-6) and cytokines [22, 23]. From these molecules ATP [19, 24] and PGE_2 [25] are indicated as possible signaling agents (Figure 2.2) [26]. However, much remains unknown about the signaling pathways between the keratinocytes and the nociceptors.

Mechanical stimulation of keratinocytes by pressure or touch leads to the release of ATP in the extracellular space, as reported by Moehring et al. [23]. The keratinocytes, located close to the sensory neurons, facilitate response of the neurons to ATP through purinergic receptors (P2). Plausible receptors for this are the ionotropic P2X and the G-protein-coupled P2Y receptors [23, 27]. For instance, six of the P2X receptors ($P2X_1$-$P2X_6$) are expressed in the sensory neurons, where $P2X_3$ and $P2X_{2/3}$ are predominant in the nociceptive neurons, as well as $P2X_4$ [28, 29]. Furthermore, the RNA of the P2Y receptors $P2Y_1$, $P2Y_2$, $P2Y_4$ and $P2Y_6$ are identified in sensory ganglia [30].

To summarize, keratinocytes release ATP as result to thermal stimulation (25-35°C) of keratinocytic TRPV3 and TRPV4, and to mechanical stimulation via pressure and touch [18, 19, 22, 24]. This, in combination with the nocifensive behaviour to light activation of ChR2-keratinocytes, gives the strong indication that the same signaling mechanism is applicable for the transduction of thermal stimuli to the sensory neurons. It indicates that this is at least one of the signaling pathways, as pathways with other neuroactive molecules are still open as mentioned before. [23]

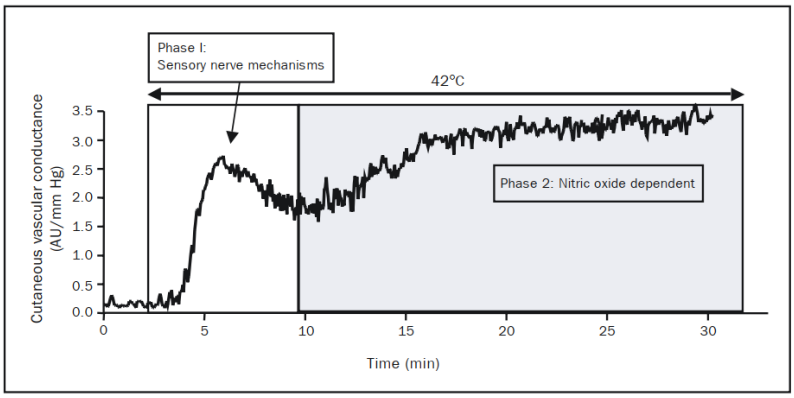

Figure 2.3 Typical course of cutaneous vascular conductance (arbitrary units/mmHg) during local heating for 30 minutes. The first part comes from local sensory nerve activity, whereas the second part depends on the attendance of nitric oxide. Reprinted from Charkoudian et al. [31]

2.1.2 Heat regulation

Local heating of the skin with heat of 42 °C and above, causes the blood vessels to dilate maximally [31]. The sensory nerves responsible for this vasodilation are primarily C-fiber afferents, antidromically releasing CGRP, SP, and NkA (Figure 2.2) [31, 32]. Within them, CGRP is responsible for vasodilation, the red coloring of the skin, whereas SP and NkA cause plasma extravasation, resulting in the swelling of the skin. This heat stimulation of sensory nerves and the reaction to this is embodied in the term neurogenic inflammation [32]. The release of CGRP, SP and NkA, results in a positive feedback loop to the afferents, sensitizing the C-fibers for thermal stimuli [32]. After several minutes, the nerve activity will be taken over by the signaling molecule nitric oxide (NO) [31, 33], as shown in Figure 2.3.

2.2 Dysfunction of the nociceptive pathways

Currently, the knowledge about nociception is limited due to lack of a sufficiently sophisticated device with reliable characteristics for assessment of pain [2], and thus in knowledge of dysfunctions in nociceptive pathways as well. Therefore, some background information is provided on possible target populations with nociceptive pathway dysfunctions, as they could benefit from a better knowledge of the physiological and psychological aspects of pain, and from better knowledge of the function of nociceptive pathways in general.

Dysfunction of the nociceptive pathways can be classified as any sensation that is perceived as pain, but not triggered by a nociceptive stimulus. The sensation of pain to a non-nociceptive stimulus is called neuropathic pain, which is officially defined by the International Association for the Study of Pain (IASP) as “pain caused by a lesion or disease of the somatosensory nervous system” [34]. Neuropathic pain can be divided into pain originating in the central nervous system (CNS) or in the peripheral nerves. Examples of neuropathic pain on the CNS are multiple sclerosis, spinal cord injury, and central post-stroke pain [35, 36]. Peripheral neuropathic deficiencies are for instance: post-herpic neuralgia, phantom limb pain, post-mastectomy pain, Guillain-Barré syndrome, neuropathic cancer pain, complex regional pain syndrome (CRPS) (type I and II), chronic lumbar root pain, trigeminal neuralgia, peripheral nerve injury (PNI) and several neuropathies (painful diabetic neuropathy, HIV neuropathy, painful polyneuropathy and chemotherapy induced neuropathy) [35, 37].

2.2.1 Current assessment

Quantitative sensory testing (QST) is a non-invasive technique that can be used as tool for assessment of patients with peripheral neuropathy or other neuropathic dysfunctions. This psychophysical method is used to quantify somatosensory function in healthy subjects and patients [8]. QST consists of several tests to examine certain physiological sensations, such as touch, vibration, pinprick/sharp pain, warmth, cold, painful warmth and painful cold [8]. To test thermal sensation for example, the subject should indicate whether the warmth stimulus was sensed or not. This makes it under liable to a psychological component. Therefore, it cannot be used as a stand-alone diagnostic test for neuropathic pain, as patients with language and cognitive difficulties, anxiety or litigation can (involuntarily) influence the outcome [8]. Nevertheless, QST can be a valuable tool for early detection, therapy selection and assessing the gain or loss of sensation over time.

Figure 2.4 The standard 30x30mm thermode. Reprinted from Medoc [38]

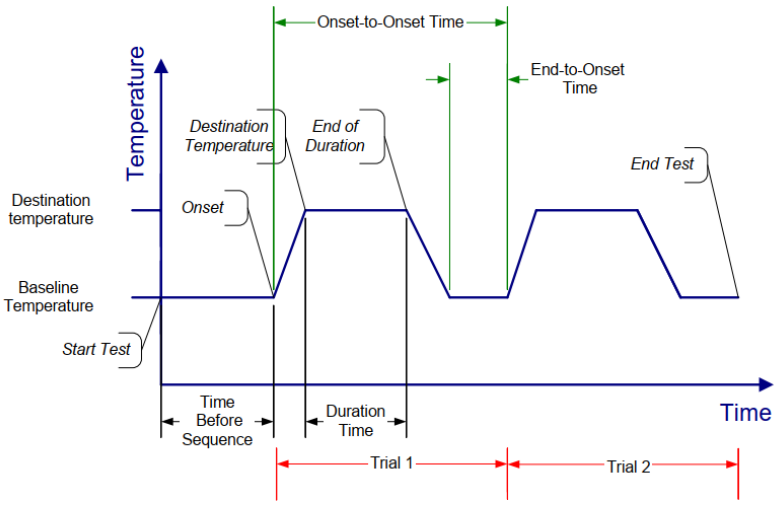

Figure 2.5 Overview of a temperature protocol for the TSA2, with all the specific properties marked in the diagram. Reprinted from the TSA2 operation manual [39]

2.2.2 Characterization

Neuropathic dysfunction can be characterized by hyperalgesia (increased sensitivity to pain), allodynia (pain response to a non-painful stimulus) and hypoalgesia (decreased sensitivity to pain). When nociceptive pathways are affected (e.g. by a disease), the sensory pathways are often affected as well, which can be helpful in diagnosing a disease [37]. For the non-nociceptive pathways, neuropathic dysfunction can also be characterized by hypoesthesia (decrease in sensitivity to sensation, numbness) and hyperesthesia (increase in sensitivity to sensation). CRPS has for instance a higher prevalence of hyperalgesia to cold, heat, blunt pressure and pinprick, and dynamic mechanical allodynia. PNI on the other hand has a high prevalence of hypoalgesia for cold and heat pain [37]. More details can be found in the research of Maier et. al [37]. Altogether, this gives a small indication of the population of interest, as there are several neuropathic dysfunctions where the thermo-electric stimulation electrode could be useful for in diagnosing or revealing the course of the disease.

2.3 Current Methods

Selective activation of nociceptive fibers can help to get insight of the nociceptive pathways. Several methods are based on the ability of nociceptors to detect (noxious) heat via TRPV receptors and on the difference in depth of the nerve endings. Specifically, the nociceptors terminate in the epidermis, whereas tactile fibers terminate in the dermis, as mentioned before. Examples of methods are thermal stimulation by admission of noxious temperatures via laser or contact heat stimulation [2, 3] and intra-epidermal electrical stimulation (IES) [4, 5].

2.3.1 Laser stimulation

Laser stimulation is an effective tool to thermally stimulate nociceptive fibers. The small, almost parallel, beam makes it possible to apply a high energy density at a small spot. This allows for a fast and high heat transfer via radiation, which facilitates ramps of several thousand degree Celsius per second [2]. This means that nociceptors can be activated within a few milliseconds. At the same time, laser stimulation asks for safety precautions. If the stimulus is not applied briefly and with care, it can cause damage to the skin or eyes, which is a major problem [2, 3].

2.3.2 Contact heat stimulation

An alternative to laser stimulation is contact heat stimulation via a thermode. Commonly used are the TSA2 of Medoc (Israël) and the MSA of Somedic (Sweden) [40]. The focus of this research will only be on the TSA2, as this one is available at our research group Biomedical Signals and Systems (BSS). Rolke and colleagues listed the properties of both devices in more detail [40]. The 30x30mm thermode of the TSA2 (Figure 2.4) uses a technique based on thermoelectric heating [39]. These elements make use of several thermocouples, which will generate a current flow when they are heated. Conversely, when a current is applied, the thermocouple will increase in temperature as well. Therefore, it is possible to heat or cool a surface with the thermode. The temperature can range from 0 to 53°C, which can be applied without any direct harm to the skin. When longer

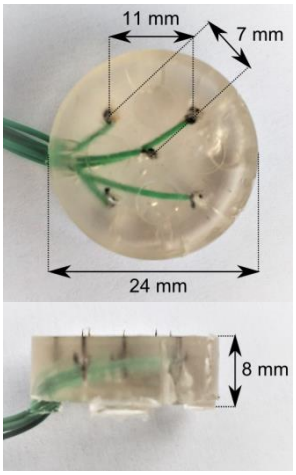

Figure 2.6 The IES-5 electrode currently used for intra-epidermal electrical stimulation.

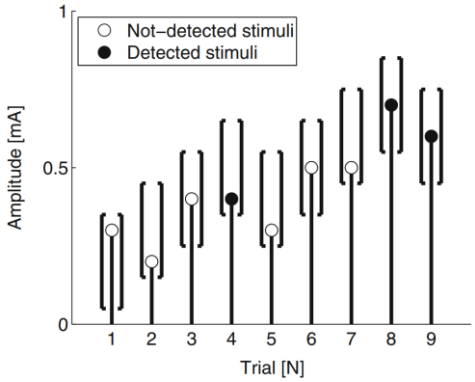

Figure 2.7 An example of the adaptive staircase procedure, where the brackets represent the sets wherein the stimulus randomly will be chosen. The next set will be increased when not detected, whereas it is decreased when the stimulus is detected. Replicated from Doll et al. [41]

durations are desired, temperatures of 10 to 45°C can be applied without any time restrictions. Otherwise there are duration restrictions ranging from 60 seconds at 47 °C to 0.4 seconds at 52 °C at warm temperatures and 80 seconds for temperatures between 0-6 °C. The temperature change rate ranges from 0.1 to 13°C/s for the standard 30x30mm thermode. Furthermore, applied temperature by the thermode has an accuracy of ±0.3°C [39].

With the thermode, it is possible to specifically stimulate the thermosensitive C and Aδ fibers, to provide information about their function [7]. This method can help to detect or measure the progression of the disease or dysfunction of the small sensory fibers in more quantified results [7, 39]. The stimulation can be completely regulated via the included software program of Medoc. It has the benefit of a build in safety protocol and the controlled temperature regulation. For the purpose of the experiments, it is desired to have a constant temperature, such that it is well controlled, accurate, and reproducible. This can be realized with prior created protocols, with properties such as baseline, target temperature, duration of the stimulus, increase or decrease rate of the temperature, as shown in Figure 2.5.

2.3.3 Intra-Epidermal Electrical Stimulation

At our research group, a method is used for measuring psychophysical nociceptive detection thresholds (NDTs). Measurements are performed with help of our own developed IES-5 electrode (Figure 2.6), which has five needles with a length of approximately 0.5 mm protruding from the silicone [41]. When used, the IES-5 is gently put on top of the skin, such that it only protrudes for roughly 0.2mm. Herewith, it is possible to stimulate the nociceptive Aδ and C fibers intra-epidermally with small electrical currents of around 0.1-1mA. This is right around the detection threshold of sensation, to estimate the pain sensitivity. However, IES is very sensitive: when a double pulse stimulus of two times the detection threshold is applied, it is no longer selective for nociceptors and it activates low threshold tactile fibers as well[4].

NDT method

For determining the NDT, an adaptive staircase procedure is used for the applied electrical stimuli. This procedure is often used in other comparable research at our research group, as tool to overcome prediction of the next stimulus and to compensate for the non-stationary threshold, due to subject's habituation [41-43]. A set of five amplitudes is defined at the initial detection threshold. A stimulus amplitude will be randomly selected from this set for the next stimulus. When detected, the following will be decreased by a certain step size, otherwise it will be increased (Figure 2.7). In this way predictability will be prevented, and accounted for habituation.

Impedance at the electrode-skin interface

Usage of an electrode to measure or stimulate the skin, will always involve electrical impedance. The stratum corneum (SC) has a high influence on this, as it is electrically insulating, due to its dead cells, and a humidity of only 20 percent [44]. Therefore, the resistance of the SC is significantly higher than that of the underlying layers of the epidermis, resulting in impedance that is closely related to the thickness of the SC [44, 45]. The

electrode-skin interface can be modelled in an electrical scheme, as shown in Figure 2.8 [46, 47]. In this scheme, the hair follicles and sweat glands affect the resistance property, whereas the lipid bilayer determines the capacitance property [44]. The resistance and capacitance of the SC are in the order of 10^5 Ωcm^2 and 30 nF cm^{-2}, respectively [45].

The electrode-skin impedance is often used to evaluate how effective the charges are transferred from the body to the electrode (and vice versa) [46]. Too high impedances will lead to unreliable measurements, as a higher pulse must be given to overcome this impedance. This pulse then does not provide information about the stimulation threshold of the fibers, whereas it will about the impedance of the SC. Therefore, the impedance of the skin should be improved. For instance, wet electrodes with an electrolyte gel minimize the impedance of the skin by hydrating it and forming a conformal electrical contact with its textured surface (Figure 2.8) [45]. Another improvement is skin preparation by cleaning it with alcohol and scrubbing the top layer of the skin [48]. This removes the oily layer and dead skin cells from the SC, decreasing the impedance.

The impedance of the electrode-skin interface can be modelled with an RC model (Figure 2.9). To model this accurately and consider the layered structure, it will give a complex model with several parameters (>20) [44]. And still, this model will not represent the complex skin structure. Lu et al. mentioned as well that the skin could also be modeled with a constant phase element (CPE) instead of a capacitor [44]. This model will take into account the biological characteristics, such as humidity and heterogeneity. The impedance of CPE (Z_{cpe}) is defined as:

$$Z_{cpe}(\omega) = \frac{1}{Q(j\omega)^{\alpha}} \qquad (2.1)$$

with Q and α independent of the frequency. α represents surface heterogeneity and humidity [44, 49] and is a measure of the leak current of the system [50]. If the skin was a perfect insulator, α would be 1 and will act as an ideal capacitor. For increasing humidity of the skin, α will decrease and will act as a non-ideal capacitor, which is characteristic for a CPE [49]. For the human stratum corneum α has a value of ~0.8 [49], whereas for sweaty skin a value of 0.5 is used [44].

For analysis of this model in the time domain, $\alpha \neq 1$ gives difficulties in the inverse Laplace transform of this system since it has no standard form when oriented parallel to another element. Therefore it is complicated to solve, hence only the value of $\alpha = 1$ is used for analysis.

2.4 RESEARCH IMPLICATIONS

The sensitivity of the selectivity of the IES-5 electrode might be improved by combining the thermal and the intra-epidermal stimulation. Therefore, the Thermal-Electrical Stimulation for Specific Activation (ThESSA) electrode is developed. This electrode combines the thermal advantage of specificity and the electrical advantage of well timed, double pulsed and shaped stimulation.

The electrode will be designed and developed following a design cycle, which includes a list of requirements, a morphological map, several concepts, evaluation of the concepts, development of the best concept into a prototype, and testing of the prototype on the specific requirements. This iterative process will continue until a functional electrode is developed, such that it can be tested on several subjects.

For designing the new electrode it is important to keep in mind that there is no clear-cut activation of nociceptors via thermal stimulation: it is not a simple on or off. The activation of nociceptors will gradually increase as interplay of activated keratinocytes and nociceptors. Thus, thermal stimulation will also affect neurogenic vasodilation, which has influence on the temperature of the skin. Furthermore, it is important to understand that the type of electrical conduction (surface or needle) has impact on the transmission to the skin, and thus on the activation of the nociceptors. This will all be kept in mind while the electrode is developed.

3. DESIGN

3.1 ANALYSIS OF THE PROBLEM

3.1.1 PROBLEM DEFINITION

The current assessment method for patients with peripheral neuropathic deficiencies could be improved with a more specific stimulation electrode, as QST is subjected to subjectivity, whereas IES is subjected to a small range of stimulus intensities. Therefore the goal of this design research is to develop an p that is capable of thermo-electric stimulation of the thermal sensitive nociceptors. Usage of this thermo-electric stimulation electrode might also help to gain better insight of the nociceptive pathways, i.e. in more knowledge of the thermo-sensitive activation behaviour of nociceptors. The electrode will be developed for use on the forearm to compare it with previous IES measurements, although it might as well have potential for other body areas as well, such as the feet.

3.1.2 LIST OF REQUIREMENTS

For the development of a thermo-electric intra-epidermal stimulation electrode, some essential requirements have to be set, which are combined in a list of requirements. For clarity, when 'product' is mentioned, it refers to the combined electrode and thermode.

General requirements	
G-1	The product should be able to simultaneously stimulate the skin thermally and electrically. (It is not necessary to start simultaneously)
Functional requirements	
F-1	The electrode should be compatible with TSA2.
F-2	The product should distribute the heat equally over the surface of the skin, with minimal interference of the electrode.
F-3	The warmth of the thermode should be transferred efficiently to the opposite side of the electrode with minimal loss of heat.
F-4	The electrode should only stimulate the skin electrically by the tips of the needles.
F-5	The needles of the electrode should penetrate the skin maximally for 0.2 mm.
F-6	The product can be used by a trained researcher/clinician.
Safety requirements	
S-1	The product should not cause skin damage
S-2	The electrode should be easy to sterilize.

In addition, there are some wishes, but those are not required for approval of the product:

- Electrode should consist of an electrical conducting and an electrical insulating (but thermally conducting) part.
- The electrode should cause minimal discomfort for the patient.
- The stimulation of thermal and electrical pulses (located in time) should be computer controlled.
- The electrode should be easy to move around to overcome habituation
- Low costs for small amounts of the electrode
- Low production time

3.2 SYNTHESIS I

3.2.1 MORPHOLOGICAL MAP

To find a design that fit the requirements, the requirements are translated to several functions of the product, each with its own solutions: a morphological map. From this morphological map, the following concept designs were made: (1)(2) two designs for an etched microneedle electrode, (3) a microneedle array which is already used for other purposes, redesigned for thermo-electrical stimulation and (4) a design of an electrode with embedded needles.

Table 3.1 Morphological map

Function	Solution 1	Solution 2	Solution 3	Solution 4	Solution 5
Thermal conducting base plate compatible with solid thermode	Aluminium base plate ①④	Copper base plate ①④	Silicon ②	Already existing microneedle array ③	
Electrical conducting needles	Hollow etched needles filled with conducting material ②	Stainless steel needles ④③	Etched needles ①		
Electrical insulation of the plate to the skin	Internal insulation via insulated wires	Insulated tape, which can be punctured by the needles ①④	Anodized plate	Use properties of the silicon semiconductor ②	Insulating coating ①③④
Electrical conduction from source to needles	Soldered wires connected to the needles	Fill etched path with conducting material ②	Use conductive properties of the plate ①③④		

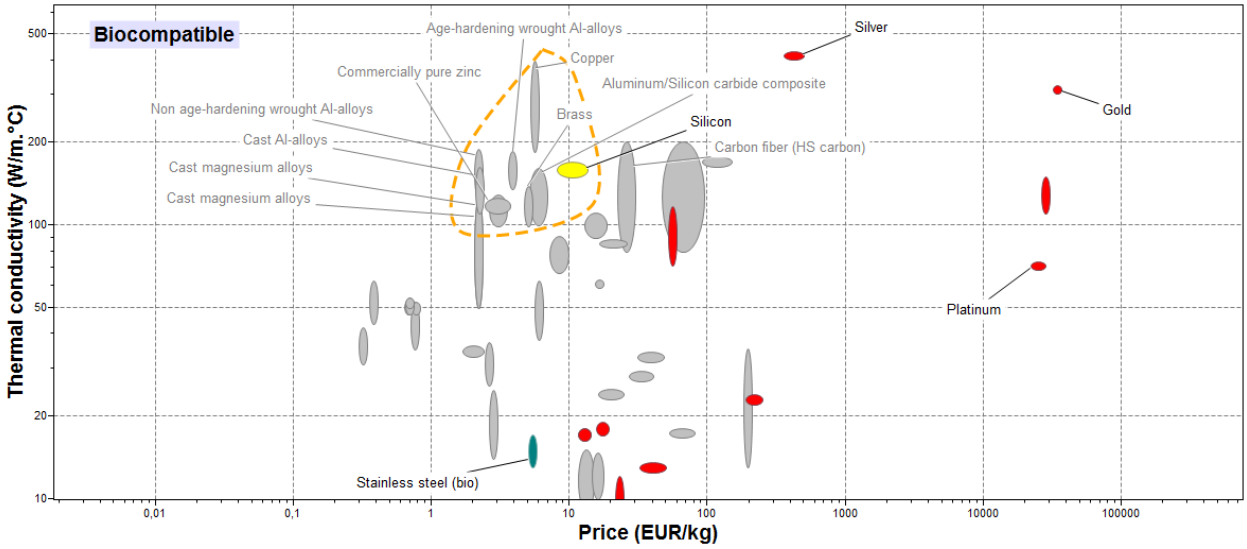

Figure 3.1 Overview of bioengineering materials. Red are metals, yellow are metalloids and green are ferrous metals. All grey materials are not biocompatible. In the orange contour, the materials are located which are favourable for their price/thermal conductivity rate.

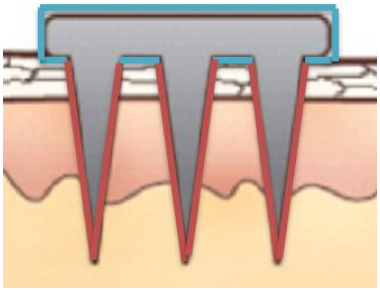

Figure 3.2 The simple etched microneedle design. Grey is the etched solid microneedle, coated with an electrical insulator (blue) and a biocompatible material (red)

Figure 3.3 The etched hollow microneedle design. Dark grey is the silicon wafer, and light grey is the electrical conductive material.

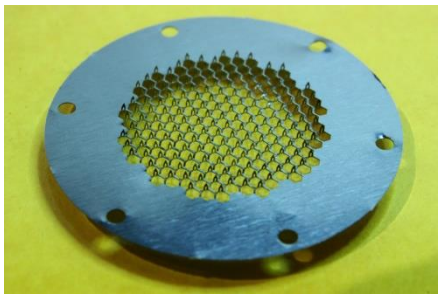

Figure 3.4 The microneedle patch AdminPatch 600 of AdminMed, with neeldes of 500µm. [51]

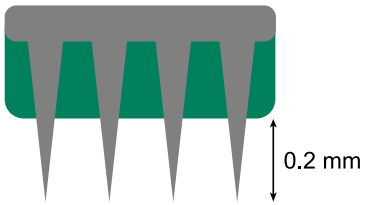

Figure 3.5 Design of an adapted microneedle array. The green layer is used to compensate for the long needles.

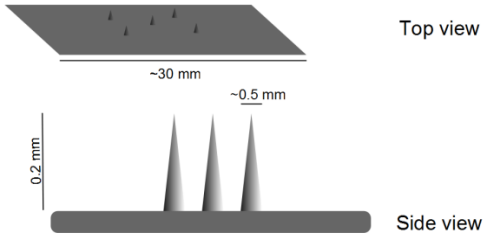

Figure 3.6 Design of an electrode with embedded needles

3.2.2 Concept Design 1: The simple etched microneedle electrode

The first design is based on the etching process and is quite simple in its composition. A solid etched microneedle is made of a good thermal conducting material, for instance copper or aluminium. The choices for these materials are based on the graph in Figure 3.1.

The 'base plate' is coated with an electrical insulator (Figure 3.2). This could be realized with insulating tape or some other insulating coating. The needles are coated with a biocompatible conducting material, for instance silver (Figure 3.2). An alternative to the biocompatible layer is using stainless steel as main material. However, stainless steel has a much lower thermal conductivity.

The production of this electrode is a bit difficult, since the production has to be done by an external company. Additionally, the design has to be developed from scratch, which requires time and collaboration with the company. However, the addition of tape or an insulating coating is a simple manual step. A pre-manufactured microneedle array would improve the feasibility, but comes with certain requirements that have to be met, which is discussed in concept design 3.

3.2.3 Concept Design 2: The etched hollow microneedle electrode

A more advanced design of concept 1 is an etched hollow microneedle array, where the base is made of silicon (Figure 3.3). The needles are filled with an electrical conducting material. The inner diameter for the needles will be approximately 10-100 µm [52]. An appropriate material for the filling (or combination of materials) should be investigated in more detail. For safety, the back side of the electrode should also be covered with an electrical insulating coat.

The production of this electrode is hard. The production can be done at the Nanolab, here at the University of Twente, but it will have a long production time, due to the training necessary for using the clean room. Again, the development of this design has to be done from scratch and research for the electrical conducting material can take some time.

3.2.4 Concept Design 3: Redesign of microneedles array patches

A pre-manufactured microneedle array would improve the feasibility, for instance with microneedles arrays used for the delivery of drugs. These are used for a less painful application and better uptake of the medicine.

For instance, the AdminPatch 600 from AdminMed could be used as basis for the microneedle electrode (Figure 3.4) [51]. This microneedle array has needles of 500µm and is made of stainless steel. Most often these needles aim for the dermis, and not the epidermis. This problem can be overcome by adding a compensation coating on the side where the needles are located, such that the needles get the desired length, as shown in Figure 3.5. The production of this electrode is rather easy, because the needles are pre-manufactured, but the addition of the coating will give it more manual work.

3.2.5 Concept Design 4: Electrode with embedded needles

The fourth design is derived from the IES-5 electrode currently used at BSS (Figure 2.6). In this design, the silicone basis is replaced with a thermal and electrical conducting base plate, such as aluminium or copper (Figure 3.6). The choices for these materials are based on the graph in Figure 3.1. For the embedded needles, a few holes will be made in the plate, such that stainless steel needles can be pinched into those holes. The plate will conduct the electrical current to the needles, but for safety reasons the entire base plate will be covered with an electrically insulating layer. This can be realized with for instance an insulating tape or some other insulating coating. For electrical conduction via the needles, the tips should be left free from insulation. The production process requires a lot of manual work, but will cost most likely less time compared to an etched electrode.

3.2.6 Design selection

To select a design out of the previous concepts, the concepts are assessed for their performance on certain properties that will be important in the development of the electrode. An overview is shown in Table 3.2. Based on the outcome of this analysis, concept design 4 is chosen: an electrode with embedded needles.

Table 3.2 Weighted evaluation of the concepts on a scale of 1 till 5, where 1 is not good and 5 is good.

	Weight (1-5)	**Simple etching (1)**	**Advanced etching (2)**	**Already existing microneedles (3)**	**Electrode with embedded needles (4)**
Mass producible	**1**	5	5	4	1
Easy to produce	**3**	3	2	4	4
Low costs for small amounts	**4**	2	1[a]	3	5
Low costs for high amounts	**1**	4	4[b]	3	5
Low production time	**5**	3	1	4	3
Low chance of health risks	**3**	2 (5)[c]	4[d]	4	5
High thermal conductivity	**3**	5 (2)[c]	5	3	5
High precision of dimensions	**5**	5	5	3	3
Easy to sterilize	**3**	3	4	4	3
Equal heat distribution	**4**	5	4	5	3
Sum of weighted average		**3.63**	**3.25**	**3.72**	**3.75**

[a] Approximately €35.- per unit per 50 pieces (without labor costs)
[b] Approximately €3.50 per unit per 500 pieces (without labor costs)
[c] If stainless steel is used instead of aluminium or copper, no biocompatible layer is needed. This biocompatible layer has the risk of chipping off. However, the thermal conductivity is much lower.
[d] Depending on the electrical conducting material.

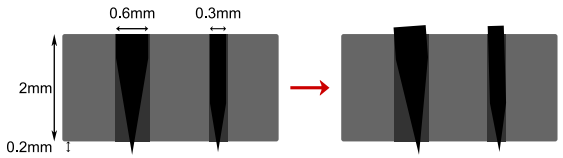

Figure 3.7 With a tick needle, it is more difficult to secure the needle, due to the length of the coned tip

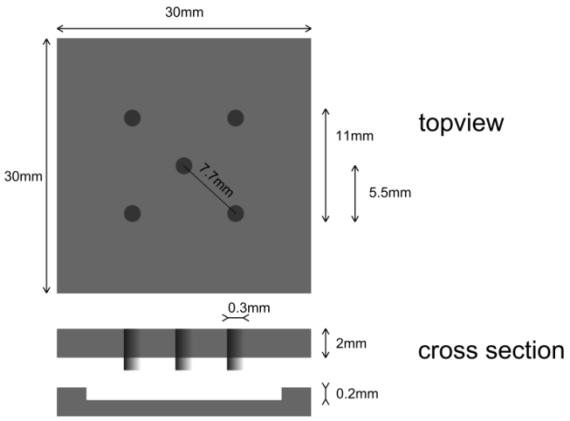

Figure 3.8 Draft of the prototype, measurements of the final prototype are shown.

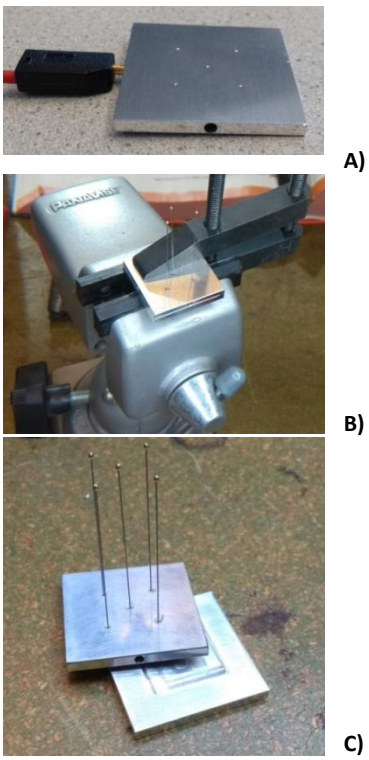

A)

B)

C)

Figure 3.9 Assembly of the needles into the base plate

3.3 Synthesis II: Development of the prototype

Several considerations must be addressed when developing Concept 4. For example, it should be taken into account that aluminium is easier to process than copper, when 0.35 mm holes are required for the needles. Since a simple production process is desired for this design, it convenient to prefer aluminium.

Furthermore, if the needles are clamped into the base plate, the length of the coned tip of the needle should be balanced with the thickness of the base plate. If the base plate is thin, the needles should also be thin, otherwise the coned tip will be too long and cannot be secured into the plate, see Figure 3.7. Currently, stainless steel needles of 0.6mm are used in the IES-5 electrode. The length of the conical shape of these is approximately 2 mm. To have good contact with the plate, the thickness of the plate should at least be ~4mm. It is desired to have a plate as thin as possible, to get the best thermal transmission. Therefore, it is desired to use needles that are as small as possible, but still feasible considering the diameter for drilling the holes.

Additionally, the electrical insulation between the plate and the skin can be realized by applying an insulation tape or an anodized layer to aluminium. Insulation tape is easier to apply than an anodized layer, as the anodization is harder to do and later modifications are difficult to make. Nevertheless, anodized aluminium has a better heat transfer.

Taking these remarks in consideration, the design can be subdivided in the following parts: the material of the base plate, needles, electrical connector and tape selection. Furthermore, it is desired to develop a holder for the electrode, such that it can be secured to the thermode. The base plate and the fixation of the needles were made at the workshop of the Techno Centre for Education and Research at the University of Twente (TCO), the other parts were produced at the lab of BSS.

3.3.1 First prototype

The first developed prototype was produced in fivefold, to prevent for possible production errors. It consists of an aluminium plate of 30x30x2.5mm and has five holes (Ø 0.35mm) for the needles (Figure 3.8 and Figure 3.9). Each side had a hole of 2mm for the connection of the constant-current stimulator AmbuStim via a 2mm banana plug, such that the orientation of the electrode does not matter. This will help also avoids delays in experiments when a pin might break, as there is no need to remove the old pin.

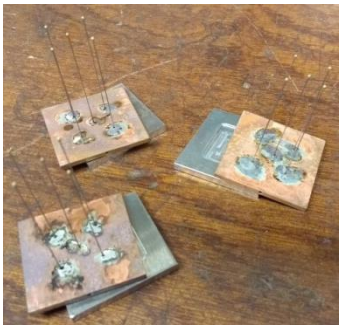
A)


B)

Figure 3.10 Assembly of the second prototype with **A)** the soldered needles, and **B)** the sanded back side.

Table 3.3 Conduction properties of aluminium and copper

	Aluminium	**Copper**
Electrical resistivity (nΩ.m)	26.5	16.7
Thermal conductivity at 300K (W/(mK))	237	401

Furthermore, an aluminium template was created, as the needles can only protrude 0.2mm from the base plate to reach the epidermis. It has a milled section of 0.2mm deep (Figure 3.8 and Figure 3.9C), such that the needles will have the correct length when placed in the baseplate. The needles have a diameter of 0.3mm and were fixated with superglue. Conduction tests revealed that the needles were insulated by the super glue, due to the capillary effect. This means that the adhesion and the surface tension of liquids become more significant in narrow spaces, resulting in suction of glue into space between the needles. Therefore, superglue was replaced with silver glue in an attempt to improve the conductivity. Nevertheless, it led to similar results in conduction.

3.3.2 Second prototype

Failure in conduction led to the change of a copper base plate, as copper adheres well with tin (which will be used for fixation of the needles). Furthermore, copper conducts better (thermal and electrical, see Table 3.3); on the other hand it is harder to process. The thickness of the plate was reduced to 2.0mm to improve thermal contuctance. In addition, the holes of the needles were narrowed to 0.30mm for better contact with the needles (Ø 0.30mm). The banana plug was replaced with a 1 mm pin connector (Han M23 P male-c 1mm, for data sheet, see Appendix B). Only three electrodes of copper were developed this time, as the production process takes more time with a copper base plate and some experience was gained from the previous prototype.

For fixation of the needles, the base plate and template were heated together on a stove, such that a beat of tin could be dropped at the back of the electrode at each needle (Figure 3.10A). This time, the capillary effect resulted in well attached needles and good electrical conduction. Afterwards the needles were shortened and sanded. A detailed description of the production process can be found in Appendix A.1.

A disadvantage of the template is that it allows shorter needles; therefore the three prototypes were tested for equal length of the needles. Only one prototype had equal lengths of the needles, therefore a rejected prototype was used for some of the remaining thermal tests to spare the approved one.

3.3.3 Tape selection

The base plate will be electrical insulated from the skin by insulation tape. TCO provided an electrical insulating tape available with a thickness of 0.063mm (Parmacel P252, see Appendix B for data sheet). The tape was attached to the surface, such that the needles puncture through the tape. For security, the tape around the needles was fastened with help of tweezers and checked under the microscope whether it was secured. The orange insulation tape of Permacel has a dielectric strength of 5500V, indicating that it also must have a low thermal conductivity (not defined in the datasheet), which is not desired. After some thermal tests the Permacel tape was changed to another tape, which conducts the heat better: Tesa 50650 (see Appendix B for data sheet). This tape did not have any specifications for a breakdown voltage; therefore the tape was tested with an insulation resistance tester (megohmmeter).

The megohmmeter showed that it has a breakdown voltage of at least 2500V. As the Tesa 50650 tape could withstand a voltage of 2500V for 8 seconds, it is sufficient to use it safely for its application. The duration of this test is much longer than the intended time, as only pulses in the range of milliseconds will be given. Furthermore, the voltage over the skin and the needle tips before breakdown will be maximally 92V (restricted by the AmbuStim). Therefore it is safe to use this tape for its intended application.

3.3.4 HOLDER

With the thermal conductivity test, it was found that the thermode can easily move over the electrode, which causes insufficient heating over the whole electrode. Therefore, a holder was designed to keep the electrode in place. Furthermore, it will also give insulation on the sides of the electrode, as currently the sides are susceptible to heat loss. The holder was designed such that it could hold the thermode, the electrode and the connection wire. When the attached holder changes orientation by movement of the subject, it could be perceived as stimuli, due to pressure of the sharp corners. Therefore, the corners are rounded off, such that they do not give false perceptions of stimuli.

While designing the holder, the unoccupied holes on the sides of the electrode were used as benchmark for keeping the electrode in place. The first attempt resulted in to large margins (0.5mm), as it was unknown how flexible the material PLA was (datasheet available in Appendix B). A narrower margin of 0.1mm led to really tight placement of the electrode in the holder, therefore the protruding benchmarks were filled off as the electrode should be placed in the holder without too much effort. The electrode is now well clamped by the holder; a technical drawing of the final design is available in Appendix F. A picture of the result is shown in Figure 3.11.

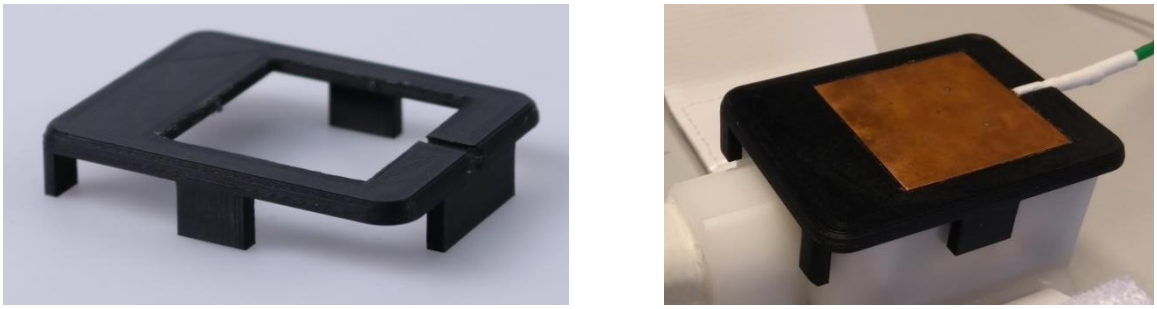

Figure 3.11 The 3D printed holder for the correct placement of the electrode on the thermode.

4. Functionality of the Electrode

In this section the process is described of the development from the idea to the prototype, with all the functional tests. It will address the method, evaluation of the measurements and its results, and some concluding remarks per functionality. The functionalities tested are thermal conduction and electrical impedance. As testing of the functionalities was a stepwise iterative process to optimize the design of the electrode, the results and discussion points will be addressed separately per step.

4.1 Thermal conduction

4.1.1 Method

For the selection of the material of the electrode and the insulation tape, several tests were performed to test the thermal conductivity. First the PT100 temperature sensor was manually calibrated, with help of the thermode, assuming that the thermode was well calibrated. This means that the raw data of the sensor was converted to the same value as administered by the thermode for several values close to the temperature threshold of TRPV1 (43 °C). Next, the thermode was attached to the skin with elastic Velcro and the temperature of the skin was measured by the sensor (Figure 4.1). Several measurements were performed to investigate the thermal conduction of the materials, in combination with the focus on the pressure of the thermode, the placement of the sensors, and the thermoregulation of the skin. An overview of all the experiments and their conditions is provided in Table 4.1.

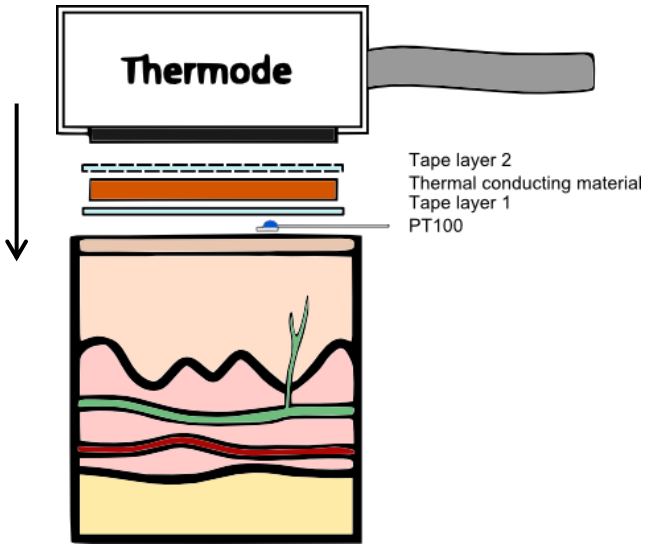

Figure 4.1 Setup of the temperature test method. The temperature sensor (PT100) is orientated towards the skin.

For some of the measurements, a few additional changes were made. In measurement 2, a second layer of Tesa tape was added to the tests (Figure 4.1) in case it was necessary to have insulation between the thermode and the electrode if the thermode was not electrically insulated from the rest of the machine. At measurement 4, it was decided that only one layer was sufficient, as the heat source of the thermode, the anodized aluminium plat, is electrically isolated from the rest of the thermode. Furthermore, the succeeding measurements were performed at least in threefold to get more reliable results, as it is difficult to draw conclusions from one or two measurements. In measurement 5, the tests were performed with four PT100 sensors, which were relocated at the same position in case of several measurements. This time, the sensors were calibrated to a calibration curve. Calibration was done with the thermode and an insulating material to press the sensors to the thermode. The calibration curve and calculation of the temperature can be found in Appendix A.3.

During the measurements, it was learned that the behaviour of the skin to temperature impulses had a major impact on the course of the measured skin temperature. Therefore the time constants were calculated to compare those in a general sense, to get a better idea of this behaviour. The time constant (τ) for increasing quantities is defined as $1 - e^{-1} \approx 0.632$ of its final value, more specifically $\tau = (-T_0 + T_{\max})(1 - e^{-1})$, with T_0 the baseline at which the temperature impulse is given.

Measurements 1 till 4 can only be interpreted dynamically (i.e. on their behaviour), not on their measured temperature, as the temperatures showed an offset, due to manual calibration. It is enough to get insight of the heat distribution behaviour, but not for drawing solid conclusions. For the purpose of these tests, this will be sufficient, and therefore these four tests will not be revised.

Table 4.1 Overview of all the measurements and their conditions. Datasheets of the tapes can be found in the Appendix B.

Measurement	Focus	Conditions
1	Thermal conduction of the base plate	Aluminium (4.0mm)
		Copper (4.0mm)
		Without material (reference)
2	Thermal conduction of the insulation tapes	Aluminium plate (2.5mm)
		Aluminium plate + Permacel insulation tape P252
		Aluminium plate + Tesa 50650 PET tape (one side)
		Aluminium plate + Tesa 50650 PET tape (two sides, see Figure 4.1)
		Without material (reference)
3	Thermal conduction of the insulation tapes with copper	Copper (2.5mm)
		Copper + Tesa 50650 PET tape (one side)
		Copper + Tesa 50650 PET tape (two sides, see Figure 4.1)
		Without material (reference)
4	Influence of pressure on thermal conduction	Copper (2.0mm) + Tesa 50650 PET tape (one side)
		Copper (2.0mm) + Tesa 50650 PET tape (one side) + holder
		Without material (reference)
5, 6, 7	Influence of the location to the thermal sensors (different subjects)	Concept electrode
		Without electrode (reference)

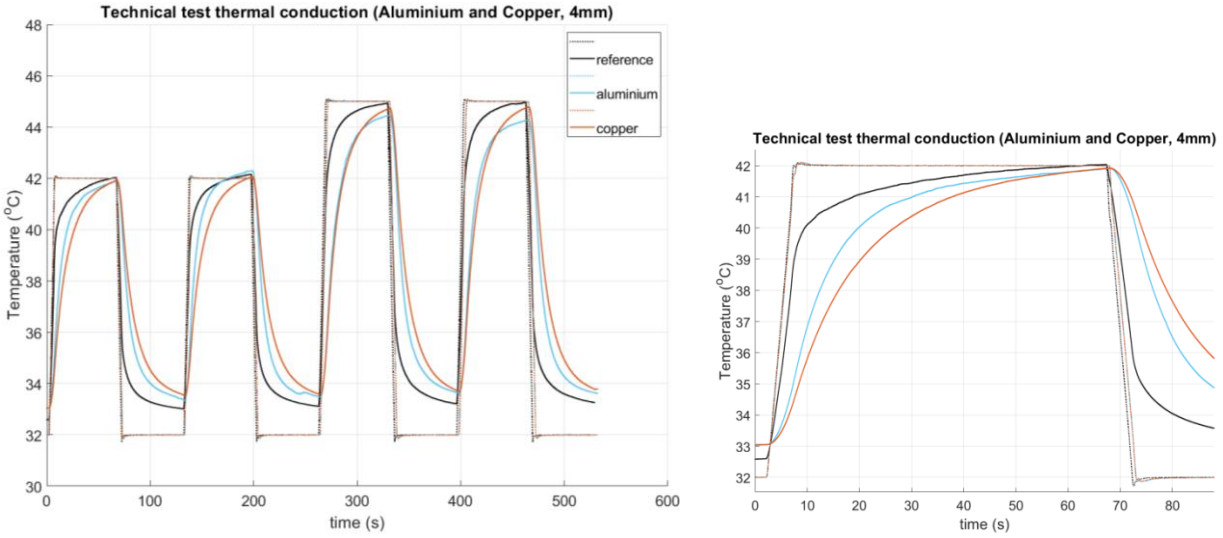

A) **B)**

Figure 4.2 In **A)** the results of the technical test of the materials are shown. The dotted line is the temperature applied by the thermode, whereas the solid lines are the temperatures measured at the skin by a PT100 temperature sensor. The graph in **B)** shows the first temperature pulse of **a)**, where the offset is higher for the PT100 sensor than the applied stimulus by the thermode. For the second pulse this resulted in a measured temperature above the actual temperature of the TSA2.

4.1.2 Functional optimization

Measurement 1: Thermal conduction of the base plate

Results

This measurement investigated which base plate conducts the temperature the best; the aluminium or the copper base plate. The results are presented in Figure 4.2, and show that the reference measurement has the fastest response to the thermal stimulus, followed by aluminium and then copper. Furthermore, copper did not reach its plateau (its steady state temperature) at the end of the two pulses of 45°C. Figure 4.2B shows an offset of 0.5-1°C in the measurements.

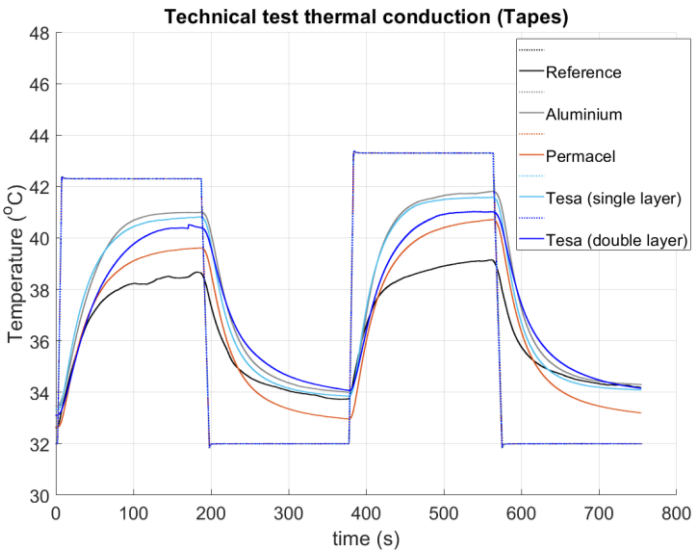

Figure 4.3 This graph shows the temperature measurements of the following conditions: only the skin (reference) (black); skin with addition of an aluminium plate of 4 mm (grey); skin with a Parmacel tape added to the plate (orange); skin with a Tesa tape added to the plate (light blue); or skin with Tesa tape added to the back and front of the plate back (dark blue). It shows some movement artifacts in the first pulse of the Tesa (double layer) and the reference measurement. Note that the reference measurement reaches only the lowest temperatures.

Discussion

The steepness of the curves indicates that the aluminium plate has better thermal conduction, as the slope is steeper than the slope of the copper plate. However, based on their thermal conductivity (Table 3.3), it was expected that the copper plate would conduct the fastest. When this is considered in combination with better feasibility options for aluminium, the aluminium base plate is preferred over copper.

Measurement 2: Thermal conduction of the insulation tapes

Results

This measurement investigated which insulation tape conducts the temperature the best: single layer Tesa tape, double layer Tesa tape or Permacel tape. The results are depictured in Figure 4.3 and show that the reference measurement reaches a lower plateau than the measurements with materials in between. Similar remarkable results are seen for the double layer Tesa tape, as it has a higher plateau than the single layered Permacel tape. When focussing on the slope, it can be seen that the reference curve is steeper in the beginning, compared to the others. Furthermore, the slope of the single layered Permacel tape is steeper than the double layer Tesa tape.

Discussion

It is remarkable that the reference measurement has a lower plateau than the other measurements in Figure 4.3, as there is no other material in between to delay or damp the temperature response. This would indicate that addition of any tested material will improve thermal conduction. However, the steeper reference curve in the beginning is contradictory to this. A steeper curve would suggest a faster response to the thermal pulse, and thus better thermal conduction when no material is in between the thermode and the skin. Further research is needed to find an explanation for this behaviour.

For this measurement, it was expected that the tapes will reduce the thermal conduction, the Permacel more than the Tesa tape because of the difference in thickness, which is 0.063mm and 0.055mm respectively. The results indicate indeed that the Tesa tape affects the thermal conduction less than Permacel; it is even very close to the aluminium curve. Unexpectedly, the double layer Tesa tape has a higher plateau than the Permacel tape. Nevertheless, the slope of Permacel is steeper, indicating faster response to a change in temperature. Based on the plateaus, double layer Tesa tape should conduct better than Permacel. Altogether, Tesa tape conducts the temperature the best, when only the single layers are compared. Therefore, Tesa tape will be used for the electrode.

At this moment the base plate was changed to copper for feasibility reasons, which means that new measurement should be performed, with the same focus as with this measurement. During the next measurement, the focus will be on the exact performance of the measurement, such that an explanation for the unexpected behaviour might be found.

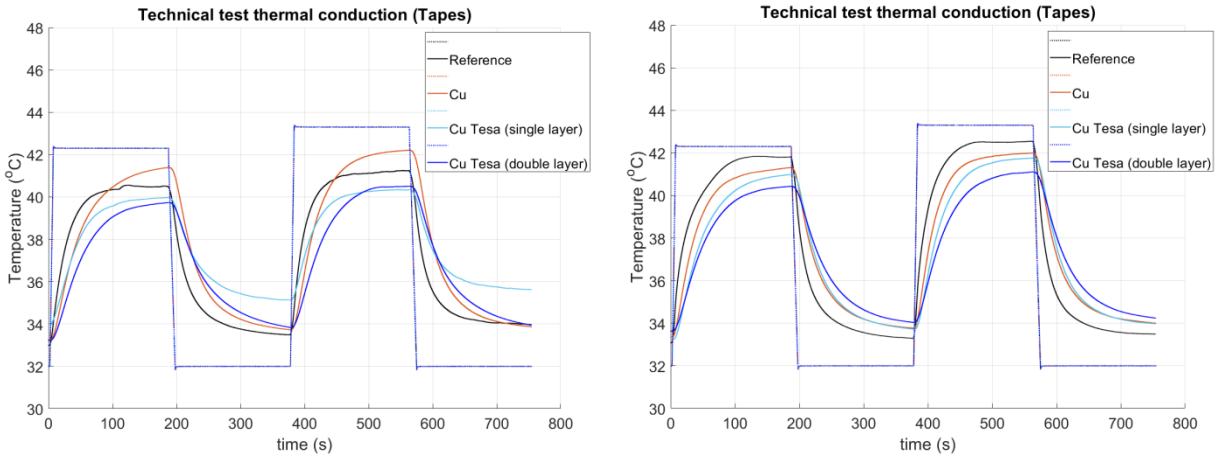

A) **B)**

Figure 4.4 This thermal conduction test with copper shows in **A)** substantially more unexpected behavior, as more graphs cross each other. **B)** shows the results as was initially expected. Nevertheless, both results are valid.

Measurement 3: Thermal conduction of the insulation tapes with copper

Results

This measurement investigated whether the thermal conducting behaviour is the same for the baseplate with Tesa tape, when copper is used instead of aluminium. The results in Figure 4.4A show that copper reaches the highest plateau, followed by the reference measurement, copper with a single layer of Tesa, and lastly copper with a double layer of Tesa. Remarkably, with the second pulse, the last two are switched, resulting in a higher plateau for the double layer, above the single layer. Figure 4.4B shows that the measurement without any material (reference) reaches the highest plateau, followed by copper, copper with a single layer of Tesa tape, and copper with double layered Tesa.

Discussion

The results in Figure 4.4A show an unexpected order for the materials, when compared on the plateaus. The expectation was that the reference curve would have the highest measured temperatures, followed by copper, copper with Tesa tape, and the lowest values for copper with a double layer Tesa tape. This is contrary to the results, without a reasonable cause; failure was suspected, although there was no clear indication for it. Thus, the measurements were executed again, to find an explanation for these results.

The new measurements (Figure 4.4B) provided more reasonable results. However, no clear explanation was found for the previous results. Thus, the question remains open wheter this behaviour can be explained and how it can be regulated better. An explanation for this behaviour could be varying pressure of the thermode on the skin. Therefore, it was decided to mark the Velcro during the next measurements, such that it had the same length, and thus the same pressure on the same location of the same subject. For the purpose of this research this will be sufficient to know whether pressure has influence on the measurements or not. Additionally, the following measurements will be performed in threefold or more for higher reliability.

Measurement 4: Influence of pressure on thermal conduction

Results

This measurement investigated whether the measurements show similar behaviour as before, when pressure of the thermode on the skin is kept constant. The results are given in Figure 4.5 and show that the curves with different conditions still cross each other and are not clustered per condition. The reference curve (solid) has for example a flatter curve, compared to the other two reference curves. This can also be seen with the dotted curve of the concept electrode (Tesa tape with the holder). Equally important is the steepness of the curve. They can be sorted from steep to less steep as ‘Reference’, ‘Tesa (single layer)’, and ‘concept electrode’. Nonetheless, the striped curve of the concept electrode is steeper than the curves with only the Tesa tape.

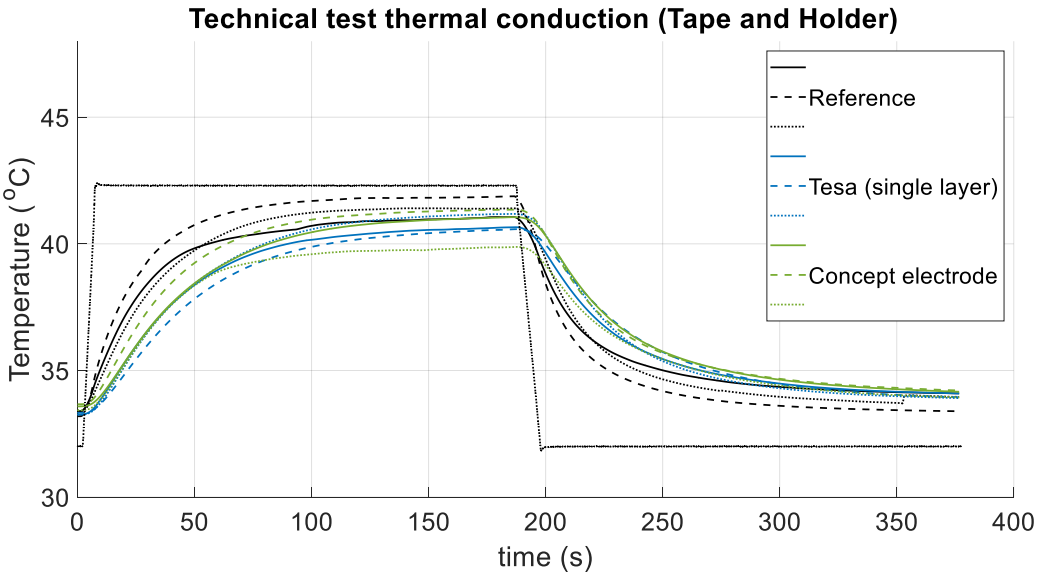

Figure 4.5 Technical measurement of the thermal conduction to the skin with the pressure kept constant. On average, the reference measurement without electrode reaches the highest temperatures, followed by the measurement with the concept electrode (electrode with tape and holder); and the measurement with only the electrode and tape.

Discussion

The results in Figure 4.5 do not show any influence of pressure on the outcome of the measurements, as no change in behaviour is noticed. This contradicts the presumed explanation for the inconsistent outcomes of the previous measurements. Plaghki stated that energy transfer of themodes is not easily controlled as it greatly depends on the pressure of the thermode applied against the skin [2]. Unlike Plaghki, Pavlakovic argues that altering the thermode pressure on the skin does not affect the thermal thresholds [53]. The results seem to support the theory that pressure has no influence on the thermal conduction. Therefore, the focus on pressure was disregarded for the following tests.

A new theory was formulated for the unexpected behaviour of the previous measurements: the location might influence the outcomes. During the previous measurements it was made sure that the sensors were placed on the same location during the measurements with and without the electrode. Nevertheless, when the pictures of the imprints were compared, it became clear that it was not that accurate, although the thermode was placed almost at the same location every measurement (Appendix A.2). Therefore in the next measurement, it should be investigated whether the precise location of the sensor has impact on the outcome of the measurement. This means that the electrode will be tested with four PT100 sensors such that location influence be investigated as well.

At this time it was also learned that the heat source of the thermode, the anodized aluminium plate, is electrically isolated from the rest of the thermode. Therefore, one layer of tape is sufficient for a functional electrode, in respect to electrical interference of the electrode on the thermode.

Intermediate measurement: Calibration of the PT100 sensors

Results

The PT100 sensors were calibrated to a calibration curve, instead of calibrating by hand for the previous measurements. Calibration was done with the thermode and an insulating material to press the sensors to the thermode. The calibration curve and calculation of the temperature can be found in Appendix A.3. The results of the first measurement with the four sensors are shown in Figure 4.6. Here it shows that all the curves are shifted to lower values due to the new calibration. The shift is approximately 1.2 °C at the base line, from ~33.4 °C in Figure 4.5 to ~32.2 °C in Figure 4.6 and 4.7.

Discussion

The shift of the temperature curves in Figure 4.6 and 4.7 cannot directly be translated to a similar shift at the peak values, as the peak values for the temperature are more influenced by thermoregulation of the skin. Furthermore, the calibration curve is an exponential curve (Appendix A.3), although this is minimal. This means that the peaks not only show the slightly exponential shift, but show location dependent temperature damping of the skin as well. This should be taken in to account by interpretation of the results.

Measurement 5: Influence of the location to the thermal sensors (subject C0003)

Results

This measurement investigated whether the location of the sensor had influence on the outcome of the measurement. From the results shown in Figure 4.6 it can be seen that the measured temperature, with and without electrode, is different per location. Remarkable is the change in the shape of the curve for the measurement with the electrode (Figure 4.6B), compared with measurement 4. It shows more damped behaviour than in previous measurements, i.e. the plateau was not yet reached within approximately 100s. Furthermore, it is indicated whether the sensor was close to a vein or not. One of the two sensors located closely to a vein, showed a more damped behaviour for subject C0003.

Discussion

The decreased slopes of the temperature curves in Figure 4.6 are remarkable, compared with the previous measurements; it might be related to bad connection of the electrode to the thermode. This could have resulted in air between the electrode and the thermode, and showed therefore a less good conduction of the temperature. On the other hand, it could also be a subject specific reaction to the temperature increase, as the measurement 5 was performed on a different subject. Therefore the measurement should be performed on another subject as well (same as measurement 4).

Figure 4.6 showed that the sensor close to the vein (sensor 4) has more damping on the plateau compared to the other sensors. This could indicate that the distance to a vein has impact on the measured temperature, although the other sensor close to the vein (sensor 3) measured the highest values for the temperature. Thus, the following measurement is also needed for drawing a more solid conclusion about the influence of the location on the outcome of the measurement.

Measurement 6: Influence of the location to the thermal sensors (subject C00032)

Results

This measurement investigated whether the location of the sensor had influence on the outcome of the measurement, and whether the decreased slope is subject specific (Figure 4.6B). The results in Figure 4.7 show similar behaviour as with measurement 5, including the change of the temperature curve when the electrode was attached. Furthermore, it is indicated whether the sensor was close to a vein or not. This time, both sensors located closely to a vein, showed more damped behaviour.

Discussion

The results in Figure 4.7B do not show any difference for the slope, compared with Figure 4.6B. As the outcome of this measurement and the outcomes of the measurements 1 till 4 (which were all on the same subject), it could be assumed that the abnormality was not subject specific. As the decrease in slope is not subject specific, the problem might originate from the electrode. Therefore, the electrode was closely inspected, to see whether there were any irregularities or that the electrode was incorrect attached. However, no failures were found for the attachment. At the same time it was noticed that the electrode was more oxidized than at the start of the measurements (Appendix A.2). Furthermore, there were no other irregularities found. Therefore, a new measurement was performed with the electrode, free of oxidation.

In relation to the location dependency, the curves of the sensors close to a vein showed more damped behaviour than the sensors that were not close to a vein (Figure 4.7). This supports the theory that the measured temperatures are influenced by vein distance. Thus, that the skin reacts to a temperature pulse, by diluting the blood vessels; the thermoregulation system. Nevertheless, more research is needed to measure the true influence of the distance to a vein.

Measurement 7: Influence of the location to the thermal sensors (subject C00032)

Results

This measurement investigated whether the location of the sensor had influence on the outcome of the measurement, and whether the oxidized electrode had influence on the change of slope in the electrode measurements (Figure 4.6B and 4.7B). The results in Figure 4.8 show that the initial initial temperature of the baseline is not leveled before the measurement started, and a slightly different protocol was used. The target values where in this case 42.3 °C and 43.3 °C instead of 42 °C and 45 °C. Nevertheless, the curves did not reach a plateau around 100 seconds after the pulse started. Furthermore, it was not possible to determine the locations of the veins, as those were not clearly visible through the skin.

Discussion

The results in Figure 4.8B show that there was no improvement for the slope of the temperature curves of the sensors, as no plateau was reached around 100 seconds, nor at the end of the pulse (t=200s) . To get better insight of this behaviour, the past three measurements will be compared to each other on average temperature of the plateau and time constant (Table 4.1 and Figure 4.9). However, measurement 7 was not performed very accurate, due to failed levelling of the temperature of the skin, and usage of a different protocol. For this reason, these results will be given less value compared to the other two measurements in analysis of the results.

Comparison of measurements 5, 6 and 7

Results

The subjects are compared to each other to get better understanding of the deviating behaviour when the electrode is attached to the thermode, during measurements 5, 6 and 7. In Table 4.1, the maximum values per pulse are listed for each measurement (with and without electrode), target temperature (TT) (42.0, 45.0, 42.3, 43.3) and subject (C0003, C00032 (a and b)). Per subject, an average was calculated for each peak without electrode and compared to the corresponding measurement with electrode. Firstly, the table shows that the temperature difference with the TT is at least 3.1 °C and increases as TT increases. Secondly, when the electrode is attached, the minimal difference with the TT is 5.9 °C. Note that the difference per TT with the electrode is relatively constant; for 42.0 °C it is approximately 6.0 °C and for 45 °C it is approximately 7.6 °C. And lastly, when the 'average without electrode' and the 'average with electrode' are compared, it shows differences between 2.3 °C and 3.4 °C.

For further analysis, the time constants were calculated and compared with the time constants corresponding to measurement 4. An overview of the time constants is shown in Figure 4.9. The time constants from the measurements without electrode are lower than the measurements with attached electrode, due to conducting material of the electrode between the sensor and the warmth source. Furthermore, the time constants without concept electrode are similar to the time constants of subject 1 and 2 without ThESSA. When the electrodes are attached, the time constant of the concept electrode is much lower than the time constants with ThESSA. On average, the time constants were twice as high as the concept electrode (82.9 ± 10.1 compared to 40.5 respectively).

Discussion

The average was calculated for each peak in Table 4.1, as this will reduce the impact of location on the skin, i.e. whether the skin's thermoregulation system is more active or not, due to the location of the blood vessels. Reducing the impact of location is important, as comparing the subjects on individual temperatures is not useful, because the true contribution of the vessel to the individual temperature is unknown. It is assumed that the vessels have an equal influence on the average, which will make them comparable.

An increased difference with the TT (e.g. 3.1 °C to 4.2 °C) when TT is increased (e.g. 42.0 °C to 45.0 °C) is reasonable, as these results show the relation with the skin's thermoregulatory system. The higher the temperature administered to the skin, the more the skin is expected to suppres this temperature rise.

The constant difference per TT with the electrode attached is reasonable (e.g. 6.1°C and 5.9°C for TT=42 °C), as it can be explained by the fact that the temperatures measured at the skin are not that high (35.9 °C and 36.1°C), and therefore not that much influenced by thermoregulation via the blood vessels.

The differences between the 'average without electrode' and the 'average with electrode' show values from 2.3°C to 3.4 °C. This could indicate that that temperature submission via the electrode is not very constant.

However, this variance is mostly attributed by the measurements without electrode, i.e. the averages with electrode (35.9 °C, 37.4 °C, 36.1 °C, 37.5 °C) vary less than the averages without electrode (38.9 °C, 40.8 °C, 38.3°C, 40.2°C). Therefore some other explanation must give a reason for these differences.

An explanation might be found when only the measured temperatures of the skin are analyzed. As the temperatures of the tests without electrode are higher than the tests with electrode, evidently the higher temperatures impulses are subjected to more impact of dilution of the blood vessels. This impact depends strongly on the vessel-sensor distance. With an attached electrode, the temperature impulses at the skin are slower, due to slower heat transfer through the electrode. Hence, less regulation of the temperature in the skin is required. Therefore, these measurements depends less on the vessel-sensor distance, and thus attribute less in the variance of the difference in average between an attached or unattached electrode. Altogether, these results do not give clear evidence for the stability of the temperature conduction from the electrode to the skin, although it indicates the high dependence of the temperature regulation system.

Figure 4.9 showed that the time constants of subjects 1 and 2 (with ThESSA attached) were twice as high as the concept electrode. This indicates that indeed something went wrong during measurements 5 to 7, as measurement 4 has similar behaviour to measurement 1 to 3. However, these results do not give a clear indication for a probable cause. Therefore, more research should be done to explain this change in behavior.

Altogether, these results do not give clear evidence for stable temperature conduction from the electrode to the skin, although it does show the high dependence of the thermoregulation system. As to the functionality of the electrode, the results of measurement 5 till 7 show that the electrode does not conduct the temperature as was expected from the first measurements.

4.1.3 Overall Discussion

The first four measurements of the thermal conduction test could not be interpreted on their measured temperature, as the calibration was done by assigning the applied temperature of the thermode to the measured voltage with the PT100. Later on, the sensors were calibrated to a calibration curve. This gave the insight that manual calibration resulted in an offset. Although the results of the first four measurements could therefore only interpreted dynamically, it is sufficient to get insight in the thermoregulatory behaviour of the skin, as the temperatures will still show the thermal differences between the materials. Therefore, these four tests were not revised, as new measurements will not provide substantial new insights that could not be determined by measurement 5 to 7.

Technically, testing the stability of the electrode should only involve the electrode, the thermode and the PT100 sensors. However, without skin it will strongly depend on the surroundings, and these results are not that interesting, since it will always be used in contact with the skin. Therefore, it is necessary to know the influence of the skin on the system (electrode, thermode and sensors). Still it could be valuable to perform a measurement without contact to the skin, such that the results can be compared to each other. Consequently, the true influence of the skin can be better characterized, although the current results give already a clear impression. For further research of thermo-electrical stimulation via the ThESSA electrode, characterization of this system will be important.

Considering the thermoregulation system as possible explanation for the deviating behaviour, the results from previous measurements can be viewed in a different perspective. The deviating results might be dominated by thermoregulation, and thus not show the true behaviour of the materials. Nevertheless, revising the experiments will not change the decisions made for the design.

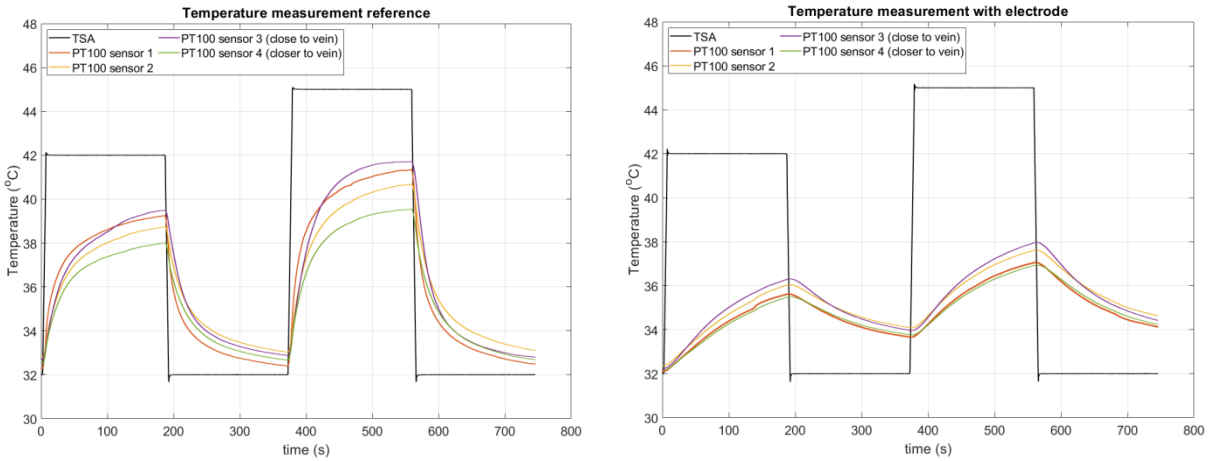

A) B)

Figure 4.6 These graphs show the results of subject C0003 without any electrode (**A**) and with ThESSA (**B**). Note that sensor 3 (purple) and sensor 4 (green) were located closer to a vein, compared to the other two.

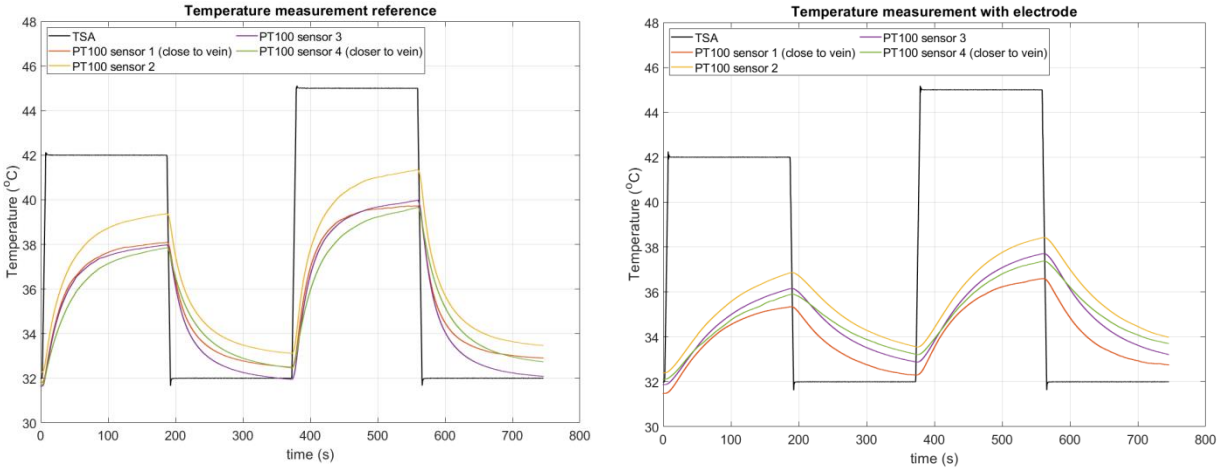

A) B)

Figure 4.7 These graphs show the results of subject C00032 without any electrode (**A**) and with ThESSA (**B**). Note that sensor 1 (orange) and sensor 4 (green) were located closer to a vein, compared to the other two.

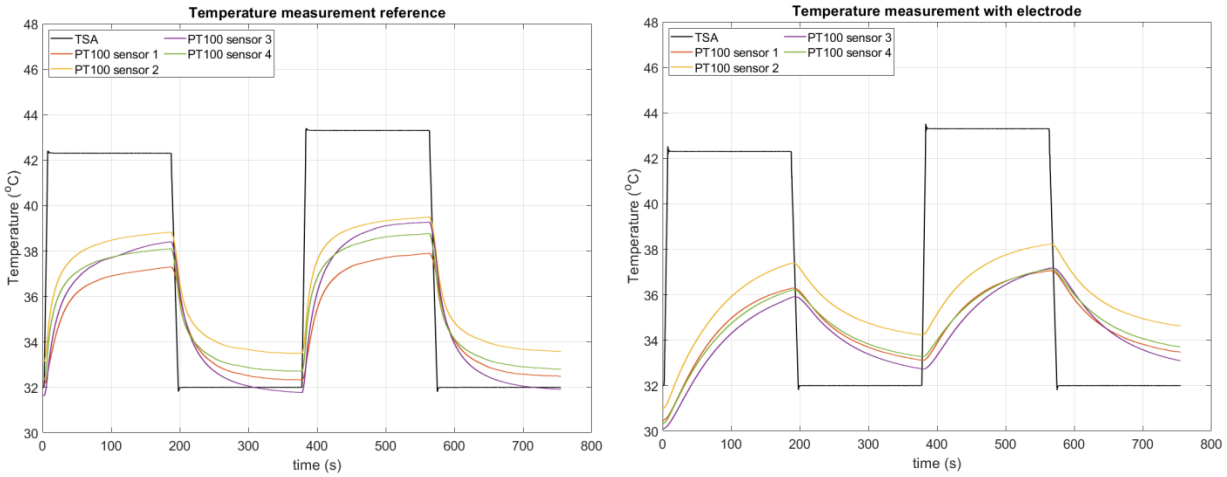

A) B)

Figure 4.8 These graphs show the results of subject C00032 without any electrode (**A**) and with ThESSA after cleaning of the electrode (**B**). There were no clear visual indications of a closely located vein to the sensor.

Table 4.1 Measured peak temperatures of the skin for the measurements of Figure 4.6-4.8. Values in italic are values of a sensor close to a vein.

	Sensor	C0003		C00032a		C00032b	
Target temperature (°C) (TT)		42.0	45.0	42.0	45.0	42.3	43.3
Without electrode (reference)	1	39.3	41.4	*38.1*	*39.7*	37.3	37.9
	2	38.7	40.7	39.4	41.3	38.8	38.8
	3	*39.5*	*41.7*	38.0	40.0	38.4	39.3
	4	*38.0*	*39.6*	*37.9*	*39.7*	38.1	38.8
	Average	**38.9**	**40.8**	**38.3**	**40.2**	**38.2**	**38.7**
	Difference from TT	3.1	4.2	3.7	4.8	4.1	4.6
With electrode	1	35.7	37.1	*35.4*	*36.6*	36.3	37.1
	2	36.1	37.6	36.9	38.4	37.4	38.2
	3	*36.3*	*38.0*	36.2	37.7	35.9	37.2
	4	*35.5*	*36.9*	*35.9*	*37.4*	36.2	37.1
	Average	**35.9**	**37.4**	**36.1**	**37.5**	**36.5**	**37.4**
	Difference from TT	6.1	7.6	5.9	7.5	5.8	5.9
Difference in average		**3.0**	**3.4**	**2.3**	**2.7**	**1.7**	**1.3**

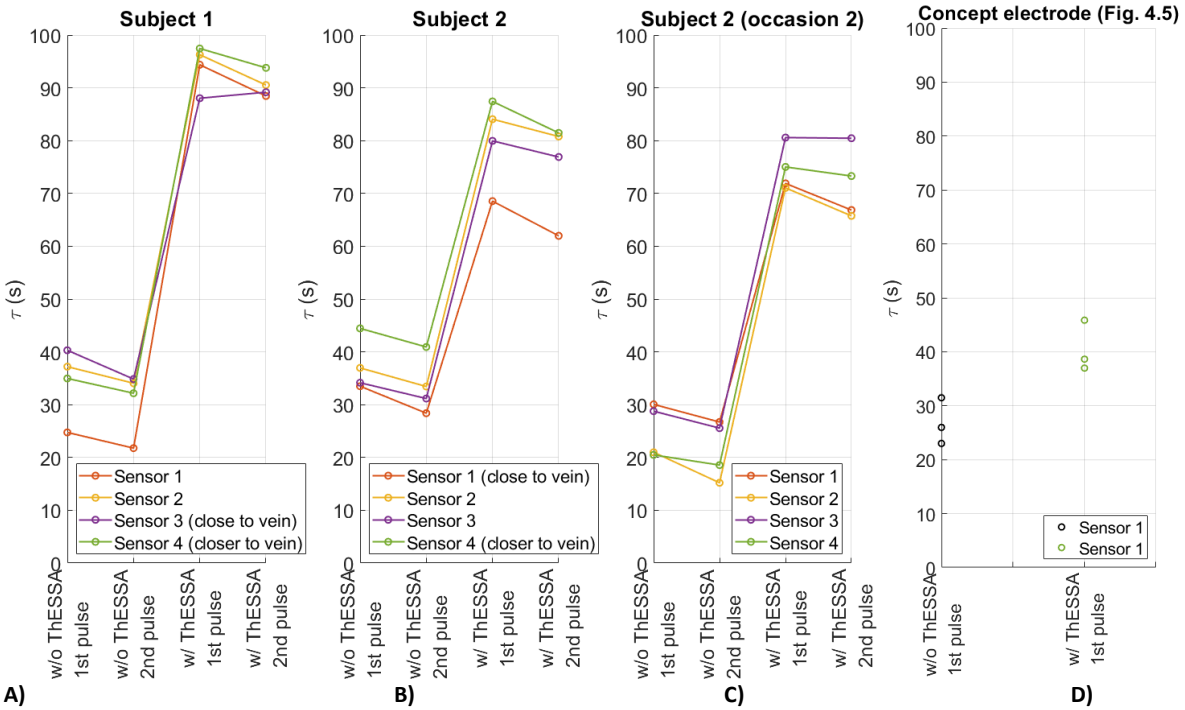

Figure 4.9 Overview of the change in time constant over the different measurements.

4.2 Electrical impedance

4.2.1 Method

Electrical stimulation of the skin will always incorporate some impedance of the skin. As mentioned in the background it is important to know whether stimulation via this electrode might result in (too) high impedances. As well as it helps to reveal any differences in impedance between the IES-5 and the ThESSA electrode, as this might help in explaining contrasting behaviour. Therefore, several impedance measurements were performed to learn how the skin behaves when electrical stimulation is applied. The setup for the impedance measurement is shown in Figure 4.10. During the thermo-electrical stimulation measurements with the subjects, the electrode will be placed at the (right) forearm to compare with other (previous) IES-5 measurements. Hence, the impedance measurements were performed at the same location on the arm. Important characteristics were investigated, such as different temperatures, the influence of the type of ground, and the number of the measurement.

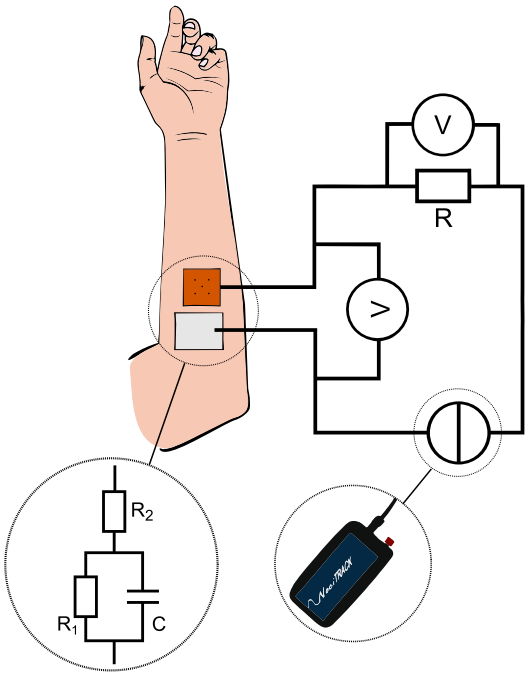

Figure 4.10 Schematical drawing of the setup for the impedance measurements.

Simulation

The skin-electrode impedance model presented in the background (Figure 2.9) was implemented in MATLAB. In this way, the obtained results from the measurements can be compared with some results of the model, which will make it easier to interpret the measured impedances. Given the scheme of Figure 4.10 the impedance Z can be calculated in the following way:

I_s was set with the AmbuStim at 1 mA with a pulse width of 3ms, which can be verified by calculating the current through the resistor of 100 Ω, as the voltage over the resistor is measured. With this, the voltage/current rate can easily be calculated as well:

$$Z = \frac{U_{skin-electrode}}{I_s} \qquad (4.2)$$

The behaviour of U can be modeled with the electrical scheme given in Figure 4.10. Following this scheme, Z can be described as:

$$Z = \frac{R_1}{1+sCR_1} + R_2 \qquad (4.3)$$

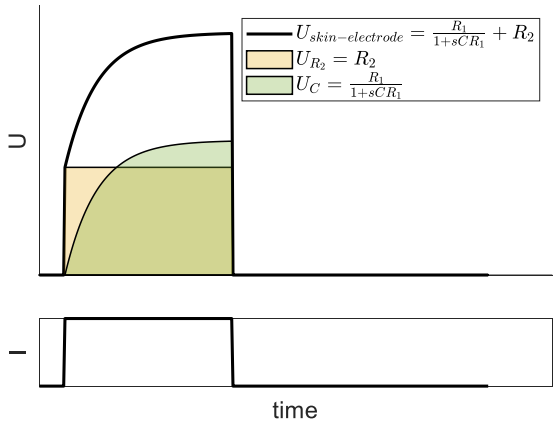

Figure 4.11 The general behaviour for the skin-electrode voltage over time, as well as for the separated terms.

with $s = j\omega$. Combining Eq. 4.2 with 4.3 gives a description for $U_{skin\text{-}electrode}$:

$$U_{skin-electrode} = \left(\frac{R_1}{1+sCR_1} + R_2\right) \cdot I_s \qquad (4.4)$$

The model is only described in a general sense, as it already provides the necessary information for the interpretation of the impedance measurements. The behaviour of this system is shown in Figure 4.11.

Filter

Some pre-processing was needed to get signals that can be interpreted easier. Therefore, a 4th order low pass Butterworth filter was used with a cut off frequency of 0.004 Hz. This was done for all signals.

4.2.2 Evaluation

Number of the pulse

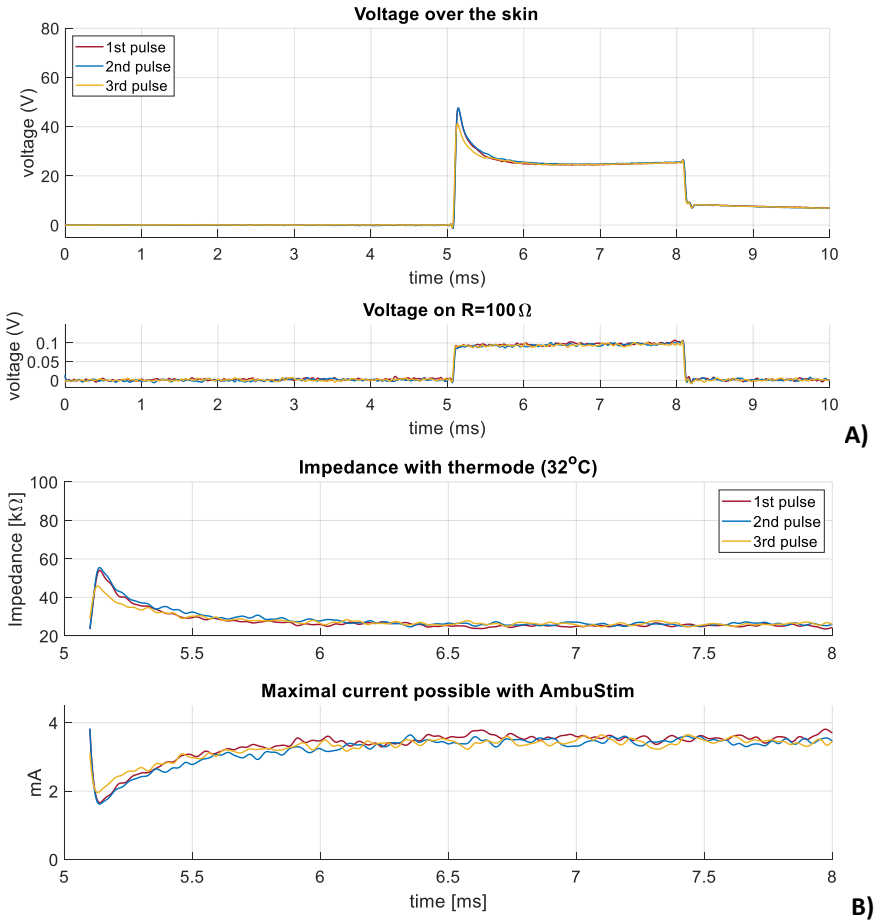

Figure 4.12 In **A)** the measured voltages are shown over the skin (upper graph) and the resistor (lower graph) with the ThESSA electrode at a temperature of 32 °C. **B)** The calculated impedances (upper graph) and its corresponding currents that will be possible (lower graph). These tests depict the distinction between the first, second and third measured pulse.

Figure 4.12 shows the measured voltages (Figure 4.12A) and the calculated impedance with its corresponding current (Figure 4.12B) that could be applied to the skin via the AmbuStim. The first pulse (and sometimes the second as well) shows clearly a higher voltage peak as a response to this electrical impulse. Furthermore, notice that after the pulse, the initial baseline does not returns directly back to the value before the pulse. It gradually returns from 8.2V back to the baseline of zero (not shown).

Figure 4.12 demonstrates that impedance depends on the number of the pulse. The decrease of the impedance could be explained by the fact that current follows the path of the least resistance. Whenever an optimal pathway is found, the next pulse will experience less resistance, as cells migrate slightly under the influence of the electric field, such that conducting paths are created [44, 54]. This phenomenon is also known as electrophoresis.

In the succeeding measurement the decrease of the voltage peak over the skin-electrode interface is visible as well; therefore the number of the pulse will always be presented with it. Often, the third pulse can be read as any higher number of pulse as well, since they do not differ that much as the first two pulses. The inter pulse interval (IPI) is in the order of seconds, although this is not recorded.

THERMODE OFF COMPARED TO THERMODE ON

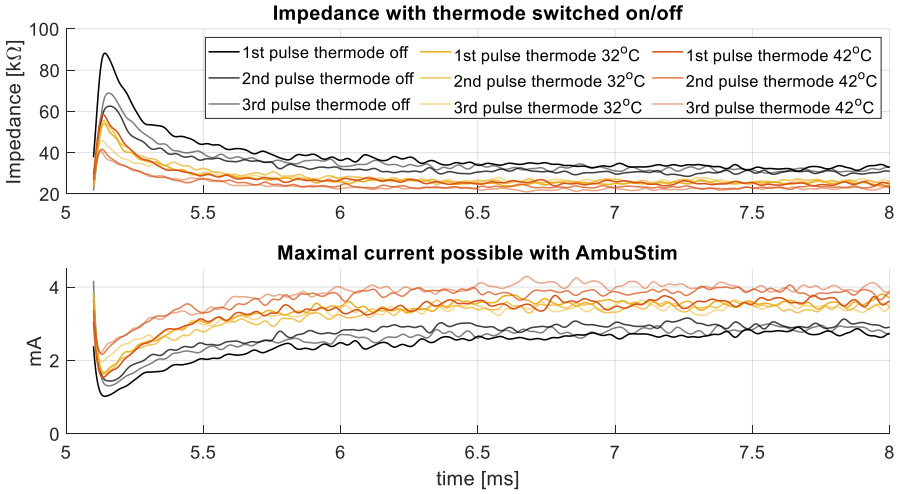

Figure 4.13 This graph shows the calculated impedances (upper graph) and its corresponding currents that will be possible (lower graph) with the ThESSA electrode. In the black shades are the measurements shown with the thermode switched off, in yellow the thermode at a neutral temperature of 32 °C, and in orange at a heated temperature of 42 °C. For every setting, the shade becomes lighter as the number of the pulse increases.

Figure 4.13 shows the impedances and currents of three conditions: with the thermode switched off; the thermode in its neutral setting of 32 °C (the same as the skin temperature); and with heat applied of 42 °C. The measured voltages can be found in Appendix A.4. Figure 4.13 shows that the first pulse always has higher impedance compared to the following pulses, as mentioned before. Furthermore, the impedance decreases as the temperature increased. Notice that these differences continue as they reach steady state. At the end of the warmed pulses, it shows similar impedances, whereas the 'switched off' pulses show ~8 kΩ higher values, which correlates with ~1mA lower amplitude for the current.

The results in Figure 4.12 showed that the number of the pulse matters in the resulting impedance of the skin. In Figure 4.13 it shows behavior that is that is even more extreme, as an increase in temperature decreases the impedance. This can be explained by the thermodynamic behaviour, as an increase in temperature causes an increase in entropic forces. Therefore, pathways can be formed easier under the influence of a higher temperature.

It could be argued that the impedance decreased because the measurements were performed in the order of 'switched off' to 'neutral' to 'heated'. However, the electrode was every time replaced, such that it had to overcome this initial impedance again. Therefore it is presumed that the order of the type of measurement does not have impact on the outcome.

THESSA COMPARED TO IES-5

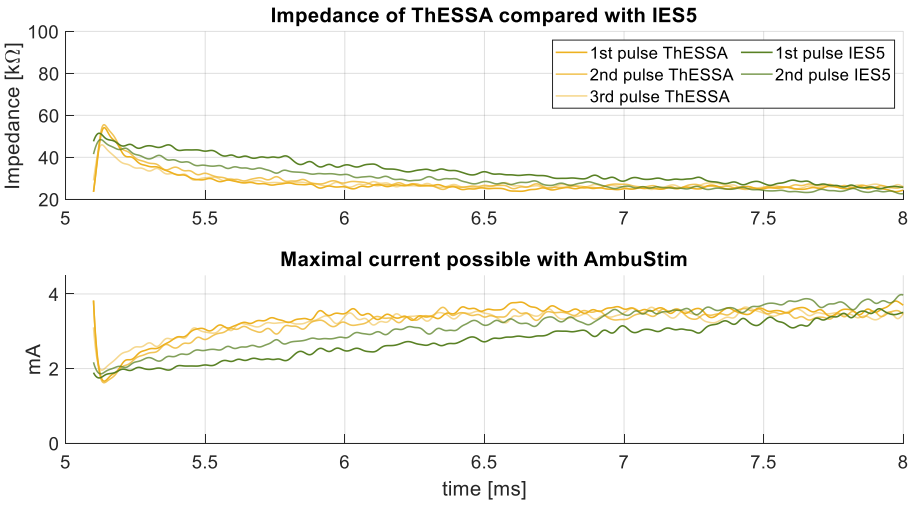

Figure 4.14 Comparison of ThESSA and the IES-5 electrode for the impedance and its corresponding current. The temperature of ThESSA was set to 32 °C.

This measurement compared ThESSA (at 32 °C) to the IES-5 electrode. Figure 4.14 shows that the peaks of the IES-5 electrode are a bit lower than ThESSA. On the other hand, ThESSA decreases faster to its steady state compared to IES-5.

The difference in decrease is interesting, as the IES-5 impedance is almost linear, although it looks still slightly exponential. It might have to do with certain dynamics in the electrode-skin interaction. If the first part could be explained by establishing the conducting path, the second part should relate to maintaining this path. At the same time, the skin dynamics are not changed, other than the temperature. However, ThESSA shows the same dynamics when the thermode is switched off. Therefore the temperature could not be the reason for this behavior. Thus it might be related to the design of the electrode.

ThESSA with an Ag/AgCl ground electrode

Figure 4.15 compares the standard ground to the Ag/AgCl ground, both with ThESSA as counter electrode. The response with the Ag/AgCl electrode does not show the large peak at the start of the pulse for both temperature conditions. However, the voltage (Figure 4.15A, upper graph) and impedance (Figure 4.15B, upper graph) show evidently higher values compared to the standard ground electrode. Remarkable are the decreased values for the voltage and the impedance after the temperature increase; both grounds show similar decreased responses in combination with the ThESSA electrode. Furthermore, Figure 4.15A shows that the Ag/AgCl electrode returns slower to the (temporally increased) baseline after the pulse.

In relation to the number of the pulse (Figure 4.12) and comparing the grounds (Figure 4.15) some additional measurements were performed to show more explicit the impact of the number of the pulse (Figure 4.16). The 0^{th} measurement was an initial test to check whether the setting is working. For completeness, it is also included in the figure. In contrast to Figure 4.15, the new tests show actually that it does have an initial peak at the beginning of the pulse. However, it is not clearly visible anymore for the third pulse and higher numbers of pulse, as mentioned before.

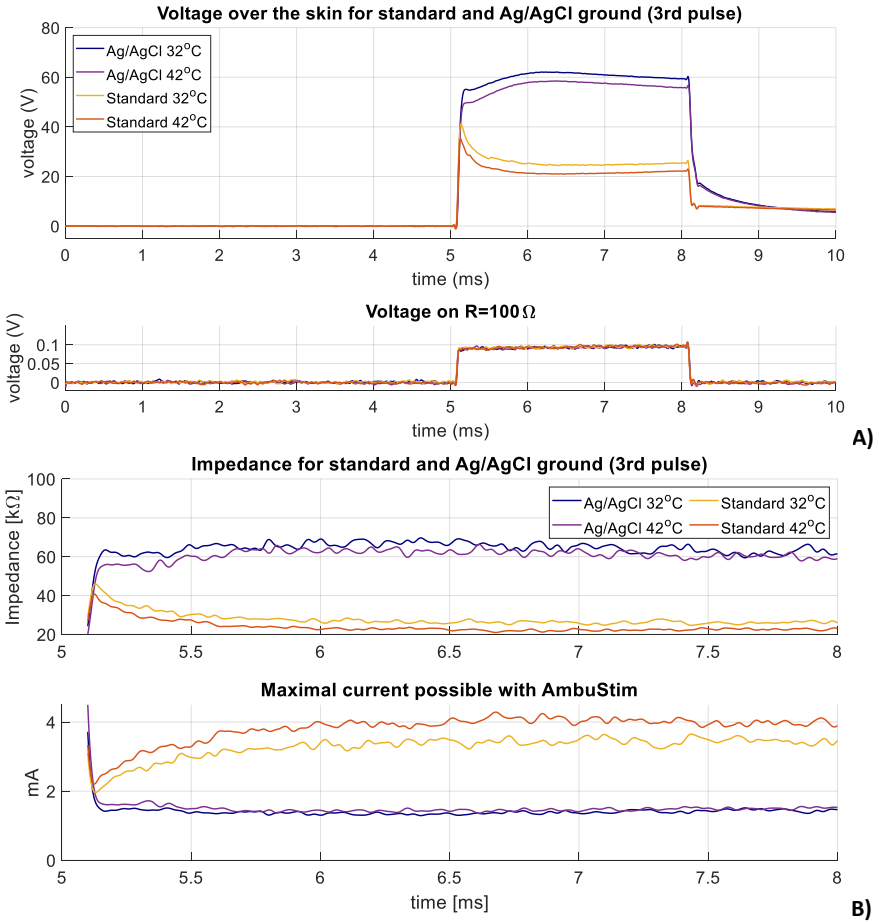

Figure 4.15 The comparison of two grounds (standard and Ag/AgCL) in combination with ThESSA. **A)** The Ag/AgCl electrode does not have a large peak in the beginning of the pulse (upper graph), and the characteristic shape stays constant when the temperature is adjusted. It is only shifted down when the temperature is increased for the voltage and the impedance (**B**). Similar behavior for the impedance can be seen for the standard ground in relation to a change in temperature.

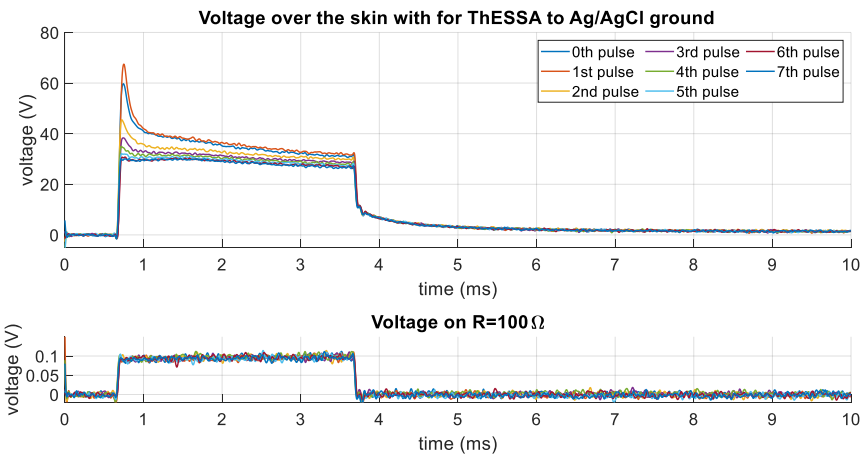

Figure 4.16 A train of pulses for the ThESSA to AgAg/Cl setup, with an interpulse interval in the order of seconds. It shows the decrease of the initial peak at the beginning of the pulse, when the number increases.

CONTRIBUTION OF AG/AGCL OR STANDARD GROUND ELECTRODE TO THE TOTAL IMPEDANCE

For measuring the impedance over the skin-electrode interface, it always shows the behaviour of two electrodes: ThESSA and the ground electrode. Therefore, it is important to know how two similar electrodes behave. As only one single ThESSA electrode can be tested due to absence of a second thermode (and electrode), the ground electrodes should be paired. This will show the contribution of the ground electrodes to the ThESSA-skin-ground impedance.

Figure 4.17A shows the measured voltage over the Ag/AgCl-skin interface, while Figure 4.17B shows it for the standard ground-skin interface. For both ground electrodes there is no initial peak, and it does not matter which number the pulse has. Furthermore, it shows some capacitive behaviour, the Ag/AgCl electrode more than the standard ground. In addition, the Ag/AgCl electrode reaches values of ~22.0 V, whereas the standard ground, only reaches ~10.5 V

This shows that the contribution of the Ag/AgCl electrode is at least twice as large as the standard ground. Hence, the differences in steady state in Figure 4.15 can be explained as well. Further on, it will be discussed with the computational model as well.

The missing peak might be explained by the difference in conducting surface. The needle electrodes have a conducting surface of ~0.1mm^2, whereas a surface electrode has a conducting surface of approximately 1cm^2 or more. This makes that the starting (or ending) point of the conducting path with a needle electrode is already set, while with a surface electrode the point can be anywhere of this surface. This means that when a needle electrode is used, a potential is built up before a conducting path is established, until it is high enough that a conducting path is formed and the potential decreases. The next pulse can take the same path, as it will have less resistance, which explains the decrease of the peak as the number of the pulse increases.

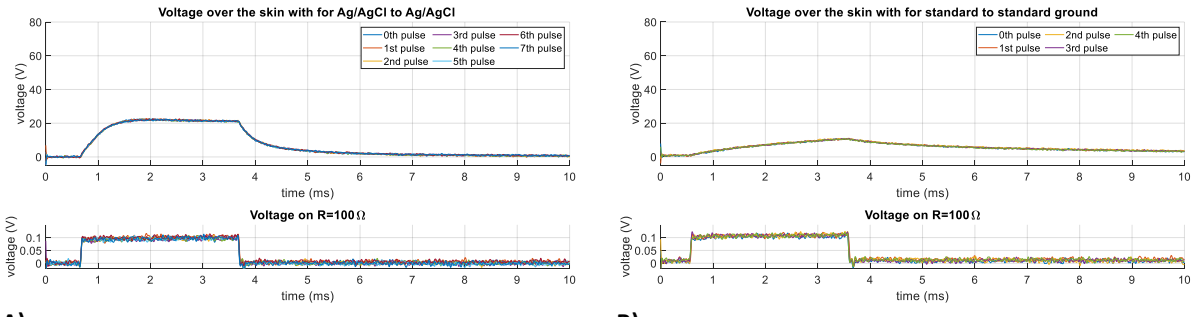

A) **B)**

Figure 4.17 Contribution of the ground electrodes to the ThESSA-skin-ground voltage. **A)** The voltage over two Ag/AgCl electrodes. **B)** The voltage over two standard electrodes.

COMPUTATIONAL MODEL

The shown impedance results do not agree with the model proposed in literature; see Section 2.3.3. This is clearly visible when the general behaviour shown in Figure 4.11 is compared with the obtained results from the measurements. As mentioned in the analysis of the ground electrodes, is there a difference in conducting surface (~0.1mm^2 for ThESSA, compared with >1cm^2 for a gound electrode), which argues for a different schematic electrical representation for needle electrodes.

R_2 represents the electrical transfer from electrode to skin, therefore it is highly expected that R_2 does not behave as a normal resistor, as R_1 and C_1 represent the conduction within the skin, which is still the same. This means that the contribution of the R_2 term will be different than a normal resistor (Figure 4.18A, R_2 is replaced with R_2^*), it would probably behave as shown in Figure 4.18B. The step response for R_2^* has now some exponential component in it, which provides a similar response as e.g. in Figure 4.15. Even if the contribution of R_2^* is slightly adjusted, it will show behaviour comparable to the ThESSA-Ag/AgCl response (Figure 4.18C).

Although both contributions show already some similarities with the measured results, proper research and fitting should be done to get better insight in the actual dynamics of the system. Due to time limitations, this could not be done yet. Still, the expected contribution of R_2^* will help to interpret the obtained results from the impedance measurements.

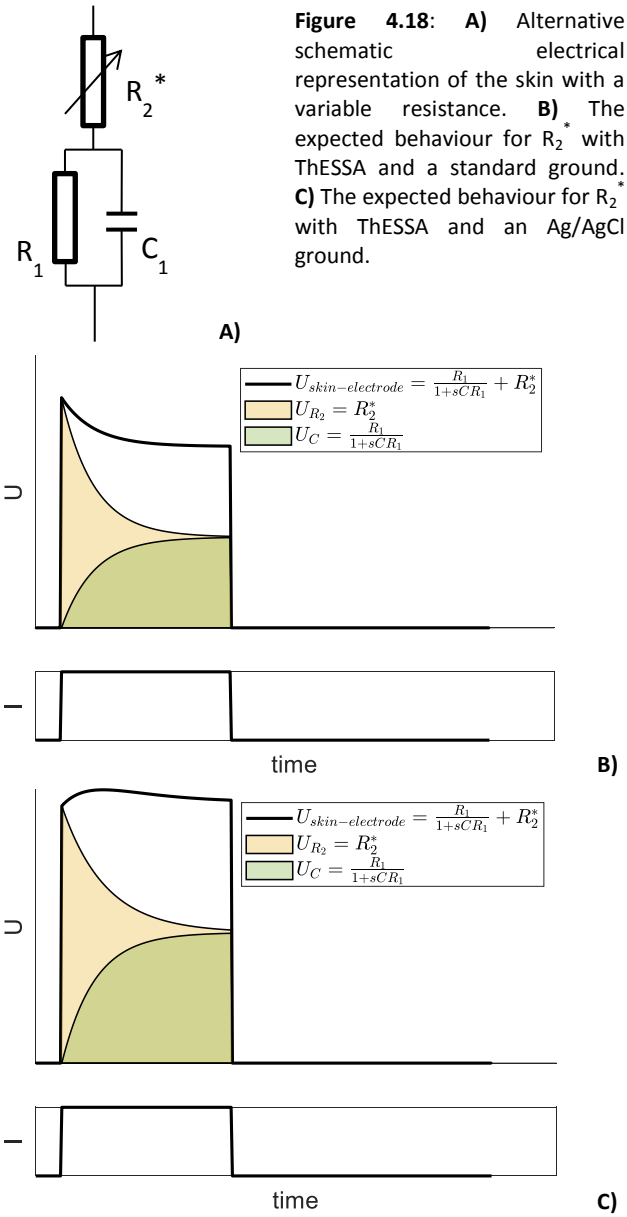

Figure 4.18: **A)** Alternative schematic electrical representation of the skin with a variable resistance. **B)** The expected behaviour for R_2^* with ThESSA and a standard ground. **C)** The expected behaviour for R_2^* with ThESSA and an Ag/AgCl ground.

4.2.3 CONCLUDING SUMMARY

From previous results, some important remarks can be made. Firstly, application of warm temperatures shows better electrical conduction in the skin. Secondly, needle electrodes have to overcome some initial resistance, before a conducting path can be formed, which cannot be represented by a normal resistor as proposed in common models. And lastly, the Ag/AgCl electrode has a contribution twice as large to the total impedance, compared with the standard ground. Therefore, the standard ground was chosen for the measurements with ThESSA.

Furthermore, these results show that ThESSA is functional whenever the current of the pulse stays below 1.6 mA for the first pulse. For later pulses, this value will increase (up to ~2 mA) as the impedance decreases with a higher number of the pulse (Figure 4.13). Since the amplitude of the pulse increases during the thermal-electrical stimulation measurement, ThESSA is functional as long as the amplitude stays under ~2 mA.

5. PSYCHOPHYSICAL EXPLORATION

As the functionality of the ThESSA is approved in terms of thermal and electrical conduction, the focus of the research will now continue on the functionality in terms of detection rate, stimulation amplitude and perception of the stimuli. This will be done in an explorative manner, such that a first insight can be obtained about the effect of thermal electrical stimulation (TES) on the nociceptive detection thresholds (NDT's). Thermal stimulation will be compared on two different temperatures: the average skin temperature (32 °C, also referred to as 'normal') and the heat pain detection threshold (HPDT) of the subject. As ThESSA is subjected to some heat loss, the skin will never reach this (painful) temperature (Section 4.1), which will help as well to stimulate just below the threshold of heat sensitive nociceptors (Section 2.4).

5.1 METHOD

5.1.1 SUBJECTS

After approval of the Ethics Committee of Natural Sciences and Engineering Sciences at the University of Twente, six healthy participants were enrolled after providing written informed consent. Three of the participants were male, three were female. The average age was 22.8 ± 2.9 years (range 19-26), and all except one have a dominant right hand. Exclusion criteria were skin problems at the site of the pain sensitivity measurement; diabetes; implanted stimulation device; pregnancy; pain complaints at the time of the experiment; a medical history of chronic pain; use of analgesics, drugs or excessive alcohol within 24 hours before the experiment; or an average heat pain detection threshold (HPDT) of more than 47°C. Participants received a small compensation for participation and could withdraw at any time for any reason.

5.1.2 STUDY DESIGN

The TES measurement consists of four blocks of NDT tasks, of which the second or third task includes thermal stimulation, in line with a cross over study design (Table 5.1). Assigning the programme to a subject was done via blocked randomisation with blocks of two. The subjects were blinded, to prevent for bias. In between each task, the subjects were asked some questions about the perceived stimuli. Prior to the TES measurement a preparatory HPDT test is performed. The outcome is used as input for the heated NDT (H-NDT) task. An overview of the study setup is provided in Figure 5.1.

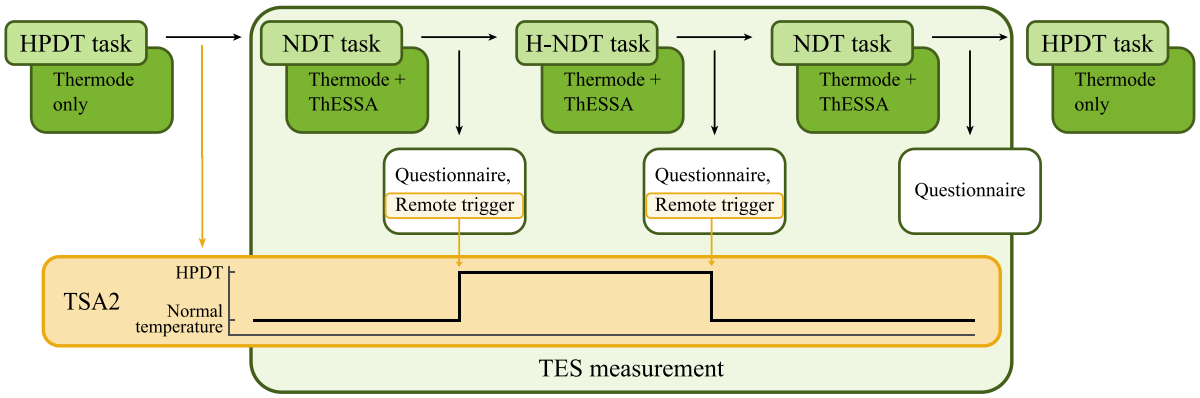

Figure 5.1 Flow of the sub-measurements. For simplicity, randomisation of the blocks is not shown; instead only one heated block is included in the diagram.

Table 5.1 Session options for the thermal electrical stimulation measurement

Session A	**Session B**
NDT task	NDT task
H-NDT task	NDT task
NDT task	H-NDT task
NDT task	NDT task

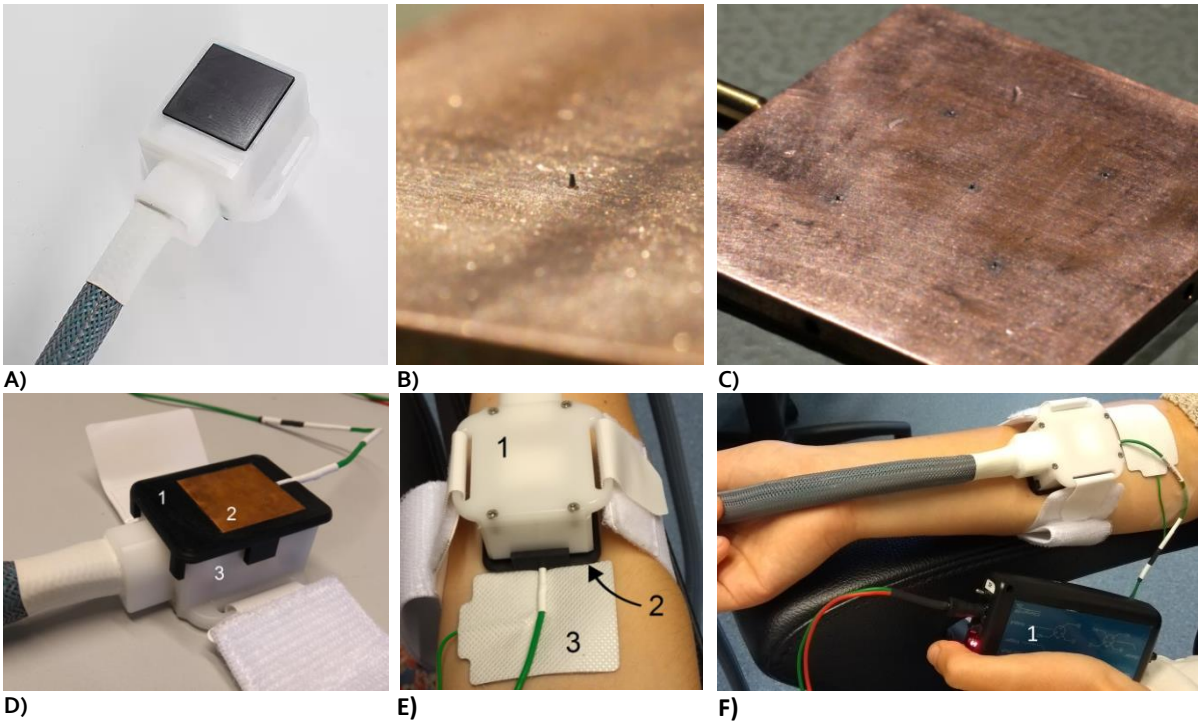

Figure 5.2 A) The 30x30 mm thermode used for heat application. Reproduced from Medoc [38] **B)** Close-up of the needle of the ThESSA electrode. **C)** The ThESSA electrode for thermo-electrical stimulation of the skin. The needles are 0.2 mm long and are spaced 7 mm apart. The surface is 30x30 mm. **E-F)** The ThESSA electrode attachment. In **(D)**, the black holder (1) with the electrode (2) is attached to the thermode (3). **(E)** Attachment of the thermode (1), with the ThESSA electrode (2), and the ground electrode (3) to the forearm. **(F)**This gives the overview of the setup, together with the AmbuStim (1)

5.1.3 Materials

Firstly, the TSA2 (Medoc, CE-certified) is used for application of heat to the skin. The thermal protocols were designed in the software supplied with the TSA2: the Medoc Main Station (MMS). Running the protocols was performed via external control in MATLAB (R2020a), meaning that the start, stop and order of the protocols were controlled via a MATLAB script, as well as the data collection. This script is also used to switch between all the different thermal protocols in the right order. The heat application for the thermal NDT task can be activated manually via a trigger button connected to the TSA2. The script used for these experiments can be found in Appendix E. Furthermore, the temperature of the skin is measured with four PT100 temperature sensors (datasheet can be found in Appendix B) which are processed with Porti7 (TMSi) and the corresponding software programme Polybench (Polybench Designer 1.34.1).

Next, the AmbuStim is used for the electrical stimulation. This is a handheld, constant-current stimulator, which is developed and tested by the research group BSS. This device is commonly used in the electrical stimulation studies at BSS. It is connected to the computer via Bluetooth to overcome electrical interference. It is controlled via a programme in LabView (2014 SP1) that applies the nociceptive detection threshold (NDT) tracking protocol, as described in the background section. Before the start of this study, the AmbuStim (device 015; backup device 011) was calibrated following the standard protocol; details of the calibration can be found in Appendix G.

Lastly, the ThESSA electrode is used for combined thermal and electrical stimulation. To optimize the thermal conduction and the alignment to the thermode, ThESSA is placed in a 3D-printed holder, which is placed on the top of the thermode (Figure 5.2D). With the elastic Velcro of the thermode, the whole product can be attached to the forearm of the participant (Figure 5.2E-F). ThESSA should be used in combination with a ground electrode (Figure 5.2E (3)); for this study the disposable adhesive ground electrode (40x50 mm) of Technomed is used. Before usage, ThESSA was subjected to a risk analysis, which can be found in Appendix D.

5.1.4 Stimuli

Thermal stimulus

The settings for the thermal stimuli in the HPDT test are as follows: the base line is set at skin temperature (32°C), and will increase with 0.5°C/s. The subject is instructed to press the button whenever the heat became "uncomfortable, unpleasant and/or painful". After the button is pressed by the subject, the temperature will immediately decrease with 8.0°C/s back to the baseline. After several seconds a new stimulus will start, and the same procedure will follow, until six stimuli were applied. The first thermal stimulus is for familiarisation, whereas the following five stimuli will be used for an average HPDT, which will be used later on. An example of the results of this protocol is shown in Figure 5.3.

For the TES measurement, a protocol was designed to apply a thermal stimulus in the second or third task via a remote trigger, such that it is independent of time. Detailed settings for the TSA2 protocol can be found in Appendix E, and an overview of a temperature protocol is provided in Figure 2.5. The details about the programmed activation of the heated task can be found in the MATLAB script, provided in Appendix E.

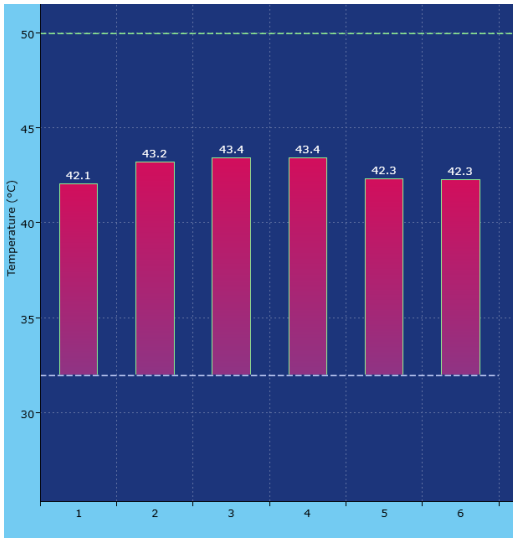

Figure 5.3 Example of the HPDT protocol in MMS. The baseline is shown as a white dotted line, whereas the heat limit is a green dotted line. The bar shows the temperature at which the subject stopped the thermal stimulus.

Electrical stimulus

The procedure for electrical stimulation starts with a normal staircase procedure, followed by an adaptive staircase procedure. The normal staircase procedure is performed tree times: one for familiarization, one for determination of the initial detection threshold for the single pulse (SP), and one for the double pulse (DP). The adapted staircase procedure will start with this initial threshold, and will continue from there.

The normal staircase procedure increases the stimulus by 0.025mA every stimulus, until it is felt by the subject. The adaptive staircase uses a set of five values for the amplitude, whereof one amplitude will be selected randomly. When a stimulus is detected, the following set will be decreased by 0.025 mA, whereas it will be increased by 0.025 mA when it is not detected. More specifications about the stimuli can be found in Table 5.2. The stimuli will be provided to the subject in blocked randomisation, such that every type of stimulus is applied the same number of times.

Table 5.2 Settings for the NDT tracking method

	Single pulse (SP)	Double pulse (DP)
Number of stimuli per block	80	80
Number of pulses (NoP)	1	2
Pulse width	0.21 ms	0.21 ms
Inter pulse interval (IPI)	-	10 ms
Vector size	5	5
Step size (within the vector)	0.025 mA	0.025 mA
Increase/decrease step	0.025 mA	0.025 mA

5.1.5 Procedure

As preparation for the TES measurement, the tape of ThESSA was checked for any ruptures, and disinfected with an alcohol pad (70%). The HPDT is determined, where only the thermode is attached to the forearm of the subject (Figure 5.1). The average temperature of this test is the input for the TES measurement, i.e. it will be the target temperature of the heated block (Appendix E).

After the HPDT measurement, the ThESSA electrode is placed on the thermode, and re-attached to the forearm (Figure 5.2 D-E). The ground electrode is placed proximal and closely to ThESSA. The other hand will hold the AmbuStim, which can be controlled by the subject by pressing the button (Figure 5.2F).

Next, three normal staircase tests are performed: one to become familiar with the stimuli and two to determine the initial values for the SP and the DP. During these tests, the stimulus strength will increase stepwise, as long as the button of the stimulation device is pressed. It will continue until the stimulus is felt by the subject, and the button is released; the stimulus has to be clearly felt for the familiarisation test and firstly detected for the initialisation. The obtained values of the initialisation tests will be used as initial strength of the adaptive staircase procedure of the NDT procedure.

In the NDT procedure, the nociceptive detection threshold is tracked over time. Whenever the subject presses the button of the AmbuStim, the electrical stimulation will start. The subjects were asked to release the button if they detected a stimulus. The stimulus will be marked as detected when the button was released within 1.0 second after the stimulus was given. The AmbuStim will apply stimuli with randomization of the amplitudes according the NDT procedure (Section 2.3). If the button is re-pressed, the stimulation will continue until the task is completed. Additionally, the H-NDT procedure has a continued heat pulse applied (Figure 5.1).

After each NDT procedure (normal or heated), the subject is asked to answer some quantitative and qualitative questions about the perception of the stimuli. This involves questions about the perception of the temperature change (large decrease, slightly decrease, no temperature change, slightly increase, large increase); the overall perception of the stimuli (not perceived, light touch, touch, tingling, shock, warm, burning and pricking); and the pain rate following the NRS scale (0-10). The detailed questionnaire can be found in Appendix C.

At the end of the TES measurement, the subject will undergo again a HPDT test, to see whether the HPDT was subjected to habituation (Figure 5.1). Afterwards the subject will be disconnected from the setup and will receive a small compensation gesture.

5.1.6 Analysis plan

The study parameters of this thermal electrical stimulation research are the detection rate of the stimuli, the stimulation amplitude, and the perception of the stimuli. More specifically, are there any differences in a stimulus detection experiment when thermal stimulation is applied with two different temperatures, when evaluated on the study parameters?

To answer this, the results will be analysed in the following way: the trails over time will be plotted against the stimulation amplitude per subject. Per task it will be indicated which stimuli are detected and which not, together with the detection rate over all stimuli. The stimulation amplitude will be analysed by an estimation of the nociceptive detection threshold (NDT) (Eq. 5.1 and 5.2), which is based on the stimulation amplitude. The NDT will be plotted in the graph, together with the applied stimuli. Furthermore, over the course of the measurement, the temperature is visualised, as well as how the stimuli are perceived by the subject.

The results will be evaluated per task on whether there are differences in single pulse (SP) or double pulse (DP). More specific, per task, the study parameters *detection rate* and the *estimated NDT* will be evaluated. Additionally, differences between the tasks will be evaluated on all three study parameters, including *perception of the stimuli*. Furthermore, it will be analysed whether a certain relation can be found between the different subjects in one of the research parameters mentioned before.

The study parameters detection rate, estimated NDT and perception of the stimuli entail the following. Firstly, in a stimulus detection experiment, stimulation at the detection threshold will theoretically result in 50% detection of the stimuli. In reality, the detection rate will be between 0.4 and 0.5, due to subject's habituation and the adaptive approach of the experiment (Subsection 2.3.3). By definition of the adaptive approach, the detection rate will be lower than 0.5, when the threshold increases.

Secondly, for analysis of the stimulation amplitude, an estimate is made for the detection threshold with a generalized linear model. This estimate can be used when tasks are compared, instead of the individual detected stimuli. The detection threshold is estimated with a generalized linear regression model (glm), based on the research of Doll et al. [41], with improvements of Van den Berg et al. [55]. The model uses the function

fitglm in MATLAB. The first 10 electrical pulses (SP and DP, detected and non-detected) are not included in the estimation of the detection threshold, as the stimuli should converge to the threshold first.

Next, only the detected stimuli are used for fitting the model to the data. The variables used for the model are the first and second stimulus amplitude and the trial number, which results in a NDT estimation that depends on SP and DP together [55]. These estimations can be described as follows, the SP estimation:

$$NDT_{est,lin,SP}(n_{trial}) = -\frac{\beta_1}{\beta_2} - \frac{\beta_4}{\beta_2} \cdot n_{trial} = NDT_{0,SP} + a_{SP} \cdot n_{trial}, \tag{5.1}$$

and the DP estimation:

$$NDT_{est,lin,DP}(n_{trial}) = -\frac{\beta_1}{\beta_2+\beta_3} - \frac{\beta_4}{\beta_2+\beta_3} \cdot n_{trial} = NDT_{0,DP} + a_{DP} \cdot n_{trial}. \tag{5.2}$$

Within these equations, NDT_0 is the estimated initial threshold, a the gradient of the NDT, and n_{trial} the trial number. β_1 represents the intercept, β_2 the first amplitude, β_3 the second amplitude and β_4 a trial number dependent variable, which represents some of the habituation of the subject. Values for β_n of the IES can be found in Appendix A.8.

When the stimuli show a gradual increase of the amplitude over trial, the generalized linear regression model is able to fit the threshold slope quite well. However, when the stimuli deviate from this course, the predictions might become less accurate. Therefore the NDTs will be evaluated whether they deviate from the course of stimuli amplitude over trial. When deviating, this will be taken into account.

For the third study parameter perception of the stimuli, two assessments are performed with specific perception indicators. Firstly, the subject has to score the pain on the Numeric Rating Scale (NRS) and secondly, it has to assess the quality of perception with predefined labels [4, 56, 57]. The NRS ranges from 0 to 10, of which 0 means no pain; 1-3 means mild pain (nagging, annoying, interfering little with activities of daily living (ADLs)); 4-6 means moderate pain (interferes significantly with ADLs); and 7-10 means severe pain (disabling, unable to perform ADLs). The quality of perception assessment consists of the following indicative labels: not perceived, light touch, touch, tingling, shock, warm, burning and pricking. Of those, 'light touch, 'touch' and 'tingling' suggest tactile activation, whereas 'shock', 'pricking' and 'burning' suggest nociceptive activation, of which the latter one also indicates thermal activation of the nociceptors [57]. 'Warm' suggests activation of the non-nociceptive thermal sensitive keratinocytes.

5.2 Results

5.2.1 Study design

During the measurements on the subjects, some deviations were made from the original session plan for two of the six subjects. This was due to time limitations (subject D0021) or a manual mistake (subject D0052). An overview of the final sessions is shown in Figure 5.5. This will be taken into account with the analysis, as far as possible. The extra H-NDT task (task 4) of subject D0052 will be ignored when the subjects are compared to each other, although individually the block will be analysed. The missing normal block of subject D0021 will leave a gap in the overall analysis of the subjects.

Furthermore, during analysis of the measurements, it was found that the temperature pulse with subject D0032 and D0041 did not continue during the complete H-NDT task (i.e. temperature pulse of only 80s), and were thus excluded. The remaining measurements of subjects D0012, D0021, D0052 and D0061 were included for the analysis of the TES measurements (Figures 5.7-5.10). As the group consists only of 4 to 6 subjects (depending on the parameter analysed), no statistical evidence can be provided to support the findings.

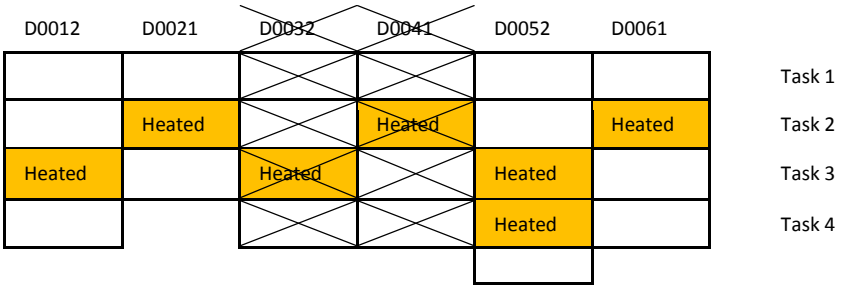

Figure 5.5 Overview of the final sessions of the measurements on the subjects. Subjects D0032 and D0041 were excluded due to failed temperature stimulation. Subject D0021 did not complete task 4 due to time limitations, and subject D0052 completed two H-NDT tasks due to a manual mistake.

5.2.2 Group-level results

The results in Figure 5.6 show comparison of the subjects on the detection rate, initial NDT threshold and NDT slope. In general, the following three observations can be made from the diagrams. Firstly, the median shows larger differences between the tasks than for the average. Secondly, the normal tasks 'N' and 'N (4^{th})' have similar values for the same subject, and lastly, it seems that the order of the tasks do not show dependence in the outcome.

Differences between normal and heated NDT tasks

For the study parameters (detection rate, NDT_0 and NDT slope), the most important observation can be found with the initial NDT threshold. For SP, it has a difference of 0.401 mA between the normal and heated task, when evaluated on the average of the four estimates. For DP this difference is 0.305 mA. Next, the NDT slope of the DP shows a difference of $0.465 \cdot 10^{-3}$ mA/trail. For the SP, however, the individual differences in slope differ too much to obtain a useful average or median to determine a trend between the different tasks. Noteworthy is the smaller spread in the H-NDT task (for SP and DP). Lastly, for the detection rate, a difference is found between the normal and the heated task of 0.0475 for SP and 0.0722 for DP.

Differences between ThESSA and IES-5

When ThESSA is compared with the currently used IES-5 electrode, the following observations can be done. For the detection rate, it is difficult to compare them, as no confidence intervals (CI) were available. But in general, it seems that the detection rates of ThESSA are lower than IES-5, although some of the detection rates are around the average of IES-5. Next, NDT_0 shows for both SP and DP higher NDT_0's than with IES-5, SP more than DP. And lastly, the average NDT slopes of ThESSA (non-heated) are within the CI of IES-5 for DP, for SP only the median (non-heated) is within the CI.

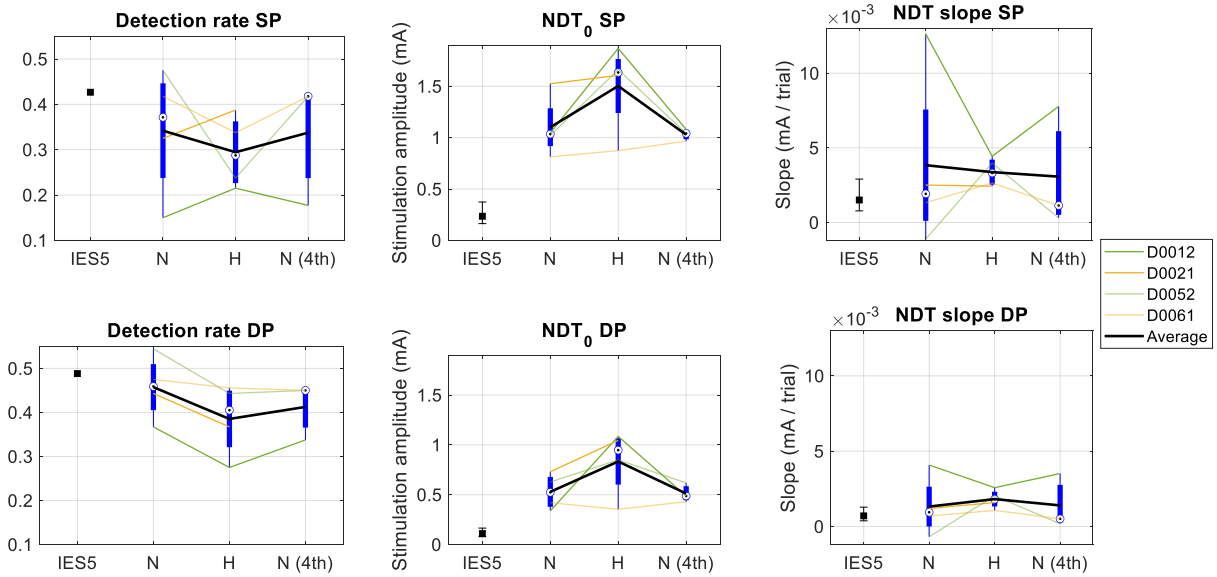

Figure 5.6 Visualisation of the subjects compared on the detection rate, NDT threshold and NDT slope. This figure shows boxplots with lines linking values of the same subject. All evaluated for the single and double pulse. The values are put in perspective with average results of the IES-5 electrode from a previous study (n=25), including 95% confidence intervals when available (represented as IES-5 in the graph) [55]. The values of these intervals are reported in Appendix A.8 (Table A.6). For the ThESSA electrode, the tasks are labelled with N for the normal task, H for the heated task, and N (4th) for the last normal task. Yellow represent subjects with the 2nd task heated, green represents subjects with the 3rd task heated.

Table 5.3 Overview of the final temperatures per subject during the H-NDT task

		H-NDT (t>900s)		**Control of TT before starting TES (t≈70s)**	
Subject	Target temperature (°C) (TT)	Average of the sensors (°C) (AS)	Difference with TT (°C)	Average of the sensors (°C) (AS)	Difference with TT (°C)
D0012	42.9	37.3	5.6	37.7	5.2
D0021	44.1	38.7	5.3	39.0	5.1
D0052	44.9	39.8	5.1	39.4	5.5
D0061	45.0	38.6	6.4	38.2	6.8

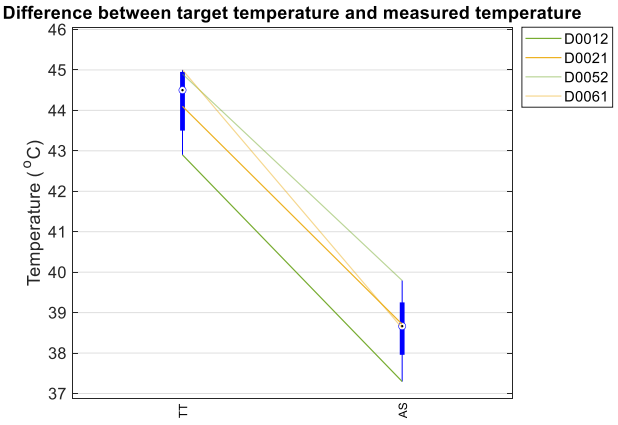

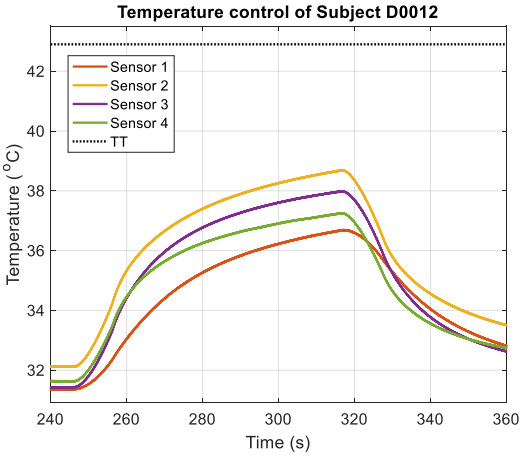

Figure 5.7 Additional figures supporting Table 5.3

Figure 5.7A Visualization of the heat loss per subject. The difference is shown of the target temperature (TT) with the average of the sensors (AS).

Figure 5.7B Example of the control of the TT before starting TES of subject D0012. Duration of the temperature is approximately 70s. TT was 42.9 °C

DIFFERENCES BETWEEN MEASURED AND TARGET TEMPERATURE

Furthermore, the maximal temperature reached with ThESSA is compared as well. An overview of the temperatures with and without ThESSA is provided in Table 5.3 and Figure 5.7. This shows that the average skin temperature has a difference of minimal 5.1°C and maximal 6.4°C with the target temperature when ThESSA is attached. Without ThESSA attached, these differences range from 5.1 to 6.8°C, although measured for a shorter duration (t≈70s). The example in Figure 5.7B shows that the temperatures of subject D0012 without ThESSA have not reached there plateau yet. Furthermore, Figure 5.7B shows that subject D0012, D0021 and D0052 have a similar heat loss, while the heat loss of subject D0061 seem to deviate from the others.

5.2.3 INDIVIDUAL SUBJECT ANALYSIS

SUBJECT D0012

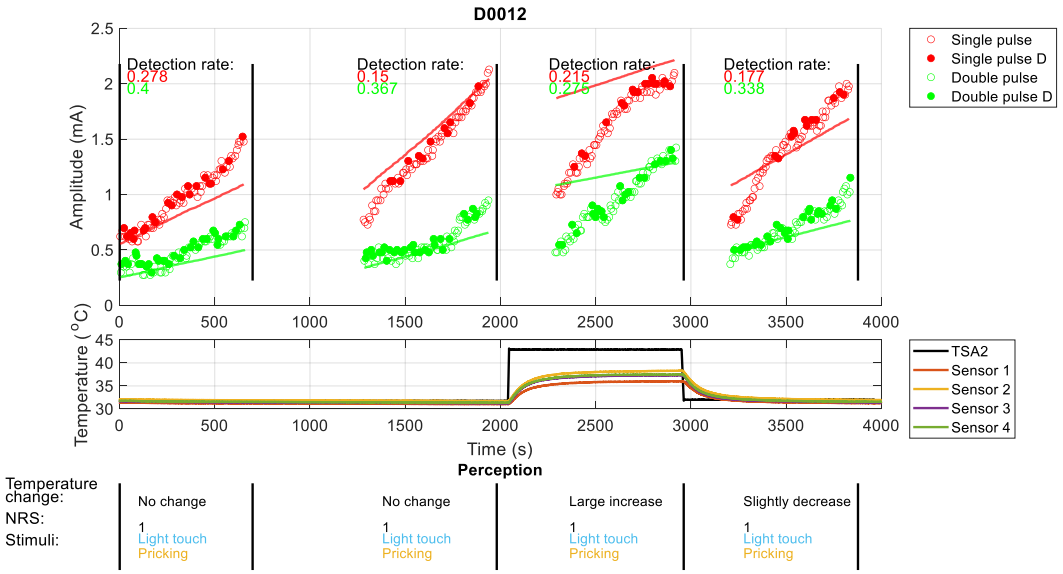

Figure 5.7 The upper graph shows the results of the NDT method, where the line through the points is the estimated nociceptive detection threshold (NDT). Solid dots are detected stimuli. The middle graph shows the applied temperature over time by the TSA2, and the temperature of the skin measured by the sensors. The target temperature for subject D0012 was 42.9 °C, average of the sensors was 37.3°C.

The detection rates are low for this subject (SP: 0.278; 0.15; 0.177; DP: 0.4; 0.367; 0.338), which resulted in strong habituation behaviour (Figure 5.7, upper graph). In the third block, when heat is applied, the detection rate of the double pulse deceases to an even lower value of 0.275. The single pulse showed a similar detection rate compared to the other single pulse detection rates (SP: 0.215).

For the estimates of the NDT, it is notable that within the H-NDT task the estimates are above the data points of the detected stimuli. Notice that the detected SP stimuli are more concentrated at the end of the task. Furthermore, it has a smaller estimated slope in relation to the course of the applied stimuli. The estimated NDT's per task can be found in Appendix A.8 (Table A.5).

In the perception of the stimuli, the subject indicated the temperature change corresponding to the temperature conditions. Furthermore, over all tasks, the NRS score and the description of the stimuli remained constant, respectively with a score of 1 and as light touch and pricking.

SUBJECT D0021

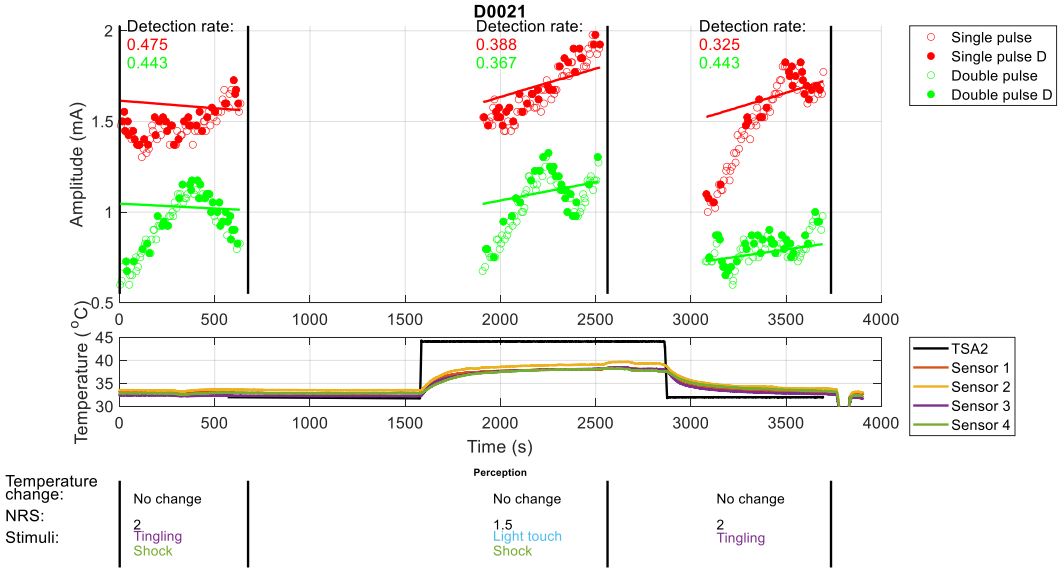

Figure 5.8 The upper graph shows the results of the NDT method, where the line through the points is the estimated nociceptive detection threshold (NDT). Solid dots are detected stimuli. The middle graph shows the applied temperature over time by the TSA2, and the temperature of the skin measured by the sensors. The target temperature for subject D0021 was 44.1 °C, average of the sensors was 38.7°C.

The detection rate is normal (SP: 0.475; 0.325 DP: 0.443; 0.433), although it shows an angle shaped detection curve, which is the result of a low detection rate in the beginning of the task followed by a high detection rate halfway on. When heat is applied, the detection rate of the double pulse decreased (DP: 0.367), whereas the single pulse decreases over the order of the tasks (SP: 0.475; 0.388; 0.325).

The estimated NDT shows a decreasing NDT over trial in the first task. Furthermore, it is notable that the DP of task 1 and 2 show a pointed shape of the applied stimuli. The estimated NDT's per task can be found in Appendix A.8 (Table A.5).

The temperature course shows that the TSA2 protocol was not started from the beginning, though the sensors show that the temperature of the skin remained constant at the desired temperature. Furthermore, a small temperature fluctuation can be seen after 2550 seconds, although this is after the second task was completed. At the end, the sensors also show the separation of the electrode from the arm.

The perception of the temperature change by the subject differed from the temperature conditions during the heated nociceptive task. The subject indicated that no temperature change was felt during the heated task. For the NRS score, the perception of the stimuli was given a score of 2 for the non-heated tasks, and 1.5 for the heated task. The characterization words chosen for the tasks are 'tingling' for the non-heated task, 'shock' for the first and second task (normal and heated respectively), and 'light touch' for the heated task.

SUBJECT D0052

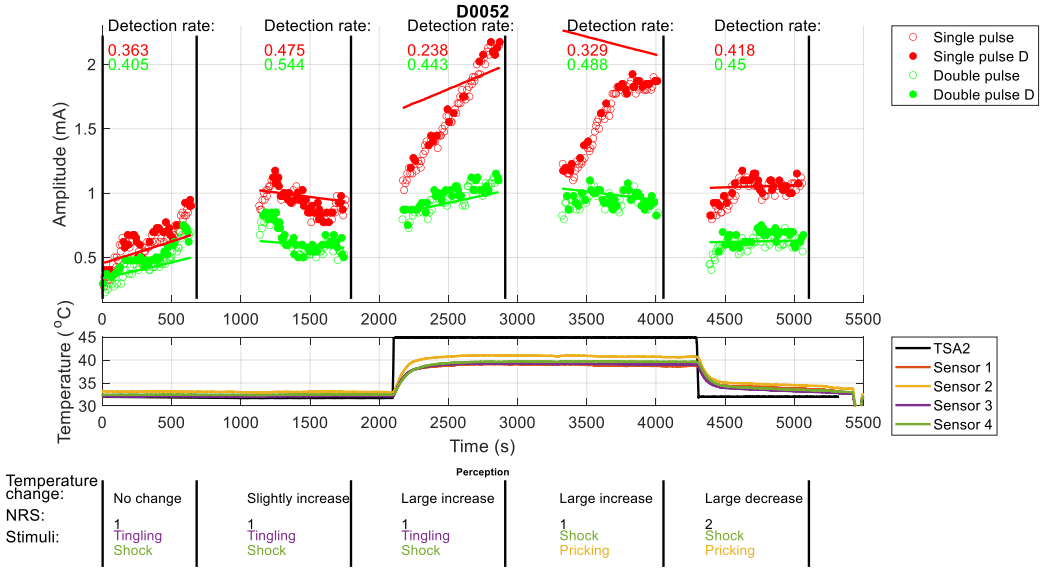

Figure 5.9 The upper graph shows the results of the NDT method, where the line through the points is the estimated nociceptive detection threshold (NDT). Solid dots are detected stimuli. The middle graph shows the applied temperature over time by the TSA2, and the temperature of the skin measured by the sensors. The target temperature for subject D0052 was 44.9 °C, average of the sensors was 39.8°C.

Detection rates for this subject are normal, although the detection rate of the single pulse during the first task is rather low (SP: 0.363; 0.475; 0.418; DP: 0.405; 0.544; 0.45). During the tasks where heat is applied, a decrease for the single pulse is visible (SP: 0.238; 0.329), whereas the double pulse shows similar rates to the non-heated tasks (DP: 0.443; 0.488).

Subject D0052 shows the clearest differences between normal and heated tasks. Both NDTs (SP and DP) of the H-NDT tasks are elevated related to the other tasks. Note that in the fourth task, SP started at low initial amplitude, followed by large increase of amplitude, until it stagnates and seems to reach a detection threshold. The estimated NDT's per task can be found in Appendix A.8 (Table A.5).

The temperature course shows the elongated temperature pulse over task three and four. Due to a manual mistake, the pulse was not ended after the first task. Furthermore, it can be seen that the temperature of the skin in task 5 remained higher than before the thermal pulse.

The perception of the temperature for task 1, 3 and 5 are consistent with the temperature course. At the second task the temperature change is perceived as a slight increase, whereas in task 4 it is perceived as a large increase. Furthermore, all the stimuli were perceived as 'shock' and the first three as 'tingling', while the last two were indicated as 'pricking'.

SUBJECT D0061

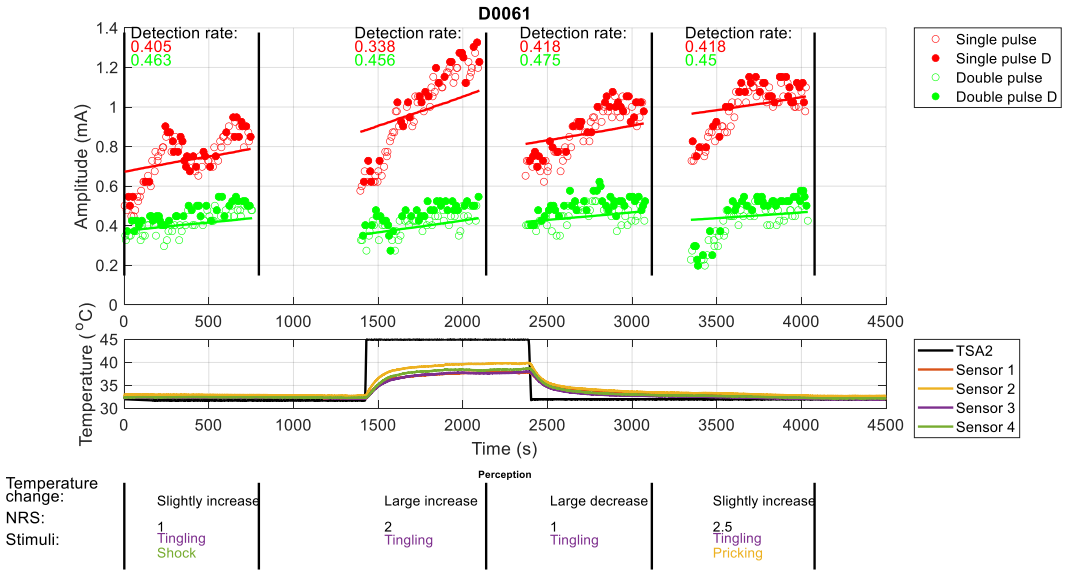

Figure 5.10 The upper graph shows the results of the NDT method, where the line through the points is the estimated nociceptive detection threshold (NDT). Solid dots are detected stimuli. The middle graph shows the applied temperature over time by the TSA2, and the temperature of the skin measured by the sensors. The target temperature for subject D0061 was 45.0 °C, average of the sensors was 38.6 °C.

The detection rates are normal (SP: 0.405; 0.418; 0.418; DP: 0.463; 0.475; 0.45). In task 2 (with heat applied), the detection rate of the single pulse decreases, while the detection rate of the double pulse remains approximately the same (SP: 0.338; DP: 0.456).

The estimations of the NDTs seem to be quit consistent with the course of the detected stimuli, although the threshold might be estimated lower than expected. The estimated NDT's per task can be found in Appendix A.8 (Table A.5).

The temperature course itself does not show any deficiencies, although the pulse started ~30 seconds later than the NDT measurement started. Note that when the sensors show a plateau of the skin temperature (at ~1600 s), the detection rate of the SP increases, although the threshold is still increasing as well.

The NSR score fluctuates from 1 to 2 to 1 to 2.5 over the different tasks, where the heated task (task 2) was rated as 2. All tasks were indicated as 'tingling' and the first and last were also indicated as 'shock' and 'pricking' respectively.

SUBJECT D0032

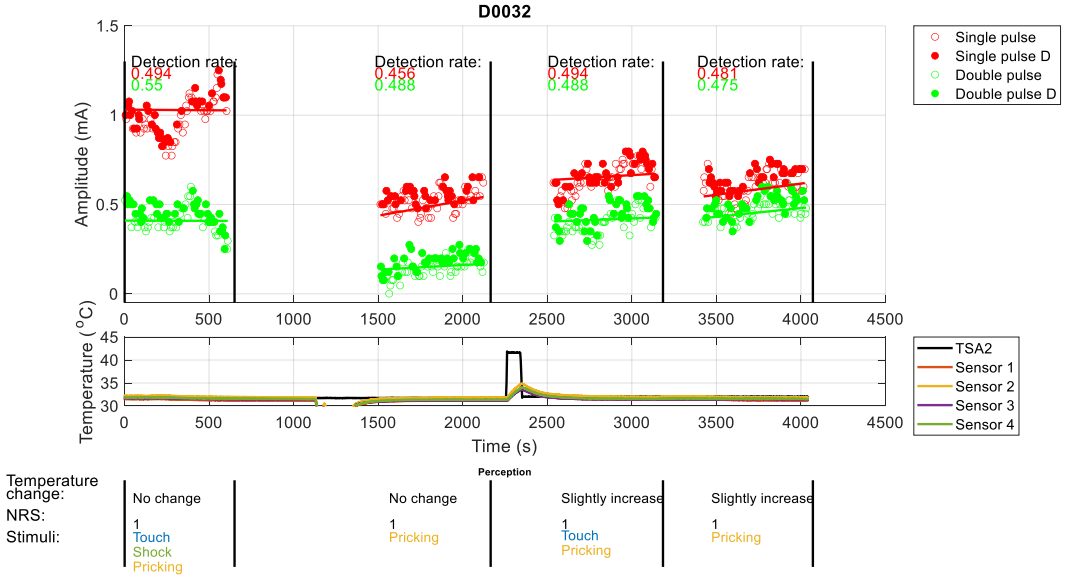

Figure 5.11 The upper graph shows the results of the NDT method, where the line through the points is the estimated nociceptive detection threshold (NDT). Solid dots are detected stimuli. The middle graph shows the applied temperature over time by the TSA2, and the temperature of the skin measured by the sensors. It shows that the heat pulse stops after ~80 seconds.

The detection rates for subject D0032 are normal (SP: 0.494; 0.456; 0.494; 0.481; DP: 0.55; 0.488; 0.488; 0.475). The electrode is re-attached between the first and second task, as can be seen in the temperature decrease of the sensors (Figure 5.11). For the second task, it shows that threshold decreased after the electrode was re-attached, and increased slowly over the succeeding tasks. The single pulse stays lower, while the double pulse amplitude returns to the same value as with the first task. It shows light habituation over the last three tasks for both single and double pulse. The estimates of the threshold seem to fit the detected stimuli well. The estimated NDT's per task can be found in Table 5.4. Note that the NDT_0's are lower than the average depicted in Figure 5.6 and the detection rates are higher than average.

In the middle graph in Figure 5.11, it can be seen that the TSA2 only applies heat for ~80 seconds, and thus does not heat the skin during the intended heated task. As such, the NDTs are only analysed over the tasks, and not in comparison with other subjects.

The perception of the temperature within the last two tasks is qualified by the subject as 'slightly increase', even for the fourth task, were no heat was applied at all. The NRS score remained constant at 1, and perception of the stimuli for all tasks was indicated with 'pricking'. For the first and third task, 'touch' is mentioned as well. As last, the stimuli in the first task were also indicated as 'shock'.

Table 5.4 Overview of the estimated NDT's per task for subject D0032

	Task 2	Task 3	Task4
SP	$0.440 + 0.0013 \cdot n_{trial}$	$0.638 + 0.0004 \cdot n_{trial}$	$0.545 + 0.0010 \cdot n_{trial}$
DP	$0.136 + 0.0004 \cdot n_{trial}$	$0.405 + 0.0003 \cdot n_{trial}$	$0.424 + 0.0008 \cdot n_{trial}$

SUBJECT D0041

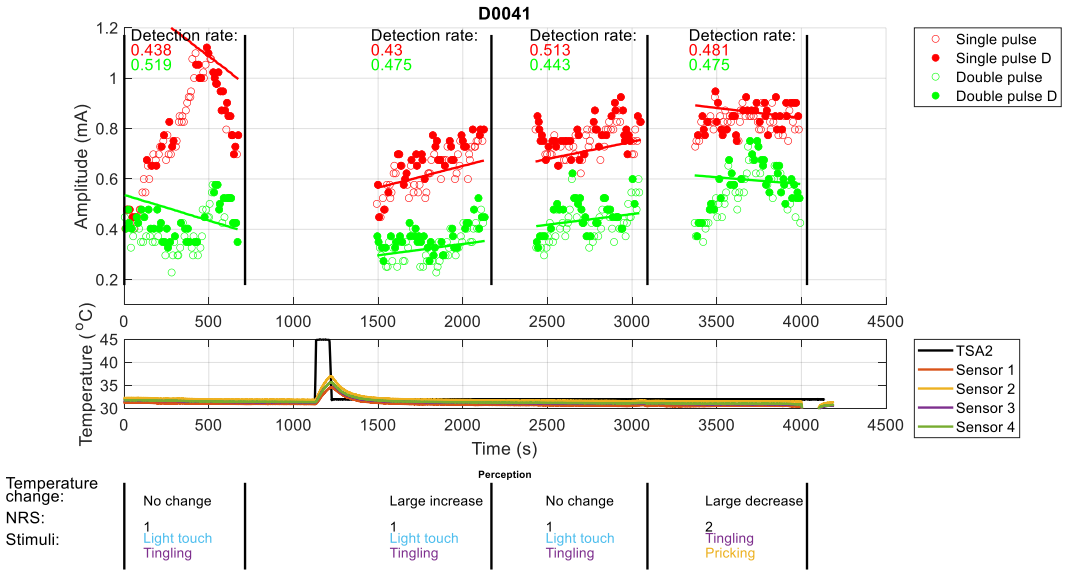

Figure 5.12 The upper graph shows the results of the NDT method, where the line through the points is the estimated nociceptive detection threshold (NDT). Solid dots are detected stimuli. The middle graph shows the applied temperature over time by the TSA2, and the temperature of the skin measured by the sensors. It shows that the heat pulse stops after ~80 seconds.

The detection rates are normal (SP: 0.438; 0.43; 0.513; 0.481; DP: 0.519; 0.475; 0.443; 0.475). The first NDT task shows not a gradual increase in amplitude of the stimuli for SP and its course of applied stimuli is deviating compared to the other tasks of this subject. Furthermore, task 4 shows a small decreasing NDT and a point shaped course of applied stimulation amplitude for DP (similar to subject D0021). Over the last three tasks, a slight habituation is visible. The estimated NDT's per task can be found in Table 5.5. Note that the NDT_0's are lower than the average depicted in Figure 5.6 and that the detection rates are higher than average.

The temperature course does not show any deficiencies other than the short temperature and the delayed start of the TSA2 (~330 seconds). The time of the pulse is again ~80 seconds, similar to the temperature pulse given to subject D0032.

The perception of the temperature during the tasks is consistent with the temperature for the first three tasks, while the last task is perceived as a large decrease of the temperature. The NRS is scored as 1 for the first three tasks, whereas the last task is scored as 2. In the perception of the stimuli we see a similar pattern; the first three tasks are indicated as 'light touch', and the last one as 'pricking'. All the stimuli were indicated as 'tingling' as well.

Table 5.5 Overview of the estimated NDT's per task for subject D0041

	Task 2	Task 3	Task4
SP	$0.565 + 0.0044 \cdot n_{trial}$	$0.669 + 0.0011 \cdot n_{trial}$	$0.892 - 0.0006 \cdot n_{trial}$
DP	$0.296 + 0.0007 \cdot n_{trial}$	$0.412 + 0.0007 \cdot n_{trial}$	$0.614 - 0.0004 \cdot n_{trial}$

5.3 Discussion

5.3.1 Technical feasibility of the study protocol

Exclusion subjects

Two measurements could not be included (D0032 and D0041), due to a technical failure within the setup. This had the result that the intended task was not heated. It is remarkable that the temperature pulse of subject D0041 had a similar duration as the pulse given to subject D0032. This might indicate a structural problem and not a manual mistake. A possible explanation for the failed temperature pulse could be that the remote trigger was frozen in the software, such that the protocol already continued to the next event, without manually activating it. For further usage of this protocol, the protocol should be thoroughly tested, such that the problem can be identified and resolved. Furthermore, as the focus of these experiments it to compare electrical stimulation on two different temperatures, these measurements were excluded from further analysis.

Failure risks

Of the 4 included measurements, one measurement was deviating from the original programme due to manual failure (subject D0052). In combination with the other excluded measurements, this shows that the protocol has a high chance of (manual) failure, as four different programmes are ran together: electrical stimulation via Labview; temperature of the skin via Polybench; the order and data storage of the TSA2 protocols via Matlab; and the remote trigger activation for the protocol in MMS (Figure 5.1). In the design of the procedure was already partly anticipated on this, as the assessment for perception indicators were performed on paper, instead of digitally. For further experiments, the process should be improved. On short term, this could be done by including a checklist of the protocol on the assessment form, such that mistakes as with subject D0052 can be avoided. On long term, the trigger for the HPDT-temperature should be given automatically, when the H-NDT task is started. This could be achieved by linking Labview to the MATLAB protocol, or by sending a trigger to the *TTL IN* port of the TSA2. A detailed elaboration to this can be found in Appendix A.5.

For unknown reason, the MMS could not export the data of measurements with duration longer than 40 minutes. Therefore, the control and data storage of the TSA2 was performed via MATLAB. Downside to this was that MATLAB had sometimes difficulties to hold the connection with TSA2, often only in the order of milliseconds. Although this is short, the protocol stopped measuring due to the loss of connection. The script was adjusted to this, but the problem was not solved, therefore it is recommended to do the external control via a more solid programme, for instance with Python. Medoc already provided code that could be used [39].

Administered Temperature

Per subject, a different target temperature (TT) is used in the H-NDT task, as the thermal pain threshold depends on the local structure of the skin, and differs per subject. Therefore, the TT was determined with the HPDT protocol, instead of a standard temperature of 40 °C as reported in literature [2]. Although this approach is liable to subjectivity to the HPDT criteria, it will account for subject differences in perception and local structures of the skin.

Resulting from the temperature curves, it could be said that the setup of the experiment fails in applying the correct temperature to the skin in the beginning, as the measured temperature is still increasing rapidly in the first three minutes (and the electrical task starts before this). However, from the functionality tests of the temperature it is known that the measured temperature of the skin is not the same as the perceived temperature. The experience is that the temperature is sensed (by the nociceptors and keratinocytes) directly whenever the thermal pulse is applied, although it takes time before the skin under the sensor is heated to the same temperature, therefore there will always be a delay in the measured temperature compared to the perceived temperature. This should be considered in the interpretation of the results.

5.3.2 Group-level results

Comparing only 4 subjects is difficult (Figure 5.6), as it are too few measurements to have a rigid median or average. Therefore both are depicted, together with the individual values, such that the spread per task is visualized as well. With this, the consistency of the individual measurements with the average/median can be taken into account as well. In addition, the median showed larger differences between the tasks than the average. Therefore, analysis was performed on the average, as a valuable difference in average means that this difference exists for the median as well.

Differences between normal and heated NDT tasks

The NDT_0 and the NDT slope are put in perspective with average values of the IES-5 (n=25) and their CI's. When it is assumed that those CI's are purely based on subject variability, a similar CI can be assumed for ThESSA. With this, the differences between the normal and heated task can be put in perspective as well. For NDT_0 SP, the upper bound of the CI has a difference of 0.139 mA with the average. With similar assumed sizes of CI, the difference between normal and heated of 0.401 mA is presumed to be outside the CI of ThESSA (non-heated). For NDT_0 DP, the IES CI has a difference of 0.055mA with the average. The difference between normal and heated of 0.305 mA is presumed to be outside the CI of ThESSA (non-heated) as well, which might indicate an effect of heat on NDT_0 for SP and DP.

The NDT slope (DP) on the other hand, the IES-5 CI has a difference of $0.578 \cdot 10^{-3}$ mA with the average. The difference between normal and heated of $0.496 \cdot 10^{-3}$ mA is presumed to be inside the CI of ThESSA (nonheated), which indicate no direct effect of heat. For the NDT slope of SP, comparing IES-5 with ThESSA results cannot be done, as there are too much individual differences. Therefore, more measurements should be performed to compare valuable results.

For the detection rate, no CI's were available of the IES-5 to compare with the detection rates of ThESSA. Therefore, as rule of thumb, a difference of 10% between the normal and heated task was assumed as meaningful. This results for SP in a decrease of 13.9% in the detection rate. For DP this is a decrease of 15.8%. This indicates that heating might be of influence on the detection rate, although more measurements are needed for statistical evidence of this presumed relation.

Differences between ThESSA and IES-5

When ThESSA is compared to IES-5, the detection rate gave difficulties to compare. Some of the subjects performed worse than the average of IES-5, which resulted in a lower average detection rate for ThESSA. It cannot be said that these lower detection rates indicate worse performance of ThESSA, as it could also depend on performance of individual subjects, as known from previous performed measurements within our research group. This is as well supported by the higher detection rates of the excluded subjects D0032 and D0041 when the normal tasks are compared (Figure 5.9 and Figure 5.10). Therefore, the current results should be compared with the CI's of IES-5 as well, such that this can be supported, although it is more important to perform extra measurements to rule out that it depends on the performance of ThESSA.

For the NDT_0's it is unknown what could explain the higher NDT_0's of ThESSA. Although this should be placed in perspective when compared on the normal tasks, such that the excluded subjects can be taken into account as well. Namely, the NDT_0's of the excluded subjects (D0032 and D0041) are lower than the average depicted in Figure 5.6 (Table 5.4 and 5.5), showing that it is possible to have a NDT_0 closer to the average of IES-5. Nevertheless, the NDT_0's remains higher than the NDT_0's of IES-5.

An explanation for a higher NDT_0 could be related to the design of the electrode, as it might be possible that ThESSA does not penetrate the skin for 0.2mm due to flexibility of the skin. However, it would be expected that this would show up in the impedance measurements (Section 4.2). Although it shows a small difference in the course over time, it was not assumed to result in these differences in NDT_0's. Another explanation in relation to the impedance might be different attachment of the IES-5 to the skin; for the reported impedance measurements, the IES-5 electrode was put gently on top of the skin. It could be that the IES-5 was attached differently (e.g. deeper into the skin) in the research used for comparison with ThESSA. Therefore, it is recommended to measure the depth of the needles into the skin, such that the flexibility of the skin can also be taken into account in future prototypes. This should be done for ThESSA, IES-5 (gently placed on top of the skin), IES-5 (flat to the skin), and possibly the electrode of Inui as well [58].

For the NDT slopes, the average values of ThESSA are within the CI of IES-5, thus these are assumed to be similar for both electrodes. As the slope is assumed to be a parameter for measuring the habituation of the subject, this might indicate that there is no difference in reaction of the nociceptive system to the different stimulation methods over time. Nevertheless, more measurements are necessary to support this.

To summarize, on the research parameters detection rate, NDT_0 and NDT slope the following things can be said: the detection rate seems to be affected by application of heat, the NDT_0 seems to change when the skin is heated, and the NDT slopes seems only to be closer together during the heated task. In comparison with the IES-5, it seems that ThESSA could improve in obtaining lower NDT_0's. Nevertheless, more research is needed to statistically support these preliminary findings.

Differences between measured and target temperature

In relation to requirement F-3, the temperature measurements during the experiments are of interest for determining the true effect of the electrode on the final skin temperature. The ThESSA electrode showed temperature differences of minimal 5.1 °C, which seems large. When these values are compared with the temperature differences without electrode, it has the same minimal difference. However, Figure 5.7B shows that the temperatures have not reached their plateau, due to the short duration, as this measurement was only intended to test the TT before starting the TES measurement. Nevertheless, the temperature course might be estimated based on previous performed temperature measurements (Subsection 4.1).

It was learned that within approximately 200s the temperature curve has reached it plateau (when no electrode is attached). Thus, when the curves in Figure 5.7B are extended in a similar way (up to 200s), it is expected that it will only increase 1.0-1.5°C. This places the differences in more perspective, and shows that the difference to TT is much larger than the expected difference in temperature when the ThESSA is attached or not. This seems to indicate as well that thermoregulation has a large influence on the measured temperature of the skin, instead of ThESSA. In relation to the functionality of the electrode, ThESSA seems to be able to transfer the warmth of the thermode efficiently to the opposite side of the electrode with only a small loss of heat (Requirement F-3). However, to confirm the expectation of an increase of only 1.0-1.5°C, additional measurements with and without ThESSA should be performed on multiple subjects as well, with durations longer than 200s.

These findings show that thermoregulation has major impact on the temperature measurements. Therefore, it is recommended to gain more insight about the behaviour of this system. For instance with a COMSOL model of the skin that has the blood flow embedded, such that simulations can be performed with different temperature pulses applied. In this way, one might be able to anticipate better on the thermoregulation of the skin in future studies related to thermo-electrical stimulation.

5.3.3 Individual subject analysis

Subject D0012

The results of subject D0012 show a low detection rate, which might be the result of the medical history of the subject. Inclusion of subject D0012 was done, as the chronic pain complains were related to headache, and not to peripheral perception. However, the medication for this might be of influence on the perception of the stimuli, which might have been neglected in the consideration. In retrospect, it might have been better to exclude this person, although given the exploratory nature of this study, it may provide additional insights.

The estimated NDTs for the H-NDT task are higher than the applied stimuli. This might be the result of the low detection rate of this subject, as the reliability if the NDT depends on the detection rate. However, the SP detection rate is higher than those of the second and fourth task. When task 3 in Figure 5.7 is closer inspected, it shows that the detected stimuli are more concentrated at the end of the task, whereas in the other tasks it is more spread over time. This input for fitting the NDT might result in this deviating NDT, although it is difficult to indicate how this will affect the interpretation of the results, as this remains how the glm is defined.

The subject indicates the quality of the perception for all tasks 'light touch' and 'pricking', which might indicate tactile and nociceptive activation respectively. This could indicate that no selective activation was achieved. Due to the high speculative character of this method, these outcomes should be considered together with the outcomes of the other subjects to say something about the functionality of the electrode.

SUBJECT D0021

Subject D0021 completed only three tasks as the duration of the experiment took longer than expected. This meant that the last normal block could not be done in time and thus left a gap for comparing the subjects. However, the data could still be useful for exploration of the functionality of ThESSA on the detection rate, NDT and stimuli perception.

The pointed shape of the DP detection curve in the first and second task is remarkable, as this behaviour is more common for SP detection. It might be a too low initial amplitude for the DP, although this would not result in a decrease of amplitude in the end of the task, as it is expected to result in stagnation of the amplitude. Another reason could be uncertainty about the detection criteria or adaptation of the criteria during the trial by the subject, which was confirmed at the end of the experiment by the subject. Nevertheless, it remains unclear what causes this deviating behaviour without further investigation, which is out of the scope of this research.

The detection curve of the single pulse shows a rapid decrease at the end of the third task. It might indicate loss of attention by the subject, which is common in this type of experiments. Loss of attention is often visible in the single pulse and leaves the double pulse untouched. This means that the estimation of the threshold could be less accurate, as it is influenced by the distraction of the subject. However, as the NDTs depend on both SP and DP, the NDT of the SP is less affected by loss of attention, and has therefore low impact in the comparison of the subjects.

With some subjects (D0021, D0032, D0041), the temperature curve shows that the start of TSA2 protocol is delayed. This is not concerning for the application of the temperature, as the baseline of the TSA2 is the same as the stimulation temperature of the first task. The only consequence is that the thermal and the detection results cannot be aligned via a trigger. This is resolved by manually aligning the measurements on the absolute time. For further usage of this protocol, it is important to simplify the start of the thermal and NDT measurements, such that it becomes more synchronized and alignment will be more robust.

The small temperature fluctuation after 2550 seconds, are a possible movement artefact. Similar artefacts were found with previous pilot studies, which were known to be caused by movement. It shows the responsiveness of the sensors, but this artefact has no further consequence for the measurement, as it happen after completion of the NDT procedure.

It is remarkable that no temperature change was reported by the subject at the heated task. This might be explained by possible misinterpretation of the question ‘How would you describe the temperature change?’, as indeed during the task the temperature did not change. Formulation of a question always has influence on the interpretation of the receiver. This was kept in mind with designing the questionnaire, although success depends on proper usage and following the questions formulated. Although this might be a plausible explanation for reporting a different perception from the measured temperature conditions, it still could be the case that the subject indeed did not felt a temperature change.

SUBJECT D0052

The temperature of the skin of subject D0052 remained higher in the fifth task than before the thermal pulse. Although, similar behaviour can be seen with subjects D0021 and D0061, the behaviour of the skin’s temperature of subject D0052 is the most notable. It might indicate that the skin is subjected to neurogenic inflammation due to the elongated temperature pulse. This has the consequence that the last NDT procedure might be influenced by this and thus should be interpreted with this in mind.

With the perception of the temperature, subject D0052 indicated the fourth task as ‘large increase’, while the temperature remained constant. However, it is debatable whether this indicates that the subject perceived again a large increase of temperature, or that it was interpreted as a large increase related to the first two tasks. This difficulty of interpretation of the question arises due to the unintended double heated task. Therefore, the perception of the temperature of task 4 will be given less value.

The perception per tasks might indicate activation of both tactile and nociceptive fibers in the first three tasks, whereas the last two tasks might indicate only activation of the nociceptive fibers. This is remarkable for the last task, as this one is not heated. However, it might be subjected to neurogenic inflammation as mentioned

before, which might explain this perception. This is also supported by the increased NRS score for only the last task. This has direct consequences, as the assessment of perception is only a control.

Subject D0061

In the second task of subject D0061, the detection rate of SP decreases during the heated task, compared with the other tasks. However, the detection rate of DP remains approximately the same. This might indicate loss of focus by the subject, when a thermal pulse is applied. In contrast, loss of focus can be recognised by a decrease of stimulation amplitude, when the subject refocuses. However, this is not present in the results for this task. Therefore, there might be some other explanation for this behaviour. For instance, the thermal stimulus might cause noise in processing the perception of the electrical stimuli, which could result in difficulties with detecting SP. Noise would affect DP less or not at all, due to the character of the DP, as this pulse is easier to distinguish.

Partly related to this, the detection rate of SP increases when the sensors show a plateau of the skin temperature (at ~1600 s) due to the late start of the temperature pulse. The question arises whether there is a relation between reaching the plateau and the increasing threshold. As this phenomenon is only seen in one single measurement, no solid conclusions can be drawn from this. However, this might be an interesting theory to investigate in new experiments. Nevertheless, this should only be investigated when the protocols (and electrode) are further developed.

Subjects D0032 and D0041

The electrode has been separated from the skin from subject D0032 after the first task, as it was attached too firm to the arm. The re-attachment resulted in a changed detection threshold for the following tasks. This does not have to be concerning, as the first measurement is mainly to get more familiar with the task. Therefore, this will have no consequences for further analysis.

The perception of the temperature was qualified by subject D0032 as ‘slightly increase’, even when no heat was applied. This shows how easily perception could be misinterpreted, although this remains the perception of the subject. A similar misinterpretation can be found with subject D0041, again during the last task. This could indicate that a deviating perception might originate from the long duration of the experiment. For subject D0041, this can be supported by the increased NRS score, which might indicate an over sensitized sensory system. Therefore, those perception results should be interpreted with caution. Furthermore, analysis of perception might only be valuable when it is performed over large amounts of this perception assessment.

Remarkable are the results of the study parameters ‘detection rate’ and ‘NDT_0’ for subjects D0032 and D0041, as they perform better than average on the normal tasks. This supports the recommendation that more measurements are necessary to evaluate the functionality of ThESSA in context of NDT measurements.

6 General Discussion

6.1 Design

The material choices of concept design 1 and concept design 4 were based on the information available via Granata eduPack as shown in Figure 3.1. The figure indicated that carbon fiber was not biocompatible. However, according to Petersen carbon fiber is in fact biocompatible [59]. This material has several interesting properties that would be beneficial in the design of a thermal-electrical stimulation electrode, such as a low oxidation rate, and it is thermal and electrical conductivity. Furthermore, mass production could be done at relatively low costs [46]. Actually, a needle electrode was used by Guitchounts to record neural activity [60]. This argues that carbon fibers should be considered as material for the electrode.

Furthermore, requirement S-2 of the design stated that the electrode should be easy to sterilize. All the materials of the electrode used could endure temperatures of 121 °C (used in sterilization with an autoclave), however, the coper plate oxidised partly due to sterilization. Therefore, the electrode was only disinfected with an alcohol pad, to preserve the electrode from malfunctioning. This could be justified, as the needles only superficially protrude the skin. Nevertheless, the sterilization of the electrode, as well as carbon fiber for the basis of the electrode, should be considered in further development of the ThESSA electrode.

With the design of ThESSA is a needle length used of 0.2mm, such that it protrudes the stratum corneum, and reaches the epidermis. This design choice is made on the assumption that the needle will penetrate the skin for the same depth, without considering the flexibility of the skin, the sharpness of the needles and occasionally bended needle tips. Although the true penetration depth is not known, it presumably will not affect the measurements substantially, as a conducting path will be formed through the SC while the NDT familiarisation is applied. For further development of ThESSA it is recommended to do a penetration test on surrogate skin, such that the needle length can be adapted on the outcomes of this test.

6.2 Functionality of the Electrode

For the calibration of the PT100 sensors, it was assumed that the thermode gives an accurate temperature. In the specifications of the TSA2 it is defined that it has an accuracy of ±0.3°C [39]. This means that the calibration curve will also have an accuracy of ±0.3°C and therefore the temperature curves as well. During the temperature measurements, only the H-NDT task might be affected by this, as the HPDT is used as input for the constant thermal pulse. When the deviation is assumed to be consistent over time, this will not affect the interpretation of the results. It will only be affecting when a different thermode is used, or when the thermode is recalibrated between measurements.

6.3 Temperature measurements

The skin temperature was measured with PT100 sensors to verify whether the skin reached the desired temperature. The results in Table 5.3 clearly show that the skin temperature never reached the target temperature. However, it did not reach the target temperature either without an electrode attached. This showed that the temperature administered by the thermode (target temperature) is not the desired temperature to be measured at the skin. Instead, the desired temperature should be the temperature measured at the skin when no electrode is attached, as the measured temperature is subjected to thermoregulation of the skin. In this research the plateau of this temperature was never reached, as it was unknown that this was the desired temperature during the experiments. Therefore it could not be compared with the temperature of the skin when the electrode was attached. Nevertheless it gave the insight how it can be achieved in future research.

With the thermal conductivity test it is experienced that the measured temperature of the skin is not the same as the perceived temperature. The temperature is almost directly sensed whenever the thermal pulse is applied. This can be supported with the measured temperatures when the HPDT is applied, as the subject presses the button whenever the temperature becomes uncomfortable. The measured temperatures are substantially lower than the average temperature used for the constant thermal pulse in the nociceptive perception task. This means that the only thing that could be derived from the average temperature curves is the difference between the test temperature for the H-NDT task without ThESSA, and the constant temperature in the H-NDT task with ThESSA attached. This difference could be used to estimate the

temperature loss through the electrode, although the skin's thermoregulation might also have an effect on this.

The influence of thermoregulation might have consequences for the interpretation of the results. This could be anticipated by using different types of heat stimulation, for instance with heat stimulation through the needles only. In this way, the skin is less subjected to suppressing the temperature, as it is only applied on very small areas, and therefore the outcomes will become less influenced by thermoregulation. However, a disadvantage of this approach is that the true temperature of the skin will be difficult to measure, as the sensor will interfere more with the applied thermal stimulus then was the case in this research.

6.4 PSYCHOPHYSICAL EXPLORATION

This study investigated the functionality of a thermo-electrical stimulation electrode in terms of detection rate, stimulation amplitude and perception of the stimuli. The thermal stimulation needed for activation of thermosensitive nociceptors was obtained by completing a subjective HPDT task. Application of this temperature during the H-NDT task showed presumed affection of the detection rate. The analysis of stimulation amplitude was subdivided in an initial NDT (NDT_0) and the slope of the NDT. NDT_0 showed a presumed increase of threshold during the H-NDT task, and the slopes seem to be more concentrated to one point.

This study investigated the influence of an increased skin temperature on the NDT. The results showed an increase in NDT_0 when heat was applied. This was contrary to the expected effect of heating, namely a lower activation threshold. Continued thermal stimulation might cause an increased threshold of the nociceptors (accommodation), when the temperature is applied for a longer time. This might cause slow depolarisation of the membrane, which can initiate inactivation of the receptors such that it accommodates the nociceptor [61].

To prevent from accommodation of nociceptors, a new electrode could be developed that requires thermal stimulation via needles. This can apply more locally a temperature pulse, which might prevent overstimulation. Presumably the temperature will be less important, as any warmth pulse will be sensed by the keratinocytes which will activate nociceptors. Therefore, the temperature could for instance be set to 40 °C, as reported in literature as activation temperature of thermosensitive nociceptors [2]. With this new electrode, a research objective could be the tracking of the nociceptive detection thresholds with several simulation types, which vary in the duration of the temperature pulse, IPI between thermal and electrical stimulation, and even overlap of the pulses.

Another explanation for the higher activation threshold during the H-NDT task might come from noise originating of thermal stimulation. This could make it more difficult to distinguish the electrical pulse, which is supported by the lower detection rates for the heated tasks. This explanation would not directly give recommendations for improvements, as this would require removal of the noise (i.e. the thermal source). Nevertheless, noise originating from thermal stimulation should still be considered as explanation for the increased NDT_0.

In relation to the currently used IES-5 electrode, ThESSA obtained lower detection rates and higher NDT_0's for both SP and DP, based on the four tested subjects. Nevertheless, ThESSA was able to show some effect between the normal and heated NDT task, which was one of the research specifications. The study therefore showed that the thermo-electrical stimulation electrode ThESSA is functional for its purpose.

6.5 FUTURE PROSPECTIVE

Aside from the proposed improvements to the electrode, a few other recommendations can be made. As the temperature measurements showed high dependence of the skin's thermoregulation system, it is recommended to develop a COMSOL model to gain more insight in this system. It could help anticipating on the thermoregulation in the approach of thermal electrical stimulation in future research, as already mentioned in Section 5.3.2. Furthermore, it might be of interest to compare ThESSA with the IES-5 electrode on the same subjects. This might help to characterize the differences of these electrodes in a more sophisticated way than was done in this study. Another recommendation might be to measure the NDT in combination with EEG measurements (NDT-EP method). It might provide more information in the increased NDT when heat is applied, thus whether thermal stimulation causes noise in processing the stimuli. These NDT-EP measurements

can even be compared to NDT-EPs obtained with IES-5. Nevertheless, the last recommendations continue already with the use of ThESSA, although improvements on the ThESSA electrode and further knowledge of the thermoregulation system are of more priority.

REFERENCES

1. Breivik, H., et al., *Survey of chronic pain in Europe: Prevalence, impact on daily life, and treatment.* European Journal of Pain, 2006. **10**(4): p. 287.
2. Plaghki, L. and A. Mouraux, *How do we selectively activate skin nociceptors with a high power infrared laser? Physiology and biophysics of laser stimulation.* Neurophysiologie Clinique/Clinical Neurophysiology, 2003. **33**(6): p. 269-277.
3. Granovsky, Y., et al., *Normative data for Aδ contact heat evoked potentials in adult population: a multicenter study.* Pain, 2016. **157**(5): p. 1156-1163.
4. Mouraux, A., G.D. Iannetti, and L. Plaghki, *Low intensity intra-epidermal electrical stimulation can activate Aδ-nociceptors selectively.* Pain, 2010. **150**(1): p. 199-207.
5. Poulsen, A.H., et al., *Comparison of existing electrode designs for preferential activation of cutaneous nociceptors.* Journal of Neural Engineering, 2020. **17**(3): p. 036026.
6. NobelPrize.org, *Press release: The Nobel Prize in Physiology or Medicine 2021*. Nobel Prize Outreach AB 2021: https://www.nobelprize.org/prizes/medicine/2021/press-release/.
7. Medoc. *QST Technique*. 2020 [cited 2021 January 14]; Available from: https://www.medoc-web.com/qst-technique.
8. Attal, N., et al., *Value of quantitative sensory testing in neurological and pain disorders: NeuPSIG consensus.* PAIN®, 2013. **154**(9): p. 1807-1819.
9. Medoc, *Webinar about the capabilities of TSA2*. 2020.
10. Maan, M.J., *Combined Thermal-Electrical Stimulation of Nociceptive Cutaneous Afferents, a Mathematical Approach*. 2018, University of Twente.
11. Maan, M.J., *The Influence of Temperature on Selectively Stimulating Nociceptive Aδ Fibers*. 2020, University of Twente.
12. Manfron, L., et al., *Investigating perceptual simultaneity between nociceptive and visual stimuli by means of temporal order judgments.* Neuroscience Letters, 2020. **735**: p. 135156.
13. Justine Fenner, R.A.F.C., *Anatomy, Physiology, Histology, and Immunohistochemistry of Human Skin,*, in *Skin Tissue Engineering and Regenerative Medicine,*, J.H.H.I. Mohammad Z. Albanna, Editor. 2016. p. 1-17.
14. Lamantia, A.S., et al., *The Somatic Sensory System: Touch and Proprioception*, in *NeuroScience*. 2011, Sinauer Associates Incorporated. p. 189-208.
15. Magerl, W., et al., *C-and Aδ-fiber components of heat-evoked cerebral potentials in healthy human subjects.* Pain, 1999. **82**(2): p. 127-137.
16. Basbaum, A.I., et al., *Cellular and Molecular Mechanisms of Pain.* Cell, 2009. **139**(2): p. 267-284.
17. Caterina, M.J., *Transient receptor potential ion channels as participants in thermosensation and thermoregulation.* American Journal of Physiology-Regulatory, Integrative and Comparative Physiology, 2007. **292**(1): p. R64-R76.
18. Chung, M.K., H. Lee, and M.J. Caterina, *Warm temperatures activate TRPV4 in mouse 308 keratinocytes.* Journal of Biological Chemistry, 2003. **278**(34): p. 32037-32046.
19. Peier, A.M., et al., *A heat-sensitive TRP channel expressed in keratinocytes.* Science, 2002. **296**(5575): p. 2046-2049.
20. Purves, D., *Neuroscience*. 2012: Sinauer Associates.
21. Baumbauer, K.M., et al., *Keratinocytes can modulate and directly initiate nociceptive responses.* eLife, 2015. **4**(September 2015).
22. Talagas, M., et al., *Lifting the veil on the keratinocyte contribution to cutaneous nociception.* Protein & cell, 2020. **11**(4): p. 239-250.
23. Moehring, F., et al., *Keratinocytes mediate innocuous and noxious touch via ATP-P2X4 signaling.* eLife, 2018. **7**.

24. Mandadi, S., et al., *TRPV3 in keratinocytes transmits temperature information to sensory neurons via ATP.* Pflügers Archiv - European Journal of Physiology, 2009. **458**(6): p. 1093-1102.
25. Huang, S.M., et al., *Overexpressed Transient Receptor Potential Vanilloid 3 Ion Channels in Skin Keratinocytes Modulate Pain Sensitivity via Prostaglandin E₂.* The Journal of Neuroscience, 2008. **28**(51): p. 13727-13737.
26. Dai, Y. *TRPs and pain*. in *Seminars in Immunopathology*. 2016. Springer.
27. Dussor, G., et al., *Nucleotide signaling and cutaneous mechanisms of pain transduction.* Brain Research Reviews, 2009. **60**(1): p. 24-35.
28. Burnstock, G., *Introduction and perspective, historical note*, in *ATP-gated P2X receptors in health and disease*, A. Nistri, et al., Editors. 2015, Frontiers Media SA. p. 15-27.
29. Kobayashi, K., et al., *Differential expression patterns of mRNAs for P2X receptor subunits in neurochemically characterized dorsal root ganglion neurons in the rat.* Journal of Comparative Neurology, 2005. **481**(4): p. 377-390.
30. Malin, S.A., et al., *Thermal nociception and TRPV1 function are attenuated in mice lacking the nucleotide receptor P2Y2.* PAIN, 2008. **138**(3): p. 484-496.
31. Charkoudian, N., *Skin Blood Flow in Adult Human Thermoregulation: How It Works, When It Does Not, and Why.* Mayo Clinic Proceedings, 2003. **78**(5): p. 603-612.
32. Holzer, P., *Neurogenic vasodilatation and plasma leakage in the skin.* General Pharmacology, 1998. **30**(1): p. 5-11.
33. Kellogg Jr, D.L., J.L. Zhao, and Y. Wu, *Roles of nitric oxide synthase isoforms in cutaneous vasodilation induced by local warming of the skin and whole body heat stress in humans.* Journal of Applied Physiology, 2009. **107**(5): p. 1438-1444.
34. Finnerup, N.B., et al., *Neuropathic pain: An updated grading system for research and clinical practice.* Pain, 2016. **157**(8): p. 1599-1606.
35. O'Connor, A.B. and R.H. Dworkin, *Treatment of Neuropathic Pain: An Overview of Recent Guidelines.* American Journal of Medicine, 2009. **122**(10 SUPPL.): p. S22-S32.
36. Finnerup, N.B., et al., *Algorithm for neuropathic pain treatment: An evidence based proposal.* Pain, 2005. **118**(3): p. 289-305.
37. Maier, C., et al., *Quantitative sensory testing in the German Research Network on Neuropathic Pain (DFNS): Somatosensory abnormalities in 1236 patients with different neuropathic pain syndromes.* Pain, 2010. **150**(3): p. 439-450.
38. Medoc. *Thermodes*. 2020 [cited 2021 December 15]; Available from: https://www.medoc-web.com/thermodes.
39. Medoc Ltd., *Thermal Sensory Analyzer Operation Manual.* 2020.
40. Rolke, R., et al., *Quantitative sensory testing in the German Research Network on Neuropathic Pain (DFNS): Standardized protocol and reference values.* Pain, 2006. **123**(3): p. 231-243.
41. Doll, R.J., P.H. Veltink, and J.R. Buitenweg, *Observation of time-dependent psychophysical functions and accounting for threshold drifts.* Attention, Perception, Psychophysics, 2015. **77**: p. 1440-1447.
42. Doll, R.J., et al., *Tracking of nociceptive thresholds using adaptive psychophysical methods.* Behav Res Methods, 2014. **46**(1): p. 55-66.
43. van den Berg, B., et al., *Simultaneous tracking of psychophysical detection thresholds and evoked potentials to study nociceptive processing.* Behav Res Methods, 2020.
44. Lu, F., et al., *Review of stratum corneum impedance measurement in non-invasive penetration application.* Biosensors, 2018. **8**(2).
45. Heikenfeld, J., et al., *Wearable sensors: Modalities, challenges, and prospects.* Lab on a Chip, 2018. **18**(2): p. 217-248.
46. Yao, S. and Y. Zhu, *Nanomaterial-Enabled Dry Electrodes for Electrophysiological Sensing: A Review.* JOM, 2016. **68**(4): p. 1145-1155.
47. Chi, Y.M., T.P. Jung, and G. Cauwenberghs, *Dry-contact and noncontact biopotential electrodes: Methodological review.* IEEE Reviews in Biomedical Engineering, 2010. **3**: p. 106-119.
48. Hermens, H.J., et al., *Development of recommendations for SEMG sensors and sensor placement procedures.* Journal of Electromyography and Kinesiology, 2000. **10**(5): p. 361-374.
49. Hirschorn, B., et al., *Determination of effective capacitance and film thickness from constant-phase-element parameters.* Electrochimica acta, 2010. **55**(21): p. 6218-6227.
50. Valentinuzzi, M.E., *Bioelectrical impedance techniques in medicine Part I: Bioimpedance measurement first section: General concepts.* Critical Reviews in Biomedical Engineering, 1997. **24**(4-6): p. 223-255.

51. AdminMed. *AdminPatch® 600 microneedle array*. [cited 2021 9 July]; Available from: http://www.adminmed.com/array0600.
52. Gardeniers, H.J., et al., *Silicon micromachined hollow microneedles for transdermal liquid transport.* Journal of Microelectromechanical systems, 2003. **12**(6): p. 855-862.
53. Pavlaković, G., et al., *Effect of thermode application pressure on thermal threshold detection.* Muscle and Nerve, 2008. **38**(5): p. 1498-1505.
54. Zorec, B., et al., *Skin electroporation for transdermal drug delivery: The influence of the order of different square wave electric pulses.* International Journal of Pharmaceutics, 2013. **457**(1): p. 214-223.
55. van den Berg, B. and J.R. Buitenweg, *Observation of Nociceptive Processing: Effect of Intra-Epidermal Electric Stimulus Properties on Detection Probability and Evoked Potentials.* Brain Topography, 2021. **34**(2): p. 139-153.
56. Nahra, H. and L. Plaghki, *The effects of A-fiber pressure block on perception and neurophysiological correlates of brief non-painful and painful CO2 laser stimuli in humans.* European Journal of Pain, 2003. **7**(2): p. 189-199.
57. Steenbergen, P., et al., *A system for inducing concurrent tactile and nociceptive sensations at the same site using electrocutaneous stimulation.* Behav Res Methods, 2012. **44**(4): p. 924-33.
58. Inui, K., et al., *Preferential stimulation of Aδ fibers by intra-epidermal needle electrode in humans.* Pain, 2002. **96**(3): p. 247-252.
59. Petersen, R., *Carbon fiber biocompatibility for implants.* Fibers, 2016. **4**(1).
60. Guitchounts, G., et al., *A carbon-fiber electrode array for long-term neural recording.* Journal of neural engineering, 2013. **10**(4): p. 046016.
61. Hugosdottir, R., et al., *Investigating stimulation parameters for preferential small-fiber activation using exponentially rising electrical currents.* Journal of Neurophysiology, 2019. **122**(4): p. 1745-1752.

APPENDICES

The appendix consists of eight appendices, subdivided in the following topics.

Appendix A	Additional figures and descriptions	
	A.1 Detailed description of the production process of the prototypes	
	A.2 Additional pictures measurements	
	A.3 Calculation of the temperature via calibration curve	
	A.4 Additional figures impedance measurements	
	A.5 Study design elaborated recommendations	
	A.6 Temperature comparison of the skin	
	A.7 Temperature comparison of the first measurements	
	A.8 Estimated NDTs	
	A.9 Individual values for comparing the subjects	
	A.10 Additional pictures of the psychophysical exploration	
Appendix B	Datasheets	*Digitally available*
	Parmacell insulation tape P252	*Digitally available*
	Tesa50650 PET tape	*Digitally available*
	Pin connector	*Digitally available*
	PT100 (DM-303)	*Digitally available*
	PT100 (NB-PTCO-011)	*Digitally available*
	Ag/AgCl ground electrode	*Digitally available*
	Tough PLA	*Digitally available*
Appendix C	Ethical approval	*Digitally available*
Appendix D	Risk analysis	*Digitally available*
Appendix E	Protocols	*Digitally available*
	MMS protocol	*Digitally available*
	MATLAB external control script	*Digitally available*
Appendix F	Technical drawing electrode holder	*Digitally available*
Appendix G	Test report AmbuStim	*Digitally available*
Appendix H	Subject's Case Report Form	*Digitally available*

APPENDIX A

A.1 DETAILED DESCRIPTION OF THE PRODUCTION PROCESS OF THE PROTOTYPES

APPLICATION OF THE TEMPLATE

The template will be placed to the electrode, such that the needles can be placed through the base plate, until resistance was felt of touching the template. This approach is only suitable when the needles do not have any resistance from the holes. Therefore the holes had a diameter of 0.35 mm, whereas the diameter of the needles was 0.3 mm.

After placing them in the right position, the needles were fixated with super glue on the back side. When it dried, the needles are shortened with a wire cutter and sanding paper (grid size 220), such that they level with the back side of the plate.

With the aluminium prototype, the diameter was wider for the usage of the template. For the copper prototype, the template was used differently, as the holes became narrower. These narrower holes made it impossible to feel whether the resistance was due to the template or the narrow hole. With the new approach, the needles were inserted deeper through the plate, and were pushed back with the template to the correct height. As the needles give enough resistance to the sides, they will not fall out easily, and retain the length of the milled section of the template.

LENGTH OF THE NEEDLES

The template should provide that the length of the needles is maximal 0.2mm. However, shorter needles could still be possible. Therefore, they were checked manually with a flat plate on top of the needles, to feel whether the tips have the same length. If any, other than the middle needle, is shorter than 0.2mm the plate on top of the needles would be unbalanced. If so, the electrode is rejected or adjusted when possible.

From the three copper prototypes, only one passed the test for equal lengths of the needles. For one of the prototypes it could even be felt by hand that one needle was only slightly protruding the base plate compared to the other needles. The other one showed only little unbalance of the flat plate on top of the needles. The last one was sufficient enough to continue with this electrode in further tests. To presevere this one, a rejected prototype was used for some of the remaining thermal tests.

As only one prototype passed the needle length test, it shows the delicacy of the fixation of the needles. If one of the needles had less friction from the hole, it already had more risk of having a different length than the others. A light touch of the tip of the needle before fixation could already result in a shorter needle length when not paying attention to it. Therefore, this should be kept in mind whenever new prototypes have to be developed.

FINISHING THE BACK OF THE ELECTRODE

Independent of the fixation method (glue or thin), the needles were shortened with a wire cutter and sanding paper (grid size 220), such that they level with the back side of the plate.

A.2 Additional pictures measurements

Imprint electrode thermal conduction measurement 4 (with the concept electrode)

A) B)

Figure A.1 A) Imprint of the electrode and sensor during the measurement of 26 May **B)** Imprint of the electrode and sensor during the measurement of 27 May

Oxidation of the electrode

A) B)

Figure A.2 A) shows the oxifation of the ThESSA electrode after several weeks. The heating of the copper increased the oxidation. The upper right electrode and the one in the holder were used in combination with the thermode, wheras the upper left was not (it was earlier on disqualified, and therefore not used).
B) The top of the electrode is less oxidized due to the covering tape.

A.3 CALCULATION OF THE TEMPERATURE VIA CALIBRATION CURVE

```
R0=100;
a=3.9083e-3;
b=-5.775e-7;
R=@(T) R0*(1+a*T+b*T.^2);
for n=1:length(T)
    I(n)=(U(n)*10^-3)/R(T(n));
end
par(:,q)=polyfit(U,I,2); %gives parameters of the function I=c1*U^2+c2*U+c3
p=@(z) polyval(par,z) %make a quadratic function with the calibration
parameters

u=data.TMSi{n};
Rm=u*10^-3./p(u);
T_cal(:,q)=(-a+sqrt(a^2-4*b*(1-Rm./R0)))/(2*b); %Rewritten equation from
the PT100 datasheet (the earlier defined 'R').
```

Here, U is the average current on a small time interval at the end of each temperature step of the calibration curve, and T the true temperature. u is the data of a measurement, $R0$ is the initial resistance, and Rm the measured resistance with the PT100 sensor. T_cal is the calculated temperature via the calibration curve.

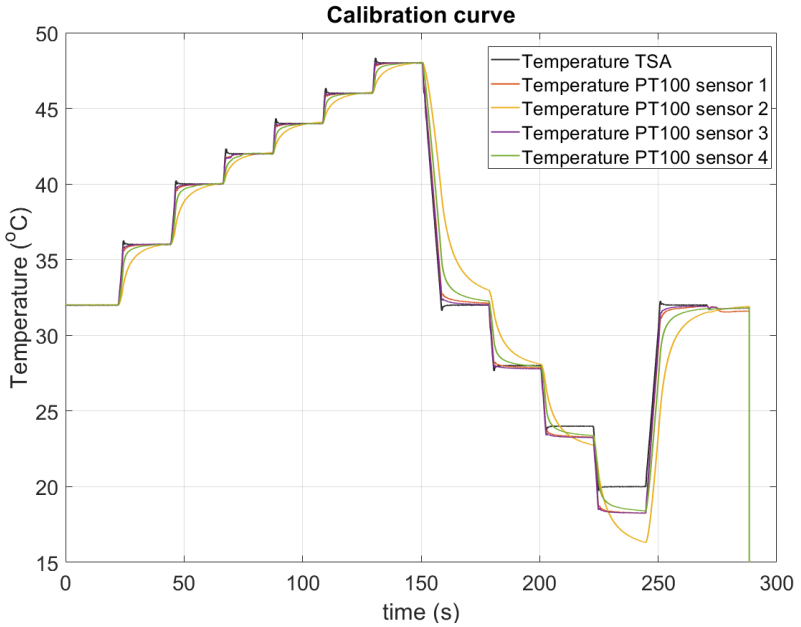

A)

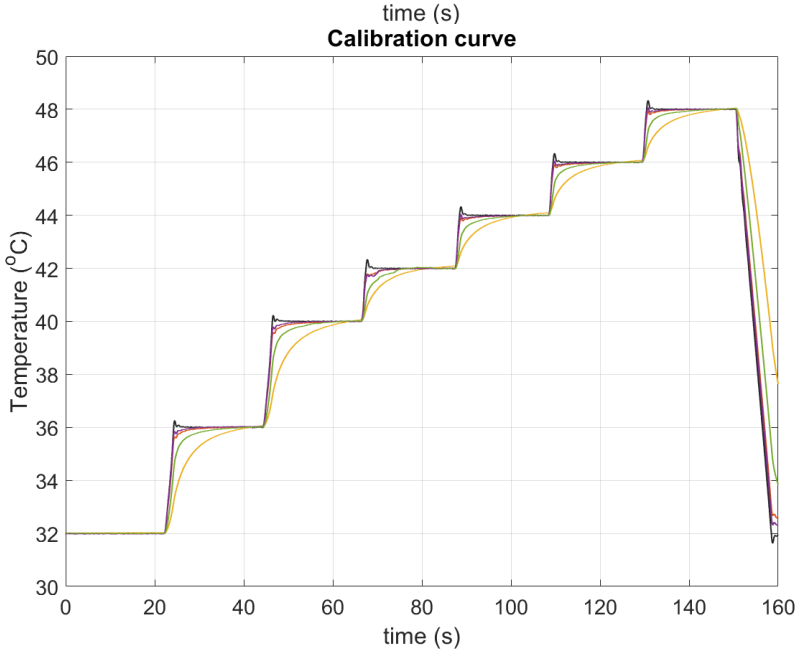

B)

Figure A.3
A) The original calibration curve. The curves of the decreasing temperature are not very accurate, and slow in its reaction to a temperature change, probably due to not using a true insulator in the calibration measurement.
B) The actual values used for the calibration. This shows that sensor 2 and sensor 4 are not adapting fast.

A.4 Additional figures impedance measurements

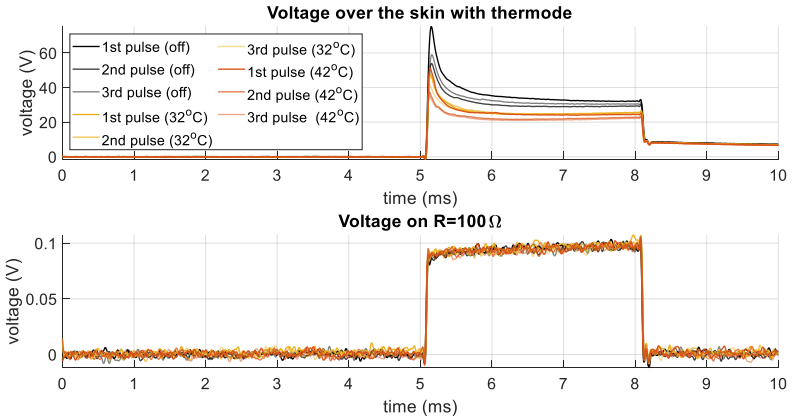

Figure A.4

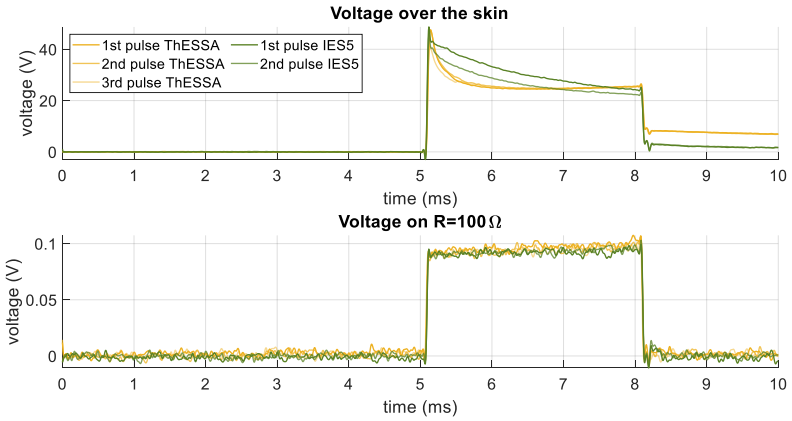

Figure A.5

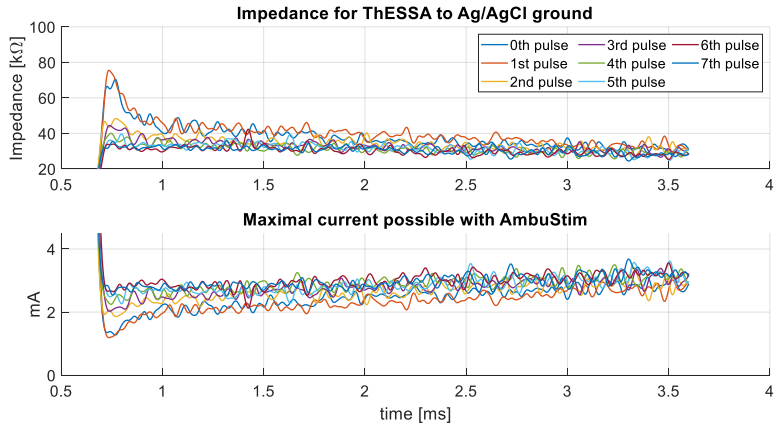

Figure A.6 The impedance of a train of pulses for the ThESSA to AgAg/Cl setup, with an interpulse interval in the order of seconds. It shows the decrease of the initial peak at the beginning of the pulse, when the number increases.

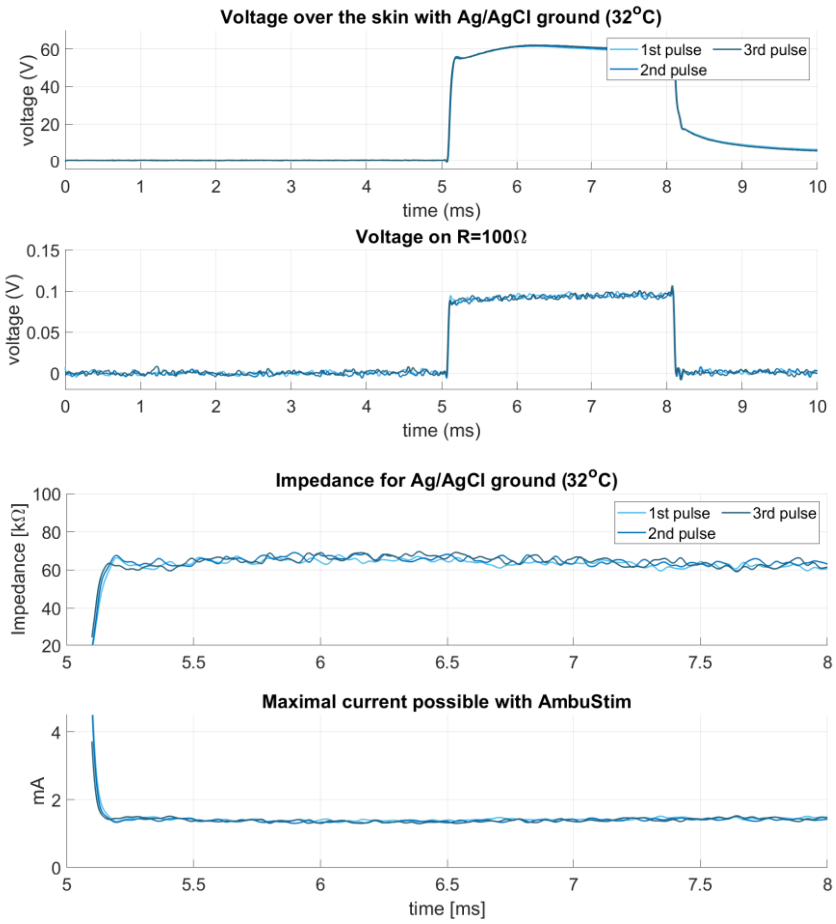
Voltage over the skin with Ag/AgCl ground (32°C)
1st pulse
2nd pulse
3rd pulse
voltage (V)
time (ms)
Voltage on R=100Ω
voltage (V)
time (ms)
Impedance for Ag/AgCl ground (32°C)
1st pulse
2nd pulse
3rd pulse
Impedance [kΩ]
Maximal current possible with AmbuStim
mA
time [ms]

Figure A.7

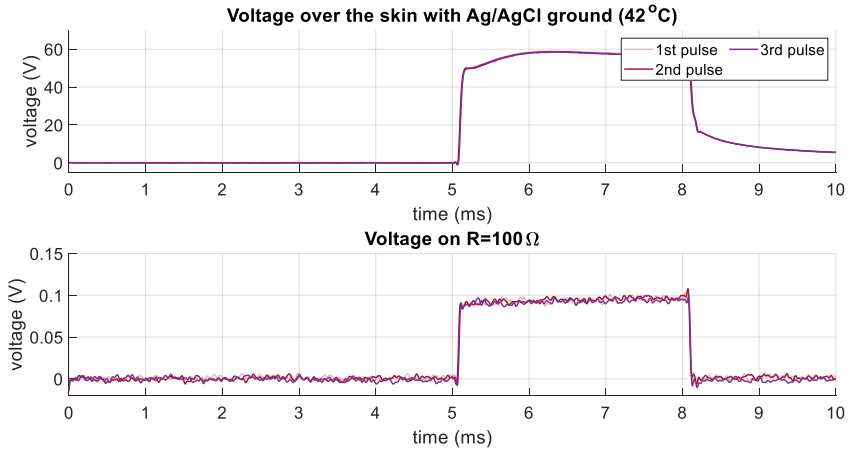
Voltage over the skin with Ag/AgCl ground (42°C)
1st pulse
2nd pulse
3rd pulse
voltage (V)
time (ms)
Voltage on R=100Ω
voltage (V)
time (ms)

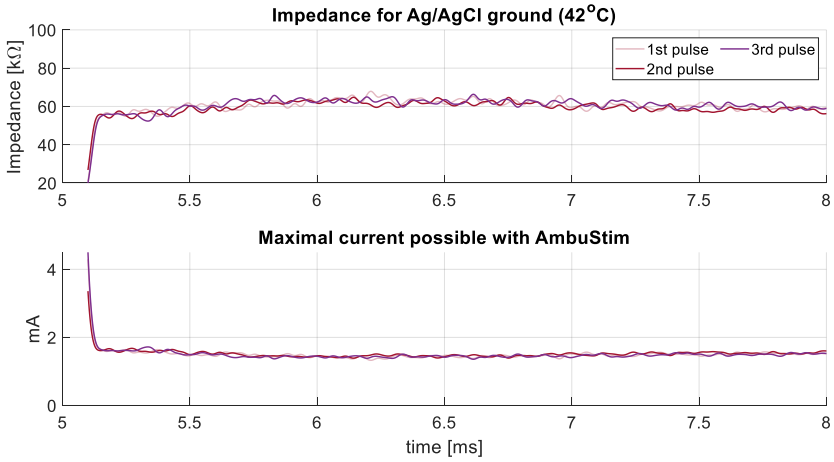

Figure A.8

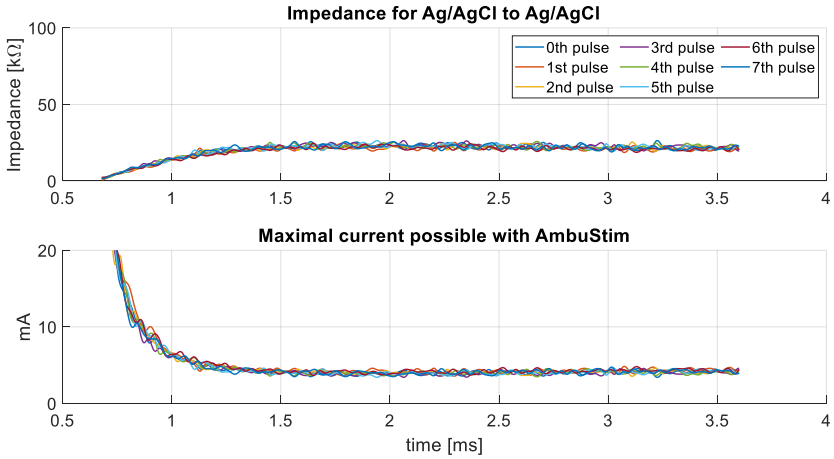

Figure A.9

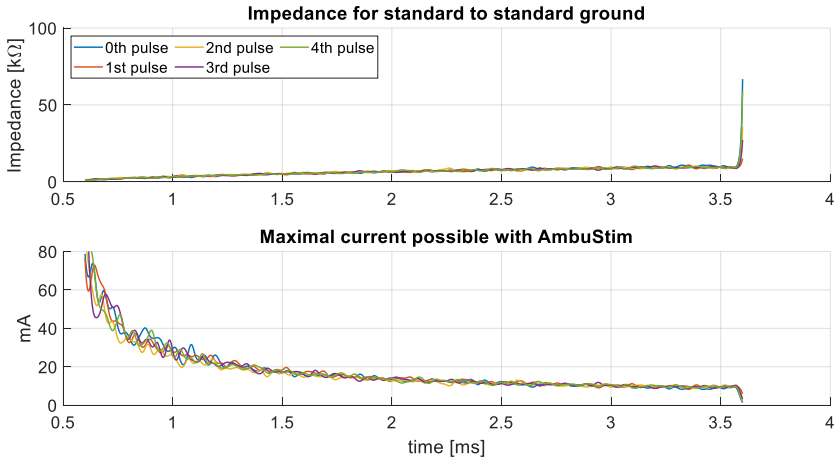

Figure A.10

A.5 STUDY DESIGN ELABORATED RECOMMENDATIONS

For automatically trigger the H-NDT task for the HPDT-temperature, Labview should be linked to the MATLAB protocol or a trigger must be send to the *TTL IN* port of the TSA2. For linking Labview to the MATLAB script, a command should be built into the Labview programme, such that it sends a trigger to MATLAB when the programme is opened. This means that two actions (opening programme and sending remote trigger) are now combined into one, which gives less chance on manual mistakes. Disadvantage of this method is the expectation that the whole MATLAB script should be rewritten, and thus the design of the experiment.

The second option, sending a trigger to the *TTL IN* port of the TSA2, could be realized by the Arduino trigger box which is already in use for other NDT research at our research group. This entails that a currently used script for the trigger box should be adjusted, such that it suits the TSA2. Furthermore, only small adjustments of the MATLAB script are necessary. Therefore this improvement is presumed to be more feasible.

A.6 TEMPERATURE COMPARISON OF THE SKIN

In Table A.1 the data is presented of the temperature of the skin for different subjects. During the experiments the HPDT was tested for 60s whether it was durable for the subject. This was performed without ThESSA as control for the obtained HPDT. This control made it possible to compare the skin temperatures with and without electrode at t=60s. Table A.1 shows that at 60s, the skin temperature is approximately 3.5 °C lower when the ThESSA is attached. These results were not included in the main report, as at 60s the temperature curve without electrode is closer to its horizontal asymptote than with electrode.

Not approaching the asymptote of the curve can be confirmed with the temperatures presented in Table A.2. This table shows the differences between the temperatures at t=60s and t>600s. On average a difference of approximately 3.6 °C is measured over this time interval, indicating that at t=60s the curve has not approached its asymptote. Thus at t=60, the curve is not at a steady state level, and therefore not suited for comparison of temperatures with and without ThESSA. The best way to compare these is to take the time at which both curves approach their asymptote. Therefore no solid conclusions can be drawn from this, but for initial insight they are presented here.

Table A.1 Measured skin temperatures with and without ThESSA at t=60s.

	Target temperature (TT) (°C)	Sensor 1 (°C)		Sensor 2 (°C)		Sensor 3 (°C)		Sensor 4 (°C)		Average sensors (AS) (°C)		Difference sensors (DS) (°C)
		w\o	w\	w\o	w\	w\o	w\	w\o	w\	w\o	w\	$AS_{w\backslash o} - AS_{w\backslash}$
D0012	42.9	36.7	33.3	38.7	34.7	38.0	34.1	37.3	34.3	37.7	34.1	**3.5**
D0021	44.1	37.8	35.2	40.7	35.7	38.7	34.8	39.0	34.4	39.0	35.0	**4.0**
D0052	44.9	39.5	35.7	40.0	37.0	38.0	35.9	39.9	35.5	39.4	36.0	**3.3**
D0061	45.0	37.4	34.6	39.9	35.9	37.0	34.3	38.4	34.6	38.2	34.9	**3.3**

Table A.2 Measured skin temperatures with ThESSA at t=60s and t>600s.

	Target temperature (TT) (°C)	Sensor 1 (°C)		Sensor 2 (°C)		Sensor 3 (°C)		Sensor 4 (°C)		Average sensors (AS) (°C)		Difference (°C)
w\		60	end	60	end	60	end	60	end	60	end	$AS_{end} - AS_{60}$
D0012	42.9	33.3	36.0	34.7	38.3	34.1	37.3	34.3	37.5	34.1	37.3	**3.2**
D0021	44.1	35.2	38.4	35.7	39.7	34.8	38.5	34.4	38.2	35.0	38.7	**3.7**
D0052	44.9	35.7	39.1	37.0	41.0	35.9	39.2	35.5	39.7	36.0	39.8	**3.8**
D0061	45.0	34.6	37.9	35.9	39.9	34.3	38.0	34.6	38.7	34.9	38.6	**3.8**

Furthermore, in Table A.3 the difference with TT is compared with the average hours of sport per week. It might show a relation between difference in TT and subject specific vessel structure, as this is presumed to be related to the average hours of sport per week. The complete overview of the case report forms can be found in Appendix H.

Table A.3 Presumed relation between difference in TT and average hours of sport per week.

	Average hours of sport per week	Difference with TT (from Table 5.3)
D0012	3.5h	5.6 °C
D0021	3.0h	5.3 °C
D0052	2.0h	5.1 °C
D0061	1.0h	6.4 °C

Table A.4 Overview of the final temperatures per subject during the H-NDT task, including the individual values.

	Target temperature (TT)	Sensor 1	Sensor 2	Sensor 3	Sensor 4	**Average of the sensors (AS)**	**Difference with TT**
D0012	**42.9**	36.0	38.3	37.3	37.5	**37.3**	**5.6**
D0021	**44.1**	38.4	39.7	38.5	38.2	**38.7**	**5.3**
D0052	**44.9**	39.1	41.0	39.2	39.7	**39.8**	**5.1**
D0061	**45.0**	37.9	39.9	38.0	38.7	**38.6**	**6.4**

A.7 Temperature comparison of the first measurements

In addition to Figure 5.7, a similar figure is presented for the temperatures measured during the functionality test of the thermal conduction of the electrode.

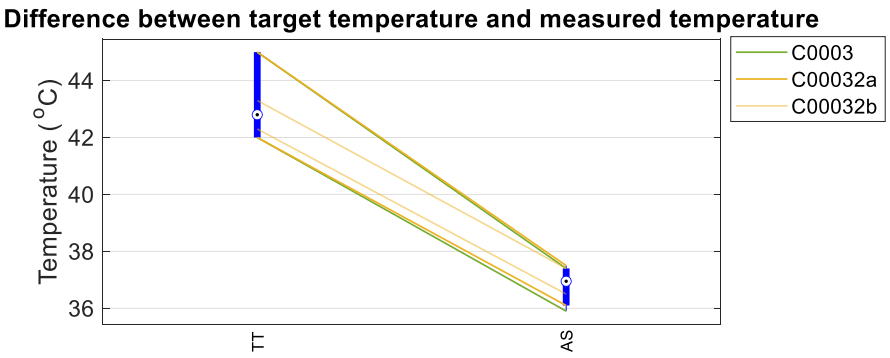

Figure A.11 Visualization of the heat loss per subject. The difference is shown of the target temperature (TT) with the average of the sensors (AS). AS is measured after a heating period of 180s.

A.8 Estimated NDTs

Table A.5 Overview of the estimated NDTs, per subject, per type of task.

		Normal	Heated	Normal (4th task)
Subject D0012	SP	$1.046 + 0.0126 \cdot n_{trial}$	$1.869 + 0.0044 \cdot n_{trial}$	$1.080 + 0.0078 \cdot n_{trial}$
	DP	$0.338 + 0.0041 \cdot n_{trial}$	$1.085 + 0.0026 \cdot n_{trial}$	$0.488 + 0.0035 \cdot n_{trial}$
Subject D0021	SP	$1.524 + 0.0025 \cdot n_{trial}$	$1.606 + 0.0024 \cdot n_{trial}$	n/a
	DP	$0.730 + 0.0012 \cdot n_{trial}$	$1.046 + 0.0016 \cdot n_{trial}$	n/a
Subject D0052	SP	$1.022 - 0.0011 \cdot n_{trial}$	$1.662 + 0.0040 \cdot n_{trial}$	$1.041 + 0.0003 \cdot n_{trial}$
	DP	$0.628 - 0.0007 \cdot n_{trial}$	$0.849 + 0.0020 \cdot n_{trial}$	$0.618 + 0.0002 \cdot n_{trial}$
Subject D0061	SP	$0.813 + 0.0013 \cdot n_{trial}$	$0.874 + 0.0026 \cdot n_{trial}$	$0.965 + 0.0011 \cdot n_{trial}$
	DP	$0.420 + 0.0007 \cdot n_{trial}$	$0.354 + 0.0011 \cdot n_{trial}$	$0.430 + 0.0005 \cdot n_{trial}$

For comparing ThESSA with the currently used IES5, the values for β_n reported in literature had to be used to derive the NDT, as only the NDT estimate is analysed and not the psychophysical curve [55].

Table A.5 Overview of the values used for comparing with IES5

	Effect size	95% Confidence interval
β_1 (intercept)	-3.70	$[-4.32, -3.09]$
β_2 (mA^{-1})	10.43	$[7.14, 13.72]$
β_3 (mA^{-1})	11.83	$[9.03\ 14.63]$
β_4 $(trial^{-1})$	$-0.0056 \cdot SD(1:450)$ [a]	$[-0.0074, -0.00038] \cdot SD(1:450)$ [a]

[a] SD(1:450)=130.048

Table A.6 CI's for the NDT_0 and NDT slope.

	SP	DP
NDT_0	[0.163, 0.374]	[0.079, 0.165]
NDT slope	[0.0008, 0.0029]	[0.0004, 0.0013]

A.9 Individual values for comparing the subjects

Table A.7 Individual values as depicted in Figure 5.6

Combined model		IES5	ThESSA		
			Non-heated	Heated	Non-heated (4^{th})
Detection rate	SP	0.427	**0.342** (0.150; 0.325; 0.475; 0.418)	**0.294** (0.215; 0.388; 0.238; 0.338)	**0.338** (0.177; -; 0.418; 0.418)
	DP	0.488	**0.457** (0.367; 0.443; 0.544; 0.475)	**0.385** (0.275; 0.367; 0.443; 0.456)	**0.413** (0.338; -; 0.450; 0.450)
NDT (mA)	SP	0.235	**1.102** (1.046; 1.525; 1.022; 0.813)	**1.503** (1.869; 1.606; 1.662; 0.874)	**1.029** (1.080; -; 1.041; 0.965)
	DP	0.110	**0.529** (0.3381; 0.730; 0.628; 0.420)	**0.834** (1.085; 1.046; 0.849; 0.354)	**0.512** (0.488; -; 0.618; 0.430)
NDT slope (mA/trial) $(\times 10^{-3})$	SP	1.507	**3.841** (12.632; 2.506; -1.110; 1.333)	**3.376** (4.437; 2.436; 3.985; 2.645)	**3.072** (7.779; -; 0.301; 1.138)
	DP	0.706	**1.322** (4.081; 1.200; -0.682; 0.689)	**1.818** (2.586; 1.586; 2.037; 1.072)	**1.399** (3.513; -; 0.179; 0.507)

A.10 Additional pictures of the psychophysical exploration

The pictures shown in Figure A.12 show the imprint of the thermode and ThESSA in the subject's skin, after the experiment. Figure A.13 shows how the sensors were attached to ThESSA.

a) D0012 Without ThESSA
Left to right (LTR):4,3,2,1

b) D0012 With ThESSA
LTR:4,3,2,1

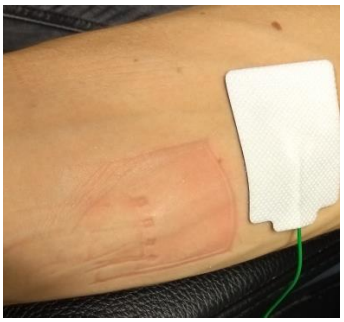

c) D0021 Without ThESSA
Top to bottom (TTB): 4,3,2,1

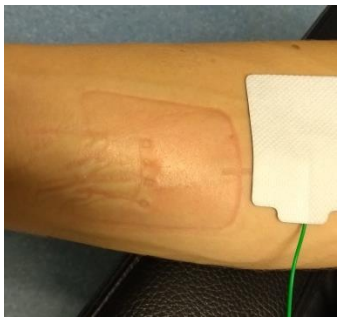

d) D0021 With ThESSA
TTB: 4,3,2,1

e) D0052 Without ThESSA
TTB:4,3,2,1

f) D0052 With ThESSA, it shows that the thermode was quite tight attached.
TTB:4,3,2,1

g) D0061 Without ThESSA
LTR: 4,3,2,1

h) D0061 With ThESSA
LTR: 4,3,2,1

i) D0032 Without ThESSA
LTR: 4,3,2,1

j) D0032 With ThESSA
LTR: 4,3,2,1

k) D0041 Without ThESSA
LTR: 4,3,2,1

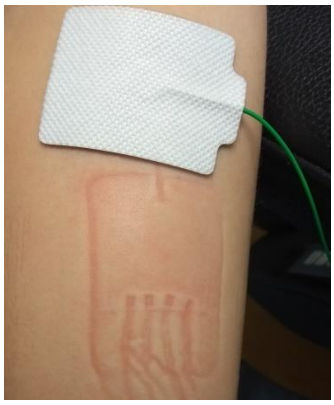

l) D0041 With ThESSA
LTR: 4,3,2,1

Figure A.12 Pictures of the imprints per subject, with and without ThESSA.

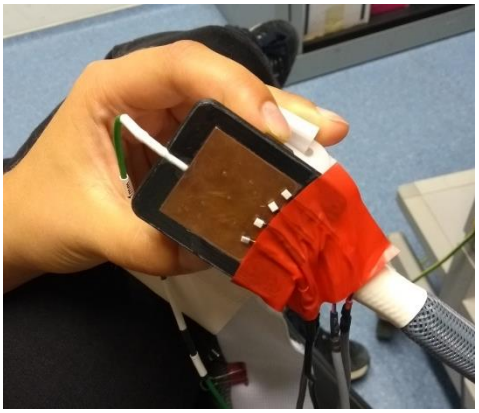

Figure A.13 Additional picture of the attachment of the sensors. From top to bottom the sensors are numbered as 4,3,2,1.